THE UNIVERSITY
of EDINBURGH

Assessment of integration of titanium to bone using acoustic emission transmission

Zinab Bodbbos

Doctor of Philosophy

The University of Edinburgh

2020

Declaration

I declare that this thesis was composed by myself, and the work contained herein is my own except were indicated, and has not been submitted for any other degree or professional qualification.

Zinab Bodbbos

September 2020

Acknowledgments

This PhD study has been an intensive learning journey for me, full of indelible memories of enthusiasm, struggle, and commitments but also of happiness and joy. I am deeply grateful to all of those who have contributed to make this journey worthwhile and successful.

I would like to express my sincere gratitude and appreciation in particular to my supervisors:

Professor Angus Walls, my principle supervisor, for giving me the opportunity and the means to make this journey, for sharing his excellent scientific knowledge and stimulating discussion, for his valuable advice and analysis which have helped me to think more deeply and value important issues I had neglected, and for his encouragement and guidance throughout my study.

Professor Robert Reuben, my co-supervisor, for his generous scientific and technical advice, for his valuable weekly discussion and for being patient enough to teach me some Engineering which helped me to develop a more comprehensive research plan, for his helpful and valuable comments and for proofreading my thesis, for his continuous guidance and support.

I would like also to thank the staff in the Department of Restorative Dentistry in Edinburgh Dental Institute, particularly, Dr Christopher Millen for his valuable advice and for his help in getting in touch with Straumann Company for offering titanium implants for the study, and Lesley-Anne Palmer for lending the GIC equipment.

I would like also to thank Dr Steven Hammer and Judith Abolle-Okoyeagu from Biomechanical Engineering Lab in Heriot Watt University for their help and advice with the AE testing and equipment during the early days of this project, and also my PhD fellow, Gabriel Boron for his technical support with the AE system.

I would like also to thank all my PhD colleagues at University of Edinburgh and Heriot Watt University for the excellent collaborative discussions, particularly,

Sharmilla Surendran for being an excellent office companion, Zoe Coyle for being such a supportive friend through emails.

I am hugely grateful to my school administrator, Jackie McGurk, for her outstanding support and assistance, for taking care of my innumerable issues, requests, forms, questions, and for being such a supportive friend who has encouraging and cheering me with her kind words during hard times.

I would like also to thank teams of people at IT and Library for their technical support and assistance.

I would like also to thank my friend, Angela Gallagher, for her linguistic advice and for her valuable tips about real life in Scotland and also for her enjoyable stories about British history.

My deepest gratitude to my parents, sisters and brothers for their continuous love and support although we are thousands of miles apart. A special thanks to my sister, Fatma, for her invaluable assistance and also to her husband, my brother-in-law Dr Farag Omar, for sharing his knowledge in AE and Matlab during my early experience in this field.

Last but not least, I would like to dedicate this dissertation to my family: my husband, Tarek, and my children: Mohamed, Arwa, Zuobair, Bara and Abdulrahman. Thank you, Tarek, for your unflagging support and limitless patience and for taking care of our new born son while I was busy with my thesis work. Thank you, my children, for your endless love, may be one day you will read this expression of appreciation for your tolerance and patience during my PhD study.

Finally, I would like to express my sincere thanks to the Libyan Ministry of Education and University of Benghazi, in Libya, for fully funding my PhD study.

Abstract

Increasingly, titanium is being used as an implantable material to make best use of its ability to integrate with bone. The replacement of missing teeth is likely the most widespread use of this technology but there is an increasing number of uses in orthopaedics and audiology. One of the challenges with this technique is being able to assess whether the bone-titanium interface is intact or is being subject to breakdown. Currently there is not a reliable and sensitive instrument able to monitor changes in bone-titanium interface.

This study sought to develop a reliable and simple-to-use test for monitoring osseointegration using dental implants as a model system with an approach that would allow early detection of compromise to the bone to implant interface. A series of systematic investigations were conducted to examine the reliability of the acoustic emission technique (AE) for measuring changes in the osseointegration of dental implants using an *in vitro* model system. The model system involved dental implants installed into bovine rib bones with models for; primary stability, partial and full osseointegration, and degraded osseointegrated interfaces.

The AE (a high-frequency ultrasonic wave) was produced by a simple source and was injected into the abutment of the implant. The transmitted energy was measured on the surface of the rib bone using a proprietary sensor. Some energy is lost at the implant-bone interface, but also in transmission along and through the bone.

The effect of bone micro- and macro-structure on acoustic transmission through and along bone has been measured in the primary stability model and a quantitative relationship developed to allow this patient-specific aspect to be taken into account in a clinical situation.

The primary stability model simply involved installing the implant using the normal surgical procedure. For secondary stability, glass ionomer cement was

used as a model interfacial material giving partial and full coverage. It has been found that the transmitted energy could distinguish between primary stability and partial and full integration.

Finally, to gauge how effective the acoustic emission technique could be in detecting early changes in the marginal bone around osseointegrated implants, simulated circumferential and vertical peri-implant bone defects of various vertical and circumferential extent were tested. It was found that the acoustic energy could effectively detect small changes in marginal bone level around osseointegrated implants. Changes in transmission of the AE signal were able to show both circumferential and narrow vertical bone defects including the most coronal 1 mm of the marginal bone.

These findings suggest a role for AE in monitoring the development of osseointegration in the weeks following implant placement and could be coupled with an assessment of bone density on an individual patient basis. The technique could also have a potential application in the early diagnosis of the peri-implantitis in the oral environment or other forms of loss of integration when used elsewhere in the body.

These findings are promising, although a number of practical issues need to be resolved before the technique can be validated in the clinical setting. Whereas the dental application is a useful model system, a clinical validation could lead to more general application in cases of monitoring bone-implant integration.

Lay summary

Dental implants are generally considered give good functional replacement for missing teeth, based on a metal screw which is driven into the jaw-bone to which a crown is attached after a period of healing.

A successful implant requires good bone to implant contact (stability), which is achieved by bone tissue growing and mineralizing onto the surface of implant following its installation during the healing period. Any subsequent breakdown in the boundary of the bone-implant contact can compromise the stability, as increased mobility of the implant may eventually lead to failure of the treatment and loss of the implant. Therefore, maintenance of health and integrity of the interface is essential for long-term implant success / function.

The methods currently used for monitoring stability suffer from a number of limitations and there is a need for a sensitive, accurate and easily used method which can offer early detection of compromised stability.

This study assessed the reliability of a novel technique, based on sound transmission, in monitoring bone-implant contact all the way from installation to monitoring for degradation after stability is established. The basic principle of this technique is to generate a controlled amount of high frequency sound waves from an impulsive source and couple them into the implant. The amount of the wave energy transmitted to a sensor mounted on the patient's face is measured, the higher this energy the better the interface.

A series of systematic investigations were conducted to test whether this technique can recognise the initial development of bone-implant contact and whether it is sensitive to any changes due to loss of the contact. A standard amount of sound was injected into implants installed in bovine bone models with different degrees of bone to implant integration. The mount of the energy transmitted through the bone-implant interface and bone was recorded by a sensor mounted on the bone surface.

The results showed that the more contact there was between implant and bone the more transmission was recorded. Moreover, the transmission decreased as the parts of the contact were removed. Furthermore, stronger (less porous) bone was found to transmit more energy to the surface. This indicates that this technique, with appropriate clinical validation, could be a useful tool for monitoring implant integration and implant stability and may also have a role in monitoring bone health in the jaw.

Planned publications

The following publications planned on the thesis work:

1. **Patient- specific aspects of acoustic emission transmission along and through bone in primary stability model**

This would be an engineering paper, most probably submitted to Proceedings of IMechE, Journal of Engineering in Medicine, where earlier work by Ossi et al. (2011, 2013) has already been published.

Draft Abstract: The effect of bone micro- and macro-structure on acoustic transmission through and along bone has been measured in the primary stability model and a quantitative relationship developed to allow this patient-specific aspect to be taken into account in a clinical situation. A titanium dental implant was tightly screwed in a fresh bovine rib bone, in primary stability configuration. Pulses of acoustic energy were generated on the abutment and collected by two sensors mounted on the bone surface; one adjacent to the implant (measuring only through-bone transmission) and one placed at various axial positions along the bone (measuring through-bone and along-bone transmission). A detailed microstructural analysis was performed for a series of histological sections of bone at each of the sensor positions and between the positions in order to assess the structure of the bone both across and along the bone sample. Strong attenuation was observed for AE signals travelling along bone and the degree of attenuation was influenced by the underlying microstructure and density of bone.

2. **Acoustic monitoring of dental implant osseointegration: an *ex vivo* animal study**

This paper could be configured for a dental audience or for an engineering audience. It is likely that it would be trailed at appropriate conferences to gather peer feedback prior to archival journal submission.

Draft Abstract: The objective of this study was to assess the potential of AE to monitor the development of osseointegration in dental implants. Three different

degrees of bone-implant contact (primary stability, partial integration and full integration) were simulated to receive pulses of acoustic energy generated on the surface of the attached abutment. The energy was collected by a sensor placed on the side of the bone, adjacent to the implant position. The results showed a positive correlation between the amount of simulated bone-implant contact and proportion of acoustic emission energy transmitted from a standard AE source to a sensor placed on the adjacent surface of the bone. These findings demonstrate that monitoring changes in acoustic emission transmission during the implant healing phase may provide valuable information on the progress of osseointegration.

3. Reliability of acoustic emission method in the assessment of various peri-implant bone loss of dental implant in bovine bone.

This paper could be configured for a dental audience or for an engineering audience. It is likely that it would be trailed at appropriate conferences to gather peer feedback prior to archival journal submission.

Draft Abstract: The aim of this study was to assess whether AE transmission could be used to monitor peri-implant marginal bone loss of osseointegrated implants. Simulated circumferential and vertical peri-implant bone defects of various vertical and circumferential extent were tested. Pulses of acoustic energy generated on the surface of the attached abutment and collected by a sensor placed on the side of the bone, adjacent to the implant position. The results showed that the transmitted energy can effectively detect small changes in the marginal bone around osseointegrated implants. Circumferential or narrow vertical bone defects were clearly detectible for the most coronal 1 mm of the marginal bone. This could have implications for the early diagnosis of peri-implantitis, the main cause of failure of dental implants.

Table of contents

List of Figures

List of Tables

List of Abbreviations

AE	Acoustic emission
AR	Aspect ratio
BIC	Bone-implant contact
Canc VF	Cancellous bone volume fraction
CBCT	Cone beam computed tomography
Cort W	Cortical width
CUS	Conventional ultrasound
FD	Fractal dimension
FI	Full integration
GIC	Glass ionomer cement
Hb A1c	Glycosylated haemoglobin
ISQ	Implant stability quotient
LS	Longitudinal section
PI	Partial integration
PIT	Peak insertion torque
PLB	Pencil lead break
PS	Primary stability
PTV	Periotest value
RFA	Resonance frequency analysis
RTT	Reverse torque test
SLA	Sandblasting large-grit plus acid-etching
Tb VF	Trabecular volume fraction
TPS	Titanium plasma-spraying
TS	Transverse section

Glossary of specialist biomedical/dental and engineering terms

Acoustic emission (AE): elastic waves generated by the rapid release of energy from sources within a material.

Acoustic impedance: the resistance of a material to the propagation of ultrasound waves.

Amplitude: the height of a voltage peak in an AE signal waveform.

Attenuation: loss of amplitude with distance as an AE wave travels through the test structure.

Bio-cortical stabilization: an approach to increase implant stability in low quality bone by engaging two layers of cortical bone.

Bone density: the amount of mineral content per unit volume of bone.

Bone remodelling: the process by which bone is renewed to maintain bone strength and mineral homeostasis.

Buccal: the surface (e.g. of teeth or gums) that faces the inner cheek.

Burst emission: discrete AE signals generated by an individual event, such as a pencil lead break.

Cancellous bone: a spongy and porous structure formed by a network of bone trabeculae surrounding the bone marrow compartments.

Continuous emission: AE generated by successive emission events from one or many sources, such as gas jet.

Compromised integration: a model configuration hypothesized in this study to refer to the disintegration in the established osseointegration of the dental implant.

Cortical bone: a dense and solid bone formed around the outer part of the bone and surrounding a porous core (cancellous bone).

Demineralization: a reduced mineral content in bone tissue.

Full and Partial integration: model configurations referring to the level/degree of osseointegration hypothesized in this study to simulate high and low amounts of bone-implant contact, respectively.

Implant abutment: a connecting piece that joins a prosthesis (e.g. crown) to an implant.

Lingual: the surface (e.g. of teeth or gums) that faces the tongue.

Longitudinal clinical study: a research method/design in which repeated observations are performed on the same subject(s) over a period of time.

Osseointegration: direct structural and functional connection between ordered living bone and the surface of a load-carrying implant.

Osteotomy: the procedure of bone drilling to prepare implant site.

Peri-implantitis: a plaque-associated inflammatory process involving tissues around dental implants, characterised by a subsequent progressive bone loss.

Primary stability: absence of implant mobility at the time of placement, attained by the screwed mechanical engagement of the implant fixture with the surrounding bone.

Quantity and quality of bone: the amount of cortical and trabecular bone and their topographical relationship in the site of implant placement.

Secondary stability: biological fixation of implant into the surrounding bone as a result of bone formation and remodelling at implant-bone interface (Osseointegration).

Trabecula: an individual structural element of cancellous bone tissue, whether plate-like or rod-like in form.

Chapter 1
Introduction

1.1 Research background

Titanium is the most popular implant material in medicine and dentistry due to its inherent ability to tightly integrate into bone, a process known as “osseointegration”. In dentistry, titanium implants are now the established approach for rehabilitation of partial and complete edentulism, supported by the high success rates indicated by long-term clinical data. The key factor in dental implant success is the establishment and maintenance of osseointegration (Albrektsson and Zarb, 1993). Brånemark et al. (1977) defined osseointegration as “a direct structural and functional connection between ordered living bone and the surface of a load-carrying implant” which can be observed using light microscopy. Several parameters have been suggested for assessing bone-implant integration, and peri-implant marginal bone condition has been reported as the main determinant of the treatment outcomes (Albrektsson et al., 2012, Dias et al., 2014, Rakic et al., 2018, Carrasco-García et al., 2019).

Monitoring bone-implant contact quantitatively during the early stages of osseointegration and, later, at follow-up examinations is valuable to assure long-term function. A number of techniques, such as radiography, Periotest™, and resonance frequency analysis, have been introduced for this purpose. However, these technologies have limitations in diagnosing compromised implants which has prevented them from gaining universal acceptance as standardized diagnostic tools for long-term clinical follow-up, (Table 6.1). For this reason, there is a need to develop a sensitive, clinically deployable methodology for early diagnosis and detection of compromised implants or implants on a path to failure.

Acoustic emission (AE) transmission is a non-invasive test that has been recently suggested to address some of the existing problems in monitoring implant stability. The AE technique is extensively used for condition monitoring

in engineering. Used conventionally (passive ultrasound), sensors placed on the surface if a structure or container can be used to detect the ultrasound emanating from such events as fluid cavitation and crack growth. In the medical field, the AE has been for such diverse applications as joint crepitus monitoring to orthopaedic surgery. Recently, acoustic emission has been suggested as an active ultrasound technique, where the ultrasound is injected into a dental implant and the amount of energy transmitted through the implant and across the bone-implant interface to a sensor mounted on the bone surface has been demonstrated to measure primary stability. However, the sensitivity of the technique to changes in the bone-implant interface either during healing or function has yet to be demonstrated.

In this PhD study, the active ultrasound approach to AE inspection is applied systematically to assess its potential to evaluate bone-implant integration in the clinic. A controlled amount of ultrasonic energy using an artificial standard AE source such as a pencil lead break (Hsu-Nielsen source) is introduced into implants installed with varying degrees of simulated osseointgration and stability into a bovine bone model. The amount of the transmitted energy is recorded using a sensor mounted on the surface of the bone. The raw AE signal is then processed and analysed in order to extract parameters that may relate to certain properties of bone-implant interface. This would help in understanding the interface behaviour in the different stages after implant placement and allow an early detection of compromise to the integration of the implant to the bone.

1.2 Aim and objectives of the study

The primary aim of this study is to evaluate the reliability of acoustic emission (AE) technique in monitoring osseointegration of dental implants using an *in vitro* model system.

In order to address this aim, the following objectives were designed:

1. Study the effect of bone microstructure on AE transmission through a primary stability model.

2. Investigate the influence of simulated osseointegration and secondary stability on the acoustic transmission.
3. Examine the potential of acoustic energy for diagnosing peri-implant bone loss of a simulated osseointegrated implant.

1.3 Research methodology

Initially a number of preliminary assessments were carried out to establish a common experimental protocol for configuring the systematic investigations. These tests provided the opportunity to establish some practical issues in order to reduce the variability within the systematic experiments.

Once the experimental setup and basic protocol were established, the initial phase of the systematic investigations focused on developing a basic understanding for the acoustic signal transmission in bone using a primary stability model of dental implant in bovine rib. This provided insight into the relationship between bone microstructure, bone-implant interface and acoustic transmission through and along bone. The second series of experiments involved establishing an osseointegration model of dental implant in bovine bone and testing the influence of various degrees of bone-implant integration (primary stability, partial and full osseointegration) on acoustic transmission.

Having established the correlation between AE and the degree of bone-implant contact, the final stage of the systematic investigations was set to assess the potential of AE in detecting early changes in the marginal bone surrounding the osseointegrated implants. Simulated circumferential and vertical marginal bone defects of various vertical and circumferential extent were created around the osseointegrated implants and systematically tested for their influence on the AE transmission.

1.4 Thesis outline

The thesis is structured in the following chapters:

Chapter 1: Introduction. This chapter describes the background which motivated the research into developing a diagnostic method for monitoring

dental implant stability using acoustic emission transmission from a simulated source.

Chapter 2: reviews the relevant current literature, which is divided into five technical topics. The first topic is concerned with clinical aspects of implant stability and the development of osseointegration. The second topic is also clinical, dealing with peri-implant bone loss with an overview of peri-implantitis and the predisposing factors. The third topic summarises the criteria for implant success and factors affecting success and failure. The fourth technical topic briefly reviews the current methods used to evaluate implant stability and osseointegration and is followed by a more detailed review of the acoustic emission technique. The final section of this chapter identifies the thesis topic, including a statement of the research problem.

Chapter 3: Materials and Methods: This chapter presents the experimental apparatus, procedures and analytical approaches used to conduct the work. The chapter is organised as follows. The first section introduces the experimental techniques, apparatus and materials used for all experiments. The second section presents the experimental procedures including the preliminary assessment tests and the systematic investigations collected into three series of experiments. The third section presents the analytical methods used for processing and analysing the AE and micro-graphical data and examining the correlations between the systematic parameters.

Chapter 4: Results and analysis part 1: Preliminary assessments. This chapter presents the results of the preliminary assessments which were carried out to establish a number of practical issues and to set-up the experimental protocol for the systematic investigations.

Chapter 5: Results and analysis part 2: Systematic experiments. This part presents, analyses and summarises the results of the systematic experiments which were conducted in three stages to investigate the effect of bone microstructure, simulated osseointegration and peri-implant bone defects, respectively, on AE transmission.

Chapter 6: Discussion. This chapter discusses and interprets the results of the experiments under the given conditions of the study. It is structured as follows: First, suitability of the models used to represent the clinical application. Second, reproducibility of the histological and acoustic emission measurements. Third, comparison of the proposed technique with existing methods. A final section discusses the clinical implications of the study.

Chapter 7: Conclusions and recommendations for future research. This chapter summarises the key findings of the study and presents suggestions for future research.

1.5 Contribution to knowledge

This thesis contributes to the current knowledge of monitoring osseointegration of titanium implants. It examines a novel, non-invasive method based on ultrasound transmission (Acoustic transmission). It has been found that the method has promise for monitoring dental implant stability, with transmission being affected by a number of aspects of micro- and macro-structure. The major finding of this thesis is a basic understanding of the relationship between various interfaces and acoustic transmission in dental implant model system. These interfaces include those within the bone and those between the implant and the bone and a quantitative assessment has been made of attenuation in terms of microstructural measures and the sizes of various interface defects. The work has the potential to contribute to the development of the technique as an efficient, reliable, and readily deployable alternative for assessing and monitoring bone-implant integration in dental and medical applications.

Chapter 2
Literature Review

This review covers five essential topics relevant to the thesis. The first of these is the concept of implant stability as it applies to dental implants. Next, the conditions that can lead to peri-implant bone loss are reviewed. The third topic is about what makes a successful implant installation and the factors affecting implant success and failure. The fourth topic reviews the methods used to evaluate implant stability and osseointegration, and, finally, the acoustic emission technique is discussed in some detail, focusing on its medical applications. The chapter concludes with a statement of the problem to be addressed in the thesis, set against the background of the existing literature.

2.1 Implant stability

Implant stability is fundamental for successful implant treatment outcomes. It is achieved in two different stages: primary stability at implant installation, and secondary stability which is accomplished during a healing period (Sennerby and Roos, 1998). Secure primary stability has been shown to enhance successful osseointegration (Davies, 1998). This success, however, is influenced by several factors related to the patient (bone quality and quantity), the implant (its length, diameter and design), and the operator (surgical technique) (Meredith, 1998). Secondary stability (biological stability) is established as a result of bone formation and remodelling at the implant-bone interface (Albrektsson et al., 1981). Primary stability, bone remodelling, and implant surface characteristics are well recognised as important parameters affecting the biological stability of osseointegrated implants (Mavrogenis et al., 2009).

2.1.1 Primary stability

Primary implant stability is an essential prerequisite to achieve optimal osseous fixation for establishing successful osseointegration (Javed et al.,

2013), particularly when early or immediate loading is adopted as a treatment modality (Javed and Romanos, 2010, Tettamanti et al., 2017). Primary stability is the absence of implant mobility after placement, and it is attained at the time of implant insertion by the mechanical engagement of the implant fixture with the surrounding bone (mostly cortical bone) (Romanos, 2009). An adequate initial stabilization and limiting micro-movements to a certain level during surgery are vital for undisturbed healing to establish firm bone-implant contact, and to avoid fibrous tissue formation at the interface between bone and implant (Gao et al., 2012).

Primary stability of dental implants is influenced by several factors, including: quality and quantity of bone at the implant site (Alghamdi et al., 2011), the design and morphology of the implant (Elias et al., 2012, Gehrke et al., 2015, Da Costa Valente et al., 2016) and the surgical technique (Bilhan et al., 2010).

2.1.1.1 Bone quantity and quality

Bone quantity and quality are normally related to the amount of cortical and trabecular bone and their topographic relationship in the region where the osteotomy site is prepared (Javed et al., 2013). Different areas of the jawbone exhibit varying levels of bone density; for example, high density bone is commonly found in the anterior mandible, the premaxilla and posterior mandible, whereas low density bone usually characterises the posterior maxilla (Misch, 2015). This variation can potentially influence the primary stability of the implant. Therefore, there are two main issues in evaluating bone tissues for implant treatment: firstly, to evaluate the sufficiency of the bone tissues at the osteotomy site, and secondly to help in predication of treatment outcomes.

Different classification systems and protocols have been proposed for evaluating bone tissue characteristics (Misch, 1989, Lekholm et al., 1994, Trisi and Rao, 1999). However, Lekholm & Zarb's (1985) classification is the most commonly applied system for bone tissue assessment in dental treatment (Ribeiro-Rotta et al., 2011). This system initially relied on radiographic examination to provide a subjective qualitative and quantitative description of

the bone tissue. Thereafter, it has been modified to include the tactile perception of bone quality during drilling.

Lekholm & Zarb defined 4 qualities according to the morphology and proportion of both cortical and trabecular bone, Figure 2.1:

Type I: Homogenous cortical bone throughout the entire jaw;

Type II: Thick cortical bone with a dense cancellous bone;

Type III: Thin cortical bone surrounding a core of dense cancellous bone;

Type IV: Extremely thin cortical bone with low density cancellous bone.

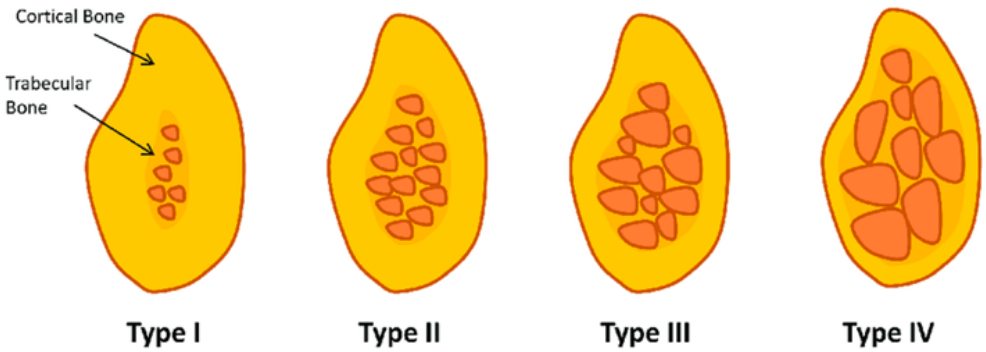

Figure 2.1: Lekholm & Zarb Classification (Alghamdi, 2018)

An alternative classification based on the macroscopic densities of cortical and trabecular bone was proposed by Misch (1989). The classification ranges from type D1 to type D4, considering both dense and porous cortical bone and both coarse and fine trabecular bone. D1 bone is homogenous dense cortical bone and is usually present in the anterior mandible. D2 bone has dense to porous cortical bone surrounding coarse trabecular bone, and it is found in either jaw but most commonly in the mandible. D3 consists of a thin porous cortical crest and lateral plates, with fine trabecular bone, and is often present in the maxilla and posterior mandible. D4 comprises mostly fine trabecular bone and is frequently located in the posterior maxilla (Figure 2.2), (Misch, 1989).

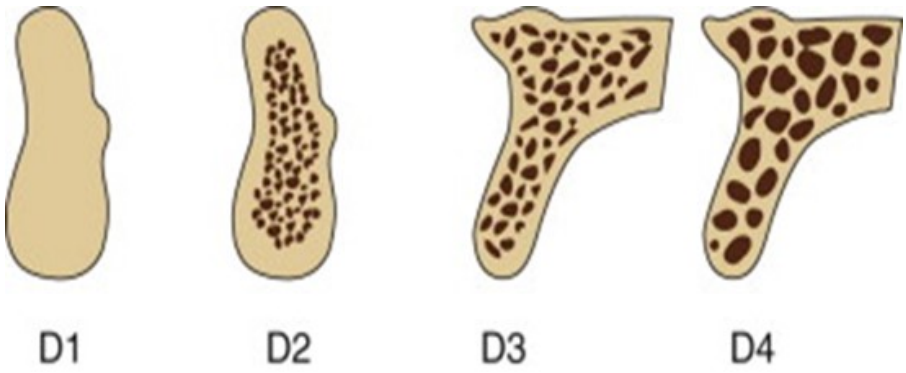

Figure 2.2: Misch Classification (Misch, 1989)

Trisi and Rao (1999) have classified bone tissue rather more simply into dense, normal and soft bone.

Insufficient quality and quantity of the regional bone have been associated with increased risk of implant failure, as either may cause progressive bone loss or impair osteogenesis (Herrmann et al., 2005). Numerous studies have reported that the primary stability of dental implants is positively correlated with bone density of the osteotomy site (Merheb et al., 2010, Marquezan et al., 2012, Salimov et al., 2014). Poor bone mineralization is commonly characterised as low-density bone, which is also referred to as soft bone (Trisi and Rao, 1999), and achieving optimum primary stability in such bone is difficult and may be associated with higher failure rates (Merheb et al., 2015).

It has been reported that the stability of the implant at the time of installation depends mainly on the thickness of the cortical bone (Mantovani et al., 2018), whereas the amount of trabecular bone has no significant effect on the stability at the time of implant placement (De Oliveira et al., 2012) but is of significant importance for the subsequent peri-implant healing (Rozé et al., 2009). Tabassum et al. (2010) reported that a thickness of 2 mm of cortical layer is crucial to establish primary stability. However, it was found in a study conducted by Merheb et al. (2010) to explore the correlation between the primary stability and different bone parameters, that primary stability is more likely to be influenced by both the cortical bone thickness and cancellous bone density at the osteotomy site. These findings are further supported by Pan et

al. (2019). Huang et al. (2010) reported that there is a strong correlation between elastic modulus of trabecular bone and primary stability values measured by resonance frequency analysis, Periotest and insertion torque, where the stability reduced for an implant placed in trabecular bone with osteoporotic structure. In addition, Kang et al. (2016) investigated the correlation between the primary stability and the microstructural parameters of cancellous bone measured by cone beam computed tomography (CBCT) and micro-CT. Their results demonstrated that a high-density bone with well-connected thick trabeculae and small marrow spaces shows high stability.

2.1.1.2 Implant design and morphology

Implant design refers to “the three-dimensional structure of an implant” including all elements and features that characterise it (Javed et al., 2013). The initial implant stability is influenced by the design (shape, diameter, length) and surface characteristics of the implant.

Implant design

It has been indicated that the implant design plays an important role in obtaining primary stability (Bhandari, 2019). Dental implants were originally developed in a parallel design (cylindrical symmetry), but this design has been shown not to be applicable to most clinical situations (Javed et al., 2013). Therefore, different implant designs have been developed to deal with the different clinical conditions. The effect of various implant designs on the primary implant stability has been examined and compared by a number of authors. Sánchez-Siles et al. (2019) compared the primary stability of tapered and cylindrical implants inserted in low density bone, and they demonstrated that the tapered implants had better initial stability compared with the parallel sided design. These results are further supported by Sugiura et al. (2019) who also reported higher stability for tapered implants than for parallel sided ones which were inserted in low density bone. Therefore, one of the suggested approaches to improve the primary stability in poor quality bone is to use tapered implants which provide a controlled level of compression in the cortical bone beneficial for poor bone implant sites.

Surface characteristics

Surface characteristics of implants have also been shown to affect the primary stability. Many different implant surface treatments have been developed with the objectives of increasing the degree of primary stability and enhancing the rate and quality of osseointegration (Le Guéhennec et al., 2007, Coelho et al., 2011). Rough surfaces have been reported to influence the primary stability positively as they provide a larger surface area and enhance mechanical interlocking to the surrounding bone (Albrektsson and Wennerberg, 2004). Dos Santos et al. (2011) compared the effect of 3 different surface finishes (machined, acid-etched, and anodized) of dental implants on the primary stability. The results showed higher primary stability (measured by insertion torque value) for implants subjected to surface treatment than that for the machined ones, which they attributed to the greater surface roughness and greater friction coefficient, which consequently required a higher insertion torque than the machined implants.

Threaded implants have generally been recommended specifically for immediate loading, as they have been shown to maintain the primary stability of the implant by minimizing micro-motion during function (Hall et al., 2005). Furthermore, they increase the surface area of the implant which consequently promotes a higher degree of bone-implant contact and enhances the secondary stability (Vandamme et al., 2007). The thread geometry (thread shape, pitch, width and depth) plays a critical role in the stress distribution at the bone-implant interface, and determines the implant stability (Oswal et al., 2016). Screw shaped implants are available in various thread shapes, such as square, v- shape, buttress and reverse buttress. Findings from studies using finite element analysis to analyse the effect of thread shapes revealed that the square thread profile exhibits the most acceptable micro-motion values and provides the best primary stability in the immediate loading situation (Chang et al., 2012).

Thread pitch “the number of threads per unit length” is another geometric feature which can significantly affect the initial insertion of the implant and determine the amount of bone-implant integration (Misch et al., 2006). A

review by Ryu et al. (2014) indicated that implants with smaller pitch produce more favourable load distribution and enhance initial anchorage by increasing the functional contact area between the implant and the surrounding bone. This may be significant for maximizing the stability of shorter implants in reduced density bone where the primary stability is a concern (Misch et al., 2006). However, there are variations in the optimal values of the thread pitch between different thread designs. Values of 1.2 mm, 1.6 mm, 0.8 mm are recommended in several studies for triangular, trapezoidal, and v-shaped threads respectively as optimal thread pitch levels which create better stress transfer and enhance the mechanical anchorage of implants (Kong et al., 2006, Lan et al., 2011).

Both thread depth and width have also been shown to affect implant insertion and surface area (Misch et al., 2008). Greater thread depth increases the amount of bone to implant contact which consequently may enhance the initial stabilization, particularly in low density bone (Falco et al., 2018). Common findings from two studies using finite element analysis (FEA) have revealed that the thread depth plays a more significant role in transferring loads to bone-implant interface than the thread width (Kong et al., 2006, Ao et al., 2010) and similar levels were also obtained from these studies which ranges from 0.18 – 0.3 mm and 0.34 – 0.5 mm for thread depth and width respectively. However, these values need to be clinically confirmed to establish a general guidelines for the optimal levels.

Implant length and diameter

The length and diameter of a dental implant also has an influence on its primary stability, increasing with increasing implant length and diameter (Obagbemiro et al., 2018). However, Barikani et al. (2014), in their study to evaluate the effect of implant characteristics on the primary stability in different bone qualities, showed that the optimum increase in the diameter and length of the implant should be considered to enhance the initial stability in cases of insufficient bone density. Their results also revealed that there is no significant effect on the stability for long implants placed in a high bone quality bed. Similar findings were obtained in the finite element analysis performed by

Winter et al. (2010) and the *in vitro* study conducted by Lachmann et al. (2011), showed a positive relationship between the primary stability and implant lengths in poor quality bone. On the other hand, Östman et al. (2006) argued that increasing length of implants may jeopardize primary stability due to exposure of the bed to more heat, generated during longer bone drilling.

Elsewhere, it has been reported that the implant diameter plays a more important role in achieving high primary stability than implant length and this has been explained by the fact that the highest loads are concentrating in the cortical area rather than dissipating along the bone-implant interface (Bilhan et al., 2010).

Gómez-Polo et al. (2016) compared the effect of the diameter and length in an *in vivo* study of primary stability and found that the diameter had a greater influence than length. Using implants with larger diameter in areas of low bone density has been proposed to enhance primary stability as it maximizes the bone-implant contact (BIC), which increases the mechanical resistance to torque loads (Hsu et al., 2017). Winkler et al. (2000) found that smaller implants (less than 4 mm) present low primary stability, although others have reported that implants with smaller diameter may provide adequate primary stability in poor quality bone (Degidi et al., 2009).

2.1.1.3 Surgical techniques

Surgical technique is one of the critical factors in establishing primary stability. Depending on bone properties at the prepared implant site, an ideal surgical protocol should be adopted to establish rigid, initial stabilization and to promote the healing process (Javed and Romanos, 2010). Different surgical protocols have been developed and introduced to enhance the primary stabilisation of implants installed in poor quality bone, which is found, for example, in the posterior maxilla of patients with osteoporosis or those who have undergone radiation therapy. A “Bone condensing” technique has been successfully applied in many clinical studies, demonstrating a positive impact on the primary stability (Marković et al., 2014). This technique, which was first used by Summers (1994), involves the use of osteotomes of increasing diameter to

compress the peri-implant bone laterally and apically in an attempt to increase its density.

Other studies advocate applying the undersized drilling technique (Turkyilmaz and McGlumphy, 2008, Alghamdi et al., 2011), in which, the implant is installed in an undersized bed. Screwing the implant in an undersized bed results in compression of the surrounding bone, increases its density and thereby maximises the stability. However, Degidi et al. (2009) have argued that reducing the implant bed in respect to the implant diameter by more than 10% may jeopardise the primary stability. A “bone expander” technique has also been reported to provide sufficient stability in the posterior maxilla (Petrov et al., 2014).

It has also been demonstrated that high success rates with immediate loading of dental implants are associated with a higher primary stability (Crespi et al., 2007, Crespi et al., 2008). In addition to reducing the treatment period, immediate loading with a flapless surgery procedure has also been demonstrated to improve the initial stability compared with conventional flap protocol (Merli et al., 2012). It has been advocated that the insertion torque can be a determinant for the primary stability, accepting values of 32, 35, 40 Ncm and above as a threshold for immediate loading (Srisuthep, 2019).

2.1.2 Osseointegration

Osseointegration is a critical and primary requirement for implant healing and secondary stability. The concept of osseointegration was first introduced by Brånemark and defined as “a direct structural and functional connection between ordered living bone and the surface of a load-carrying implant” (Brånemark et al., 1977). Albrektsson et al. (1981) further evidenced the occurrence of a direct bone-implant connection without intervening fibrous tissue under an electron microscope. Figure 2.3 shows osseointegration of a dental implant under light microscope (Misch, 2015).

Figure 2.3: Osseointegration, under light microscope (Misch, 2015)

Primary implant stability is fundamental to attaining bone-implant integration. However, this is only a mechanical anchorage and ultimately requires biological fixation. Immediately following placement, the implant is secured by mechanical friction of the threads with the surrounding host bone (primary stability) which limits the micro-movement of the implant during the early stages of healing. Subsequently, an increase in the implant stability results from bone formation and remodelling at the bone-implant interface (biological stability).

2.1.2.1 Biology of osseointegration

Peri-implant bone healing consists of a sequence of biological events that take place at the interface between bone and implant which result in establishment of osseointegration.

Following the placement of an implant, the mechanical engagement of the implant threads with the surrounding bone provides an initial stability to the fixture into the bone bed during the early stages of healing. However, the long-term maintenance of the dental implant necessitates replacing the primary stability with biological attachment of the implant body with the surrounding tissues. Healing of oral implant into alveolar bone involves a cascade of biological processes (Albrektsson and Jacobsson, 1987): clot formation,

mesenchymal tissues development, recruitment- proliferation-differentiation of osteoblast, collagenous matrix deposition, mineralisation (woven bone formation) and transformation of woven bone into lamellar bone.

Davies (1998) categorizes the mechanisms of peri-implant bone healing into three distinct biological phases: osteoconduction, osteoinduction (*de novo* bone formation) and bone remodelling. The fibrin matrix which forms after surgical placement of the implant in the space between the implant surface and the surrounding bone bed, acts as a scaffold (osteoconduction) for the differentiated osteogenic cells to migrate from the endosteal or periosteal surface to the implant surface. Differentiated osteoblasts secrete a collagen-free organic matrix which provides the nuclei for mineralisation and development of woven bone (*de novo* bone formation) at the implant surface, which represents the first phase of osseointegration. Woven bone is then progressively replaced in response to the physical strains of loading with lamellar bone (bone remodelling).

2.1.2.2 Effect of implant surface on osseointegration

Implant surface topography has a significant influence on osseointegration, especially during the osteoconduction and osteoinduction phases. It has been widely reported that rough implants encourage stronger bone response than machined implants (Feller et al., 2014, Ogle, 2015, Rupp et al., 2018). It has been demonstrated that roughness can stimulate the bone healing process by maximizing the available surface area for fibrin adherence which is essential for helping the migrating differentiated osteogenic cells to reach a surface and deposit bone (Davies, 1998).

Various surface modification techniques involving mechanical treatment, chemical treatment, coating methods or combinations of these methods have been applied with the aim of improving the biomechanical properties of the titanium surface to enhance bone integration and long-term stability. For example, etched and dual- etched surfaces have been shown to exhibit rapid bone formation due to enhanced osteoconduction and the promotion of osteogenic migration through the fibrin scaffold which is entangled into the

micro-pores that have been created on the surface by the etching. Several comparative studies between machined and dual etched surfaces have showed that the latter presents a greater resistance to the reverse torque (Le Guéhennec et al., 2007) and higher bone-implant integration (Bugea et al., 2008).

Another treatment for enhancing osseointegration is plasma spraying which is commonly used to coat implants with hydroxyapatite in order to create osteoconductive surfaces which promote cell adhesion, differentiation and synthesis of bone tissues. Cheng et al. (2013) reported enhanced bone formation on hydroxyapatite-coated surfaces compared with uncoated and sandblasted surfaces. Another comparative study reported that plasma sprayed surfaces had higher surface roughness than acid etched or grit blasted ones, providing a greater interlocking connection between bone and implant (Knabe et al., 2002). However, coating loosening and implant failure have been reported in some cases (Le Guéhennec et al., 2007). In another study, blasting and the SLA (Sandblasting plus acid-etching) processes, used to increase surface roughness and surface area, were found to be useful for improving bone integration (Jemt et al., 2015).

Several reviews have been conducted to evaluate the efficacy of surface modification methods in stimulating peri-implant bone formation and enhancing osseointegration (Alla et al., 2011, Smeets et al., 2016, Rupp et al., 2018). However, the exact role of surface alterations on osseointegration remains poorly understood, and so the quantitative surface characteristics required for optimum osseointegration have not yet been determined (Barfeie et al., 2015).

2.2 Implant stability and peri-implant bone loss

The success of a dental implant depends not only on the integration between implant and bone, but also on the integration being maintained over time. Changes in the marginal bone level and loss of osseointegration are significant factors in implant failure (Esposito et al., 1998), and such peri-implant marginal bone loss can be categorized as early or progressive.

2.2.1 Early marginal bone loss

Early marginal bone loss can be observed radiographically during the first year of function (prosthesis loading). It is thought to be an adaptive reaction to healing and loading with little effect on implant stability nor is it an indicator of progressive bone loss (Pikner and Gröndahl, 2009). The quantitative measurement of early marginal bone loss was first carried out by Adell et al. (1981). In their 15-year follow-up study, the authors reported that the mean value of marginal bone loss was 1.2 mm during the healing stage and first year after loading, whereas only 0.1 mm was lost each year thereafter. Based on these findings, Albrektsson and Isidor (1994) suggested that a successful osseointegrated implant should demonstrate “less than 1.5 mm of marginal bone loss during the first year after loading and less than 0.2 mm annually thereafter”. These radiographic features were further modified by Wennström and Palmer (1999), who proposed that a maximum bone loss of 2 mm can be accepted for a 5-year period after loading.

2.2.2 Progressive peri-implant bone loss

Initial marginal bone loss around osseointegrated implant can be aggravated by several factors which may contribute to a progressive loss and, eventually, to implant failure (Albrektsson et al., 2014). Progressive bone loss beyond marginal bone level changes during the initial remodelling process after implant installation is usually diagnosed as peri-implantitis.

2.2.2.1 Definition and prevalence of peri-implantitis

Peri-implantitis is defined as “a plaque-associated inflammatory process involving tissues around dental implants and is characterized by a subsequent progressive bone loss” (Berglundh et al., 2018).

Peri-implantitis is a major complication of dental implant treatment and the primary cause of implant loss. In a recent systematic review to estimate the overall prevalence of the disease, peri-implantitis was found to affect approximately 18.5% of patients and 12.8% of implants (Rakic et al., 2018).

Infection has been suggested as the primary cause of peri-implantitis (Zitzmann and Berglundh, 2008). This is based on a postulate that implant and tooth are similar entities and can be infected by similar microbial pathogens (Canullo et al., 2016). Peri-implant inflammation has been mostly linked to gram-negative anaerobic bacteria similar to those causing periodontitis of teeth (Da Silva et al., 2014). Nevertheless, the specific microbial composition of the disease has not yet been consistently identified (Sahrmann et al., 2020). The main diagnostic parameters of peri-implantitis include bleeding on probing, increased peri-implant pocket depth (> 3 mm) and bone loss ranges between 1.8 and 3 mm (Aguilar-Salvatierra et al., 2016).

2.2.2.2 Risk factors of peri-implantitis

Although implant treatment presents high success rates, there are several risk factors which may inversely influence the predictability of the treatment and lead to peri-implant tissue inflammation, bone resorption, and inevitably to implant loss.

Experimental and clinical studies have determined a number of factors associated with the increased risk of peri-implantitis related bone loss, to include, poor oral hygiene, history of periodontitis, diabetes, smoking, residual cement, implant surface characteristics and occlusal overload (Rosen et al., 2013), elaborated in turn below.

Poor oral hygiene

The relationship between poor hygiene and peri-implantitis has been demonstrated (Salvi et al., 2012). Implant roughened surfaces can provide retentive niches for biofilm plaque which may provoke subgingival inflammation and lead, in uncontrolled cases, to a progressive bone loss (Al-Sabbagh and Bhavsar, 2015). Poor oral hygiene is associated with the progressive bone loss in smokers where they presented a higher risk of peri-implant bone loss than non- smokers who have similar levels of oral hygiene (Meyle et al., 2019).

The effect of a history of periodontitis

Presence or prior history of periodontal disease has been indicated in the literature as a predisposing condition for occurrence of peri-implant diseases and for increased risk of implant loss. Similarities in the microbiota of dental implants and teeth support the concept that peri-implant infection may be caused by periodontal microbial pathogens (Canullo et al., 2016).

Several reviews based on prospective and retrospective data have been undertaken to explore the correlation between the history of periodontitis and occurrence of peri-implant diseases, and also to examine the potential risk for peri-implantitis in periodontally compromised patients. Claudio et al. (2016) reviewed a number of prospective studies with a minimum follow-up period of 3 years. These studies compared the severity of peri-implantitis between periodontally compromised patients and healthy individuals. They reported that periodontally compromised patients have a higher susceptibility to peri-implant diseases than the healthy subjects. Their results were consistent with the findings from a systematic review and meta-analysis conducted by Chrcanovic et al. (2014b). Similarly, Ferreira et al. (2018) in a recent systematic review reported an increased risk of peri-implantitis in patients who diagnosed or had a history of periodontitis. Furthermore, it has been proven that there is transmission of periodontal pathogens from natural teeth to implants in partially edentulous patients (Quirynen et al., 2007). It has also been found that these microbiotas can persist in the oral cavity of completely edentulous patients with a previous history of periodontitis up to one year after tooth extraction (Fernandes et al., 2010).

Diabetes

Diabetes is a risk factor for peri-implantitis and implant loss (Monje et al., 2014, Renvert and Quirynen, 2015, Decker and Wang, 2020) due to impaired wound healing and increased susceptibility to infection (Okonkwo and Di Pietro, 2017). The association between poorly controlled diabetes and peri-implant inflammation has been investigated in many studies. For example, Aguilar-Salvatierra et al. (2016), in a prospective analysis, investigated the impact of different levels of glycosylated haemoglobin (Hb A1c) on peri-implant health

for a group of diabetics. The results indicated that the peri-implant values including pocket depth, bleeding on probing and marginal bone loss increased with increasing Hb A1c levels, and the impact became greater on immediately loaded implants. These findings were in line with a previous study (Gómez-Moreno et al., 2015) which also showed a proportional relation between marginal bone loss and glycosylated haemoglobin (HB A1c) levels among diabetics compared with nondiabetics.

In addition, a cross-sectional study by Daubert et al. (2015) to build a predictive model for peri-implant disease, found a significant association between the disease and diabetes in 26% of patients and in 16% of implants after a follow-up time of at least 11 years. However, it has been reported that the risk of peri-implantitis increases in diabetes in the long-term observation with no significance during the first years after implantation. A recent systematic review by Naujokat et al. (2016) has reported that well-controlled diabetes improves osseointegration and survival rates of implants, presenting success rates close to that of non-diabetics during the first 6 years, but the risk for peri-implant inflammation elevates later in a long-term observation up to 20 years.

Smoking habits

A significant association between smoking and peri-implantitis has been reported widely in the literature (Chrcanovic et al., 2015, Vervaeke et al., 2015, Pimentel et al., 2018, Decker and Wang, 2020). Clementini et al. (2014) published a systematic review with meta-analysis, including 13 studies, to examine the effect of smoking on peri-implant marginal bone changes. The meta-analysis reported a significant increase in peri-implant marginal bone loss (0.16 mm/ year) in smokers compared with non-smokers.

Furthermore, the clinical and microbiological parameters around osseointegrated implants have been shown to be adversely affected by smoking. Findings from a prospective cross-sectional study showed that smokers had poorer gingival and plaque indices and deeper pocket depth than non-smokers as well as increased proportion of periodontal pathogens in the subgingival microbiota (Ata-Ali et al., 2016). However, a previous study had reported that smoking

does not have any significant role in changing the microbiota of dental plaque, but most likely it alters the host's response to the bacterial plaque (Machuca et al., 2000). It has also been revealed that smoking has an adverse effect on the immunological characteristics and on the healing capacity of the periodontium by increasing the levels of interleukin-1β, interleukin-6 and interleukin-10 (Leite et al., 2019).

Excess cement

Retention of residual cement in peri-implant sulcus frequently associates with cemented-implant restorations (Wadhwani, 2015, Fiorellini et al., 2019), which has recently been linked to peri-implant tissue inflammation (Staubli et al., 2017). The reason for the inflammation is most likely attributed to microbial retention by the rough surface of the cement (Wilson Jr, 2009). The author also reported that up to 81% of the implants, which presented radiographic or clinical signs of peri-implantitis, had retained residual cement. These signs subsided in 74% of the involved sites upon removal of the cement remnants. Data from several literature reviews indicated that the presence of excess cement in the peri-implant sulcus contributes to peri-implant inflammation and progressive bone loss (Smeets et al., 2014, Quaranta et al., 2017).

It has also been reported that a history of periodontitis aggravates the role of excess cement in developing peri-implantitis. Linkevicius et al. (2013) examined the incidence of cement-induced peri-implantitis in two groups of patients with different periodontal health history. The retrospective analysis showed the presence of peri-implantitis signs in 100% of the periodontally compromised patients, while it was only 65% in patients with residual cement and no history of periodontitis. Similar conclusions were drawn in a systematic review conducted by Pesce et al. (2015). Although residual cement can adversely influence peri-implant health, crestal bone loss seems to be less around cemented-implant restorations compared with the screw-retained (Lemos et al., 2016).

Implant surface characteristics

Clinical and experimental research have proven that surface-modified implants provide enhanced bone integration compared with machined implants. However, many scientific analyses have reported the significant role of the roughened surfaces in occurrence of peri-implant disease by providing niches for bacterial colonization and biofilm formation (Carcuac et al., 2013, John et al., 2015).

Marrone et al. (2013) compared clinical and radiographic data of turned and rough implants of at least 5 years, standing for a group of Belgian patients, in order to determine the potential role of implant surface treatment in occurrence of peri-implantitits. They concluded that rough surfaces created by titanium plasma-spraying (TPS) have a higher peri-implantitis rate (36.1%) than machined surfaces (19.4%). Broader retrospective observations (up to 20 years) have reported higher marginal bone loss around moderately rough-surfaced implants (Donati et al., 2018) over the smooth-surfaced (Ibañez et al., 2016). These observations are consistent with the findings of a systematic literature review by Jordana et al. (2018) which reported that peri-implantitis rates increase with surface roughness, giving the highest rate (20%) for the very rough surfaces, produced by titanium plasma-spraying (TPS) with a surface roughness (Sa) of > 2 µm. However, their results for the implants with moderate surface roughness show relative variations in peri-implantitis rates, which they attributed to the variation in the roughness and to the method of measuring the roughness. The surfaces were created by sandblasting, sandblasting and acid-etching (SLA) or anodic oxidation had a surface roughness (Sa) of 1-2 µm. For these surfaces, the highest rates were observed with the surfaces obtained by the anodic oxidation (4.14%), whereas the mean peri-implantitis rates for sandblasted plus acid-etched and sandblasted surfaces were 3.41% and 2.38% respectively.

Occlusal overload

Occlusal overloading describes the situation where the functional load of an implant exceeds the capacity of the bone that supports the implant (Esposito et al., 1999). Occlusal overload may increase marginal bone loss around

osseointegrated implants in areas where peri-implant tissues are inflamed (Chambrone et al., 2010). The correlation between excessive occlusal load and marginal bone loss has been reported in many animal experimental studies, but their causative relationship has not been determined in humans (Isidor, 2006, Fu et al., 2012).

2.3 Implant success and failures

Although high success rate of dental implants is well documented, failures still occur. Each osseointegrated implant should, therefore, be tested against and fulfil all the established success criteria (Brunette et al., 2002).

2.3.1 Criteria of implant success

Over the past decades, implant success has been evaluated by different diagnostic criteria, Table 2.1.

The most widely accepted and referenced criteria were proposed by Albrektsson et al. (1986) to provide an evidence for clinical success of osseointegrated implants. These criteria consider the radiographic monitoring of peri-implant marginal bone level as an essential parameter for implant success. Although these criteria addressed most of possible essential parameters to measure implant success, some of them either are not supported by experimental evidences or not essential for implant success (Smith and Zarb, 1989).

New parameters have been introduced in attempt to establish a more comprehensive definition of the success criteria for implant and prosthesis evaluation. These include health status and appearance of peri-implant mucosa, prosthodontic characteristics and aesthetics and patient satisfaction (Annibali et al., 2012). However, still there is a difficulty in considering the importance of these parameters when compared with the osseointegration process which remains the fundamental baseline parameter in the assessment of implant treatment (Papaspyridakos et al., 2012).

Table 2.1: Main criteria of implant success in the literature

Success criteria	(Schnitman and Shulman, 1979)	(Albrektsson et al., 1986)	(Smith and Zarb, 1989)	(Albrektsson and Isidor, 1994)	(Wennström and Palmer, 1999)	(Schwartz-Arad et al., 2005)
Absence of mobility	< 1mm in any direction	✓	✓	✓	✓	✓
Absence of pain	✓	✓	✓	✓	✓	✓
Absence of Infection	✓	✓	✓	✓	✓	✓
Peri-implant bone loss	≥ 1/3 of vertical height of the bone	≤ 1mm after the first year in service. ≤ 0.2 mm annually	≤ 0.2mm annually after the first year in service	≤ 1.5 mm during first year in service. ≤ 0.2mm annually	≤ 2 mm during the first 5 years in service	Pattern I Pattern II Pattern III Pattern IV
No evidence of peri-implant radiolucency		✓		✓	✓	
Function and aesthetic			Restoration is in harmonious position and aesthetically satisfying the patient and dentist			
Success rate	75% for 5 years	85% for 5 years and 80% for 10 years	85% for 5 years and 80% for 10 years			

2.3.2 Factors affecting success and failure of dental implants

Implant failure can be defined as “the first instance at which the performance of the implant, measured in some quantitative way, falls below a specified, acceptable level” (Esposito et al., 1998). Peri-implant radiolucency, pain, discomfort, and or persistent infection at the implant site are the most common features of implant failure.

It has been shown that most of the implant failures occur during the healing stage, while few implant losses are diagnosed during the follow-up period (Esposito, 1999).

Esposito et al. (1998) classified implant failures according to the concept of osseointegration into biological, mechanical, iatrogenic and adaptation failures.

1. Biological failure is defined as the inefficient establishment or maintenance of osseointegration by host tissues, and it is further divided into:
   1.1 Early (primary) failure which occurs before achieving the osseointegration during bone healing process.
   1.2 Late (secondary) failure involves a breakdown of the established bone-implant integration.
2. Mechanical failure includes the fracture of implants or implant components and super-structures.
3. Iatrogenic failure occurs where a stable osseointegrated implant is eliminated from the anchorage unit because it violates important anatomical structures.
4. Adaptation failure involves patient-related factors, such as aesthetic and psychological problems.

Factors contributing to implant failure are classified as: patient-, surgical - and implant-related:

2.3.2.1 Patient-related factors

Bone quality and quantity

Primary stability of the implant mainly depends on the quality and quantity of the surrounding bone. Thus, any condition affecting bone quality or density could adversely influence the survival and success of implant osseointegration. Patients with insufficient bone quality and density are at highest risk for implant failure (Busenlechner et al., 2014). Different areas of the jawbone exhibit varying levels of bone quality. Generally, cortical thickness and density of the mandible are higher than that of the maxilla, consequently, mandibular implants present higher success rates compared to implants inserted in maxilla (Carr, 2012). In addition, a higher incidence of implant failures occurs predominately in type IV bone which is commonly found in maxilla and posterior region of mandible; Jaffin and Berman (1991) reported in their 5-year analysis of 1,054 implants a 35% failure rate in type IV bone compared with 3% in types I, II and III bone. Excessive resorption of residual ridge in both maxilla and mandible results in insufficient bone available to stabilize the implant initially and consequently contribute to failure of osseointgration (Al-Sabbagh and Bhavsar, 2015).

Systemic disease

Systemic diseases (particularly diabetes mellitus and osteoporosis) may have a negative impact on the survival rate of oral implants.

Uncontrolled diabetes mellitus has been shown to increase the incidence of early implant failure (Esposito et al., 1997). This chronic metabolic disease can compromise the circulation and increase the predisposition to infection around the implant leading to delayed wound healing, and negatively affect the osseointegration (Chrcanovic et al., 2014a).

It has been demonstrated that patients with poorly controlled type I diabetes tend to have implant failures more than people who do not have diabetes (Brocard et al., 2000). Furthermore, a significant relationship between implant failure rates and the duration of this disease has also been found (Olson et al., 2000). On the other hand, many studies have reported that patients with well-

controlled diabetes may have implant survival rates similar to people who do not have diabetes, indicating that diabetes should not be considered as an absolute contraindication for implant treatment if the subject's diabetic control is stable. The results of meta-analysis by Chrcanovic et al. (2014a) indicated no significant difference between patients with controlled diabetes and those without diabetes in implant survival. Similarly, Moraschini et al. (2016) conducted a systematic review comparing failure rates of individuals with diabetes and those without. Their results showed no difference in failure rate between the groups, nor was there any difference between people with type I and type II diabetes.

A patient with osteoporosis is categorised under type IV bone according to Lekholm and Zarb classification which exhibit a high incidence of implant failure (Gaetti-Jardim et al., 2011). Osteoporosis causes alveolar ridge atrophy and decreases density of bone which may lead to inadequate bone quality and quantity at the implant site (Moedano et al., 2011). However, several reviews of the literature have reported that implant survival rates were not significantly different between patients with and without osteoporosis (Chen et al., 2013, Grisa and Veitz-Keenan, 2018).

Smoking

Smoking is another significant risk factor increasing failure rates of osseointegrated implants. Smoking has been shown to compromise wound healing at implant site (César-Neto et al., 2003). Several studies have related the higher failure rate for osseointegrated implants to tobacco smoking (Chen et al., 2013, Hui et al., 2013). For example; Zhang et al. (2017) reported failure rate of 1.3% in smokers as compared with 0.3% in non- smokers. Smoking has been reported as main risk factors of implant failure during bone-implant healing stage. According to a recent meta-analysis finding (Manzano et al., 2016), smoking may have a dose related response on osseointegration and increases the incidence of early failure 1.3-2.3 fold. This was in agreement with the findings from a retrospective analysis (Noda et al., 2015) which reported that smoking was the main indicator of failure in the preloading stage whereby

the rate of implant loss in smokers was 2.4 times higher than in non-smokers in the early stage of treatment.

2.3.2.2 Implant-related factors

Implant length and diameter

Long-term survival of the implants depends on the degree of the bone-implant contact. Therefore, the survival rate of an implant is directly related to implant length and the quantity and quality of available bone.

Many studies reported that short and narrow implants associated with higher failure rates. A reduced primary stability and increasing failure rates were reported for implants shorter than 7 mm (Olate et al., 2010) and narrower than 3.5 mm (Baqain et al., 2012). Manzano et al., (2016) concluded in a meta-analysis that there was a significant association between early implant failure and short implants (< 10 mm). One possible explanation for increased risk of failure that the short and narrow implants are usually placed in compromised area with insufficient quality and quantity of bone (As El, 1999). However, some studies have shown that the smaller and shorter implants may provide adequate primary stability and present favourable success rate in the short term in cases with poor bone quality (Degidi et al., 2009, Vicente Neto et al., 2018). A pilot randomized clinical study reported that short implants may present favourable success rate in the short term, and can be used in posterior atrophic jaws as viable replacement for long implants and bone augmentation (Esposito et al., 2011).

Implant design

Although few published studies were concerned with the role of implant shape in the treatment outcomes of dental implants, it has been shown by several investigators that implant geometry can influence treatment success. Use of cylindrical implants has been associated with greater failure rates, whereas tapered implants present high prevalence of success (Chrcanovic et al., 2014b). Tapered implants favour stress distribution to the surrounding bone by imitating the natural root shape. Huang et al. (2007) found that tapered implants can minimise stresses in both cortical and trabecular bone compared

with parallel-sided designs. In addition to the shape, implant threads and thread details are also play an important role in the treatment success. The use of threaded implants dissipates interfacial stresses, increases the contact area between the implant and bone and provides better primary stability, particularly in low quality bone (Romanos et al., 2014). Steigenga et al. (2003) reported that square thread design showed higher survival rates than V-shaped thread and non-threaded designs.

Implant surface

There have been increasing efforts to enhance bone-Implant integration and reduce the time before loading implants by modifying surface properties. Surface characteristics including: topography, physics, and chemistry may influence cell-implant surface interaction and peri-implant tissue healing which subsequently effect osseointegration and treatment outcomes.

Implants with rough surfaces demonstrated higher degree of bone to implant contact (Novaes et al., 2002), and subsequent higher success rates compared with the smooth surface implants (Jemt et al., 2015). Findings from a systematic review (Chrcanovic et al., 2014b) showed higher success rates for hydroxyapatite-coated and titanium plasma sprayed implants when compared with machined implants. For SLA implants (sandblasted large-grit and acid-etched surface), satisfactory success and survival rates have been published in several animal and human studies. In short-term retrospective study by Lee et al. (2016) the success rate for the SLA implants was 93.8%. A higher success rate of 97% and minimal bone loss have been reported for the SLA implants reviewed retrospectively over a 10-year period (Buser et al., 2012). Furthermore, anodised implants presented a clinical success rate more than 95% in cases of compromised bone and immediately extracted sockets when compared with smooth machined implants (Mishra et al., 2017).

It has been also reported that marginal bone loss around modified surface implants stabilized after the initial physiological loss in the first year of service. Jimbo and Albrektsson (2015) compared the clinical success of moderately rough implants with the minimally roughened surfaces in terms of differences

in marginal bone loss for 5 years. The authors reported that the moderately roughened surfaces (TiO blast and SLA implants) showed less marginal bone loss than the minimally roughened turned surfaces. In addition, all examined systems demonstrated a significant marginal bone loss in the first year with no further progressive loss thereafter to indicate low incidence of peri-implantitis.

Despite of the proven clinical benefits of the roughened surfaces in implant stability and osseointegration, some studies have reported that increased surface roughness of the implants enhances plaque accumulation and facilitates microbial retention which subsequently increases the risk of treatment failure due to peri-implant diseases (John et al., 2015).

In conclusion, although numerous studies have reported variable success rates for different implant surfaces, still there are lacking in the scientific evidence that support the superiority of a particular surface characteristics over the others.

2.3.2.3 Surgery-related factors

Surgical experience

Clinical experience and surgical skill of the clinician play an important role in successful implant osseointegration and treatment outcomes. However, contradictory conclusions have been reported in the literature. Lambert et al. (1997) showed higher failure rates for the implants installed early in a study compared with those for the later ones. In addition, the authors found that the failure rates of implants placed by inexperienced clinicians (placed < 50 implants) were approximately two times higher than that for the experienced ones (placed ≥ 50). Similarly, Zoghbi et al. (2011) showed higher successful osseointegrated rates for implants inserted by more experienced professionals who had placed more than 50 implants. In contrast, Jemt et al. (2015) demonstrated no significant differences in the failure rates between experienced and unexperienced surgeons.

Surgical trauma

Excessive surgical trauma is considered one of the factors that may contribute to early implant failure. Bone drilling conditions and drilling tool geometry are crucial in surgical performance and success rate (Bohra et al., 2019). Brånemark et al. (1969) highlighted the importance of an atraumatic surgical procedure at the implant site to achieve successful osseointegration. Eriksson and Albrektsson, (1984) demonstrated that overheating of the implant osteotomy site during preparation may lead to necrosis of bone around the implant and may severely interrupt its regenerative capacity. The authors reported 47°C for 1 minute as a threshold temperature to avoid osteonecrosis. Excessive heat production during implant site preparation may be attributed to factors such as excessive pressure applied during drilling, use of dull surgical drills, insufficient irrigation of the osteotomy site, and thick cortical bone (Möhlhenrich et al., 2015).

Implant placing and loading protocols

Conventional (two-stage, delayed or sub-merged) loading approach was the original approach advocated by Brånemark with a load-free healing period of 6 months for maxilla and 3 months for mandible following sub-merged implant placement (Albrektsson et al., 1981). The rationale behind this was to ovoid the microbial contamination and micro-motion in order to optimize the osseointegration before connecting the implants with the transmucosal abutment in the second surgery. Immediate and early loading protocols are alternative approaches which have been introduced to shorten the treatment duration and improve patient's comfort and satisfaction (Buser et al., 1990). In both immediate and early loading protocols, implant and transmucosal abutment are placed in a single surgery without a sub-merged healing period (one stage, non-submerged implant placement protocol).

Several studies and meta-analyses have compared the clinical and radiographical outcomes between the different loading protocols. However, the differences between them are not clear in terms of success and survival rates as well as the peri-implant marginal bone changes. Sanz-Sánchez et al. (2015) reported a greater risk of implant failure for the immediate loading

compared with the delayed loading protocol. These results support similar findings from a recent meta-analysis (Troiano et al., 2018) showing a higher rate of early implant failure for non-submerged immediate approach. In contrast, no significant differences were found in other meta-analyses (Paul et al., 2017, Zhang et al., 2017, Helmy et al., 2018). Furthermore, theses reviews have also reported that there was no significant difference in the peri-implant bone loss among the loading protocols, and the immediate approach showed less change than early and delayed protocols.

2.4 Current methods used to assess implant stability and osseointegration

Peri-implant probing has become a routine part of clinical examination for the evaluation of peri-implant condition. Bleeding on probing is a significant clinical sign of peri-implant inflammation as is increased peri-implant depth (Aguilar-Salvatierra et al., 2016). The diagnostic value of peri-implant probing is affected by several factors, including: probe tip diameter, probing force and angulation, implant shape and surface texture, and inflammatory level of peri-implant tissues (Eickholz et al., 2001). Unless healthy peri-implant conditions are present, the probe tips often fail to identify the probing attachment level between pocket bases and implant shoulder (Salvi and Lang, 2004). Furthermore, peri-implant probing has been reported to cause significantly more pain than periodontal probing (Parvini et al., 2019). This may be due to the higher degree of inflammation around the implant compared to the teeth. It has been claimed that periodontal indices are not efficient enough for diagnosing peri-implant disease or for predicting implant failure and may even lead to a false diagnosis and possibly to unnecessary treatment (Coli et al., 2017, Coli and Sennerby, 2019).

For this reason, a number of methods and instruments have been developed to improve the monitoring of implant stability.

2.4.1 Percussion test

Percussion is a simple, intuitive test, easily applied in the clinic to evaluate implant stability and integration. This technique is based on the audible sound

produced by tapping the implant or the abutment with a metallic instrument in an attempt to determine the degree of bone-implant integration. A ringing sound indicates that the implant is successfully integrated, while dull sound suggests little or no integration. However, this test is very subjective, in that it relies on the examiner's experience, and lacks precision as it provides only qualitative information which is not recorded (Atsumi et al., 2007, Sennerby and Meredith, 2008).

2.4.2 Radiographic analysis

Radiographic evaluation is the most commonly used clinical method for preoperative assessment of local bone prior to implant installation and subsequently for monitoring osseointegration and implant stability. The main objective of a radiographic assessment is to identify peri-implant radiolucency, and to measure crestal bone level, where necessary recording any changes over time. The radiographic criteria for successful implants include "less than 1.5 mm marginal bone loss after the first year of function and less than 0.2 mm loss annually thereafter" (Albrektsson and Isidor, 1994). However, the conventional technique has several limitations. The image is two-dimensional, which can only provide a lateral view for the alveolus and is not able to present cross-sections (Kuhl et al., 2016). Thus, it cannot provide information on facial bone loss which occurs before mesial or distal bone resorption (Misch, 2005). It also has low resolution so that it is not feasible to identify alterations in the peri-implant bone structure and anatomy until 40% of demineralization has occurred (Goodson et al., 1984).

Furthermore, the view is difficult to standardise because of errors due to film placement and difficulty in achieving a true parallelism between the film and implant (Garcia-Garcia et al., 2016). A paralleling technique has been introduced to standardize the periapical radiograph to better visualise the minute changes in marginal bone level, but the precision of measurements still does not exceed 0.5 mm (Schulze and D'Hoedt, 2001). Thus, the accuracy of a radiograph is not enough to show the threshold 0.2 mm bone loss which is expected to occur every year after the first year of implant loading. Therefore,

reliable and repeatable measurements of marginal bone level around implants using this technique might not be obtainable for longitudinal stability evaluation. Radiographical assessment significantly overestimates marginal bone level compared with peri-implant probing measurements (Cassetta et al., 2018).

Cone beam computed tomography (CBCT) has also been clinically accepted for evaluating peri-implant bone defects as it provides a better 3-dimensional view of the defect. However, its diagnostic value is significantly affected by the metal artefact (implant) which may hide the early changes in the marginal bone around the implant (Gonzalez-Martin et al., 2016). Because of increased radiation dose and cost, CBCT is not convenient for use in a dental clinic for either routine or long-term implant follow-up (Sachdeva et al., 2016).

2.4.3 Reverse torque test

The reverse torque test (RTT) has been used to evaluate bone-implant integration at the second-stage (abutment connection) surgery (Sullivan et al., 1996). RTT measures the critical torque threshold which leads to destruction of bone-implant contact. During this test, a counter-clockwise torque equal to 20 Ncm is applied to the implant. The test is often used in the practice as no additional equipment is required over the implant driver and wrench used for placement. This test is effectively destructive one as it may result in significant damage to the supporting tissues around the implant and then in crestal bone loss, particularly in low density bone (Meredith, 1998). In addition, proposing a specific value for threshold RTV lacks any scientific basis as it does not consider the variability in implant geometry and local bone (Atsumi et al., 2007). Furthermore, RTV provides only a pass or fail results, without giving any objective measurement for osseointegration (Meredith, 1998). Considering all of these limitations, RTT has not found a place in clinical practice (Zanetti et al., 2018).

2.4.4 Periotest™

The Periotest™ is an electronic device, originally developed to measure the damping characteristics of periodontal ligament, providing a value for tooth

mobility (Schulte and Lukas, 1992), but it has been advocated as a reliable method for objective assessment of implant stability in clinic (Tricio et al., 1994).

The Periotest technique is based on the impact hammer method, which uses a transient impulse as an excitation force. The device consists of a handpiece with a tapping metallic rod inside, connected to a small computer. The response to striking the implant or the abutment is collected and measured by an accelerometer built into the head. The stability of the implant is assessed using the contact time between the implant and the tapping rod which is converted into a value called the Periotest value (PTV). Lower readings suggest successful osseointegration, while higher values indicate marginal bone loss. However, the technique has limited clinical use because of its reported poor sensitivity and low accuracy. It has also been claimed that the device cannot discriminate between different levels of osseointegration, as only a range of (–5 to +5) over a wide scale of (–8 to +50) has been reported for the osseointegrated implants (Olivé and Aparicio, 1990).

Furthermore, it has also been demonstrated that the PTV measurement and accuracy of the method is influenced by several factors, including device angulation, position, and abutment length (Meredith et al., 1998, Zanetti et al., 2018). It has also been reported that repeated tapping of the implants with such a device may deteriorate the initial stability, especially in low-quality bone (Seong et al., 2009).

The reliability of the Periotest™ in assessment of various peri-implant bone defect has been evaluated by a number of authors. In one study, the device was able to detect circumferential bone loss to a depth not less than 3 mm (Lachmann et al., 2006). Others have found Periotest™ to show low sensitivity to vertical partial bone loss particularly in the mesio-distal direction (Choi et al., 2014, Bilhan et al., 2015). This was attributed to the difficulty of accessing the mesial and distal surfaces during testing because of the adjacent teeth. In addition, the presence of remaining bone limits the mobility of the partially integrated implants, making its differentiation from the intact implants difficult

using such a vibration-based test. Overall, the clinical usefulness of the Periotest™ is limited in diagnosing peri-implant bone defects and radiographic examination is needed to obtain supplementary information for partial bone defects.

2.4.5 Resonance frequency analysis (RFA)

Resonance frequency analysis was first described by Meredith et al. (1996) as a non-invasive and objective method for monitoring implant stability using vibrational analysis. RFA measurement is expressed as an implant stability quotient (ISQ), a numerical measurement ranging from 1 to 100, which quantifies the stiffness of the bone-implant structure and hence the stability of the bone-implant interface. Higher ISQ value means greater implant stability (Sennerby and Meredith, 2008). Currently, the commercially-available devices used to measure implant stability include: Osstell (Integration Diagnostics), Implomates (Bio Tech One) and Penguin (MultipegTM; Penguin Integration Diagnostics). RFA measures the first bending resonance frequency of a small transducer or cylindrical peg connected to the implant or abutment. However, this process constitutes a limitation in the technique, because it requires removal of the implant superstructure and the transducer to be screwed into place with a torque half that used to insert the implant. This may cause undesirable stresses at the bone-implant interface during the early stages of healing (Zanetti et al., 2018).

RFA has increasingly been used for monitoring implant stability over time in the dental clinic (Diaz-Castro et al., 2019), as it presents good reproducibility and repeatability (Jaramillo et al., 2014). However, the sensitivity of this technique is affected by a number of variables such as bone density, implant position, abutment length and implant related factors (Andersson et al., 2019). Therefore, the accuracy of the technique has become controversial and needs to be validated against the structural (histomorphometrical bone-implant contact) and mechanical (peak insertion torque) parameters of implant stability.

The histological correlation with ISQ values has been studied by several investigators. Gottlow et al. (2010) and Acil et al. (2017) reported an increase in ISQ units with time as a result of bone deposition and remodelling at the implant interface. In a simulation study, Veltri et al. (2014) investigated the effect of varying degrees of a simulated bone-implant integration on RFA measurements. Their findings demonstrated a positive relationship between ISQ values and the amount of the simulated osseointegration. Their conclusion was drawn from analysing RF measurements made on experimental specimens, constructed from polyurethane resin which lacked any anatomical variation. Denis et al. (2018) compared ISQ values for implants, placed in maxilla, taken on the first day of surgery and then 3 months later. Their results demonstrated a significant increase in the stability over time during the 3-month period. In contrast, others have failed to demonstrate any relation between ISQ and bone density and type at the implant site (Dagher et al., 2014, Fu et al., 2017).

It has also been reported that RFA is sensitive to changes in the marginal bone around implants. Shin et al. (2015) have evaluated the effect of defect type and depth on implant stability in a bovine rib bone model. They showed that ISQ values were only able to differentiate significantly implants with 3-wall, 5 mm defects from those in intact bone. In another *ex vivo* animal study, the authors reported that RFA measurements decreased as the defect depth increased, with a significant reduction when the horizontal defect extended 2 mm apically (Yao et al., 2017). In contrast, Fischer et al. (2009) showed no association between peri-implant bone loss and ISQ values over a 1-year period. The authors compared the values of marginal bone level on radiographs with the implant stability measured in ISQ at the time of surgery and then after one year. Their findings showed that ISQ values were not able to recognise an average of 1.1 mm loss in the marginal bone during the first year while it increased significantly with time from 63.3 at baseline to 66.8 after a year. This finding was consistent with other authors (Dias et al., 2014, Elsyad et al., 2014). In view of such conflicting observations, it seems that the relationship between bone structural parameters and RFA is not yet fully understood.

Conflicting observations have also been reported for the relationship between RFA and peak insertion torque (PIT) in reference to primary stability; Santamaría-Arrieta et al. (2016) reported no correction between primary stability measured by RFA and PIT, whereas a direct relationship was demonstrated by Baldi et al. (2018). In a recent review (Lages et al., 2018), the relationship between the two methods for the prognosis of immediately loaded implants was assessed. For successful immediately loaded implants, primary stability is a fundamental requisite which is achieved by using an insertion torque equal to, or higher than, 40 or an ISQ equal to, or higher than, 70. The findings from the review showed that these scores could not be related in many studies, which indicated that insertion torque and RFA are independent and not comparable. Although ISQ values can provide an objective measurement for osseointegrated implants, a threshold value to discriminate between successful and failed implants has not yet been identified (Monje et al., 2014).

In conclusion, the efficacy of RFA for clinical evaluation of implant stability has not been fully established and still needs further investigation.

2.4.6 Conventional ultrasound (CUS)

Ultrasound is a non-invasive technique which has recently been used in research to monitor implant stability (Mathieu et al., 2011). In this technique, a probe transponder (transducer/sensor) is tightly screwed to the abutment with a torque equal to 3.5 Ncm, and connected to a pulse receiver by coaxial cable. The transducer generates a broadband ultrasonic pulse which propagates through the implant until it reaches the interface where part of the pulse transmitted while the rest is reflected back through the implant to be measured by a sensor (Reuben, 2017). As the quality and quantity of bone increases on the implant surface, the acoustic impedances (related to mechanical properties) of the bone and the implant become more matched and consequently the transmission coefficient increases (Vayron and Haiat, 2015). Thus, the recorded energy decreases as the transmission of the energy through the surrounding interface increases. The ultrasound technique

essentially assesses the acoustic impedance of the interface, where well integrated implants result in little reflection of the pulse, whereas compromised interfaces result in a large amount of reflection. It has been found that the ultrasonic response of an implant reflects the boundary conditions of the bone-implant interface, confined to a zone of approximately 30 μm around the implants (Vayron et al., 2016).

The technique has shown its potential to assess implant primary stability and osseointegraion (Vayron et al., 2014a, Vayron et al., 2014b). In a recent study, the authors compared the performance of the CUS with the RFA technique and claimed that CUS provides better estimation of implant stability parameters than RFA (Vayron et al., 2018). Nevertheless, one of the limitations of this technique is the need to remove the prosthesis and connect the transponder to the abutment with a specific torque which may have a potential impact on the established interface (Zanetti et al., 2018). Considering the intra-oral environment and the complexity of the current oral probe, its clinical application could be quite difficult and may limit the reproducibility of the measurements. Currently there is no commercial version available for the clinical use.

2.5 Acoustic Emission (AE)

Acoustic Emission describes “a class of phenomena whereby transient elastic waves are generated by the rapid release of energy from a localized source within a material” (Matthews, 1983). Natural sources can include microcracking and cavitation in fluids, and the resulting elastic waves propagate in all directions in the material according to their attenuation properties (Gueiral and Nogueira, 2012).

The high frequency (typically 500 KHz) AE waves are detected by sensors placed on the surface of the material which convert them into electrical signals. AE signals are very weak and need to be amplified significantly before processing. The amplified signals also need to be filtered to remove the lower frequency vibration noise which would otherwise swamp the signal. The electrical AE signal is then processed using computer software to extract

characteristics that may relate to particular features of the material in which the signal propagates (Rashid and Pullin, 2014).

Application of the acoustic emission (AE) technique

Acoustic emission has been developed and extensively used as a non-invasive method of monitoring in engineering. AE is a well-developed non-invasive technique for real-time damage monitoring. It offers the potential of assessing and monitoring structures where a very high level of integrity is required. AE can be used to identify early signs of failure in a structure before it completely breaks down (Grosse and Ohtsu, 2008).

AE has found extensive applications in orthopaedic research. It has been used to describe the biomechanical characteristics of bone *in vitro*, and to monitor micro-damage and fracture. For example, Aggelis et al. (2015) examined AE transmission during fracture of a human femur bone while the specimen was exposed to a combination of bending and torsional stresses to produce various fracture patterns and to imitate femur neck fractures due to falls. Their findings showed that AE can recognise the initiation of cracks before these propagate into macroscopic fractures. This supported earlier studies which used AE technology to monitor micro-damage formation during bone fatigue, and recently demonstrated the ability of the technique to detect impeding fractures in the cortical bone in physically active people (Acil et al., 2017).

These findings have led to attempts to employ AE in total hip arthroplasty research, specifically to investigate the failure mechanisms within the bone-cement-implant construct (Kapur, 2016). Fitzpatrick et al. (2017) reported the usefulness of AE for wear measurements of hip replacement implants. It has also been reported that AE can be used to predict potential fractures during uncemented hip arthroplasty by monitoring the internal damage in bone during fitting of the femoral prosthesis into the femoral canal (Pechon et al., 2018). However, the full potential of AE in the orthopaedic field has yet to be established.

In recent years, AE has begun to be used within the field of dentistry, in a variety of different applications. For example, AE has been applied in

monitoring crack growth and fracture behaviour in different dental materials such as composites (Romhány et al., 2017). Also, it has been reported that AE is effective in evaluating the development of shrinkage stress and the subsequent interfacial de-bonding of composite restorations. Also in the restorative area, Li et al. (2011) have demonstrated the validity of AE technique for detecting the interfacial de-bonding of composite restorations in the real time during curing. Their results showed a positive correlation between the cumulative AE events and the shrinkage stress produced by polymerization of the composite resin. Kim et al. (2015) and Yang et al. (2016) further confirmed that AE analysis, which reflects the bond strength of the tooth-composite interface, exhibited a strong linear correlation with shrinkage stress and de-bonding at the tooth-composite interface.

In the direct area of this thesis, there has been some interest in applying AE in monitoring dental implant stability. Ossi (2013) evaluated the reliability of acoustic emission technique in monitoring primary stability of dental implant in *in vitro* animal model. He found a significant correlation between a simulation of primary stability of dental implant and the AE values transmitted from a standard source (pencil lead break) to a sensor placed on a surface of bovine bone. In addition, he reported the potential deployment of the test in the clinical situations.

2.6 Identification of thesis topic / Statement of problem

Longitudinal monitoring of implant stability and osseointegration during various stages of the treatment procedure and at follow-up examinations is valuable to assure long-term implant success. A quantitative measurement of primary stability at the time of implant surgery, and further measurements of the stability following the initial healing phase would determine the degree of the implant integration and the level of healing at bone-implant interface. Furthermore, monitoring implant stability during clinical function is crucial to allow identifying minor changes in marginal bone level and predicting the severity of bone loss.

Progressive marginal bone loss is an indicator for peri-implantitis, and is estimated to occur in approximately 18.5% of patients. Although it has been recognized that bone loss around dental implant can be triggered by biological and biomechanical factors or a combination, the predictability of this condition remains uncertain due to difficulties in detecting the small marginal bone changes by using the current measuring techniques, especially in presence of peri-implant tissue inflammation.

Current methods used for clinical monitoring of implant stability (e.g. radiography, resonance frequency analysis, Periotest™ etc.) have not been able to provide a precise prognosis of implant failure. Even the most recently developed tests have brought little improvements towards identifying compromised implants with marginal bone defects. Limitations such as lack of sensitivity and reproducibility, complexity of oral probe, cost, time to diagnosis and radiation hazards, have led to an increased need for efficient alternatives.

Acoustic emission technology has been widely applied in many medical fields to provide a highly sensitive and non-invasive method to monitor the integrity of structures. More recently, AE has shown its promise for monitoring implant stability. However, because of the complexity of sound transmission in bone, further research is required to move towards its use in a clinical diagnosis. The current work aims to build on what has been established so far and to develop a reliable and simple-to-use test to monitor the changes in the osseointegration of dental implants either during its development or maintenance phases.

Chapter 3
Materials and Methods

This chapter presents and describes the experimental techniques and procedures used to conduct this work. It is divided into three sections:

- experimental techniques, describing the experimental methods, apparatus and materials;
- experimental procedures including the rationale for the preliminary assessments used to establish the experimental protocol and the systematic experiments used to explore;
  - the effect of bone microstructure on AE transmission through and along bone in the primary stability model
  - the influence of simulated osseointegration on AE transmission
  - the potential of AE energy for diagnosing peri-implant bone loss
- analytical techniques used to process the AE and micro-graphical data and to examine the relationship between the systematic parameters.

3.1 Experimental techniques

This section describes features and specifications of the equipment and techniques used for all experiments. It is divided into three parts: sample preparation, acoustic measurement methods and histological characterization.

3.1.1 Sample preparation

3.1.1.1 *Materials*

Samples were prepared from three materials: bone, implants and glass ionomer cement, which were then assembled in various experimental configurations representative of primary stability, secondary stability (osseointegration) and peri-implant bone loss.

Bovine ribs were used in this study as a model of human jawbone because of their similar macroscopic composition of cortical and cancellous bone. The

fresh ribs (each from a different animal) were sourced from a butcher shop and were cleaned of all soft tissue residues and immediately stored in a refrigerator (4°C), wrapped with saline-soaked gauze to avoid dehydration. Bone samples were taken from the proximal part of the ribs in order to have a deep cross-section with a wide ridge to ensure that the various models are surrounded with both cortical and cancellous bone. Samples were labelled for identification and used within five days at room temperature (23 ± 2°C). For orientation, the external (convex) and internal (concave) surfaces of the rib were deemed to represent buccal and lingual surfaces, respectively. After completing the acoustic measurements, bone samples were frozen for subsequent histological examination.

Titanium dental implants (Straumann, Tissue level, Standard Plus) measuring 4.1 mm in diameter and 10 mm length were inserted in the centre of each bone sample, Figure 3.1. For each rib, the arrangement of various models along the ridge was randomized to exclude any systematic effect of the animal-specific bone structure surrounding each model. New implants were used for the majority of tests, although some were reused in order to increase the sample size. To assess repeatability of the measurements, all configurations were repeated a number of times (typically 5) installed in different bone samples.

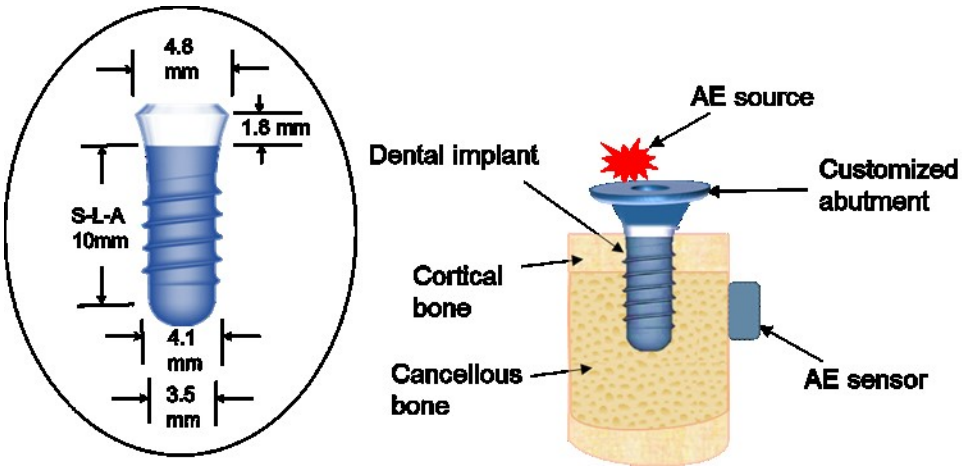

Figure 3.1: Schematic view for dental implant into bovine bone

Glass ionomer cement (GIC) was selected in this work to act as an interface between implant and surrounding bone and to simulate osseointegration. The cement has acoustic transmission characteristics close to that of bovine bone (Ossi et al., 2013) and was therefore used to simulate bone healing around implants in order to mimic the development of secondary stability during bone healing *in vivo*. Two different consistencies of the cement were tested: Ketac Fil plus Aplicap Glass Ionomer and Ketac Cem Permanent Glass Ionomer Luting Cement. Primary stability was simulated simply by installing the implants according to the normal surgical procedure with consequent interaction between the implant and the cortical bone.

3.1.1.2 *Installation of dental implants into bovine bone ribs*

Preparation of implant site

Bone samples were fixed firmly to a vice to prevent their movement during osteotomy procedure. On the upper ridge of each rib block, areas suitable for implant placement were marked every 1 cm. The osteotomy was performed using the clinically recommended drill bit with a Dremel handpiece. It was not possible to carry out the procedure using a dental handpiece for a number of practical reasons. First of all, in order to study the effect of time and sample dehydration on AE measurements, it was necessary to carry out the measurements immediately after installation of implants which required to have both the drilling tools and the AE equipment in the same laboratory. Also, to avoid concerns over cross-contamination from drilling dead animal bone in a dental surgery/laboratory it was preferable to base the experiments in an Engineering laboratory. In addition, it was not rational to purchase a dental turbine just for this work. The Dremel handpiece attached to a Dremel 3000 drill was chosen for its small size and acceptable speed range compared with a dental handpiece.

The main concern with this setup is the potential for thermal damage during drilling, given that there was no irrigation was applied. A number of precautions were taken to minimise heat generation and its detrimental effect on the bone tissues. First, the drilling was performed at a high speed (5000 rpm) to

decrease the time of exposure to the area of heat generation as this will help to dissipate the heat very quickly. Second, a predrilling (step drilling) approach was followed to minimise the total temperature elevation and prevent heat build-up. Although no irrigation was applied during the drilling, the hole was kept wet between the two steps of the drilling process. To make sure that these precautions were effective, a drilled bone sample was sectioned and observed under a stereomicroscope. On examination, there was not any obvious/gross mechanical or thermal damage to the bone tissue.

Nevertheless, it is recognised that a rise in temperature during drilling is likely to be larger in *in vitro* specimens compared with the in *vivo* because of the lack of soft tissue covering and blood flow which are important in heat dissipation (Flanagan, 2010).

According to the type of the stability configuration (primary, secondary or compromised) designated for each experiment, two simplified drilling protocols (pilot drill + final drill) were used as follows:

- for both primary and secondary stability type-1 models, the implant sites were prepared to the manufacturer's recommended dimensions using 2.5 mm pilot drill and 3.5 mm final drill.
- for secondary stability type-2 and compromised models a 2.5 mm pilot drill followed by a 5.3 mm final drill were used to produce oversized holes which were then back-filled with cement.

Implant placement

Implants were inserted into their prepared sites using either of the following placement protocols: (a) Implant was tightly screwed into a hole of manufacturer's recommended dimensions filled either with water or with luting glass ionomer cement (Ketac Cem Permanent Glass Ionomer) to create the primary stability and secondary stability type-1 models respectively. (b) Implant was embedded into an oversized hole filled with filling glass ionomer material (Ketac Fil plus Aplicap Glass Ionomer) to build the secondary stability type-2 and compromised models. Implants were placed so that the junction between the roughened surface and polished collar was flushed with the crest of the bone. Figure 3.1

shows schematically the installation of an implant into bovine bone in the primary stability configuration.

Insertion of customized abutment

A purpose-designed custom abutment was used to provide a 10 mm diameter flat circular surface for easy application of the pencil lead break test, and to transmit the AE signal to the implant through the rigid connection provided by the basal screw. The abutment was manufactured for the study by Straumann and is shown in Figure 3.2.

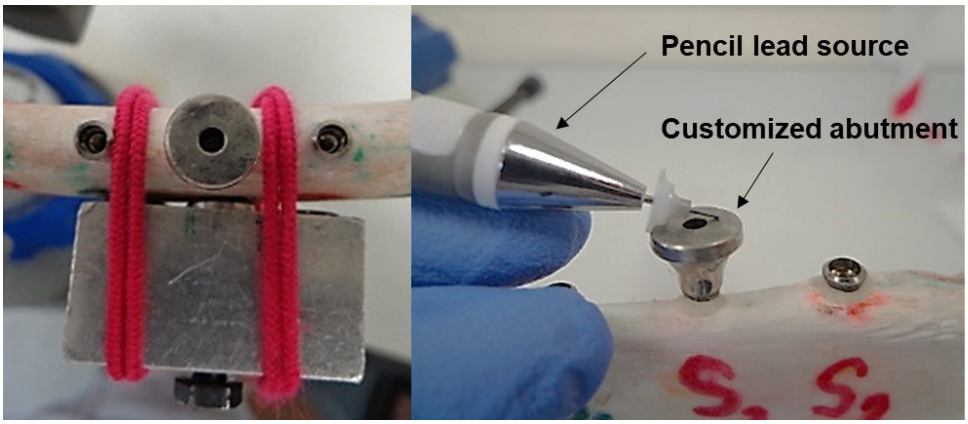

Figure 3.2: *In vitro* customized abutment connected to the implant

3.1.1.3 *Development and fabrication of experimental models*

Three configurations of bone-implant interface with different conditions of integration were prepared and developed.

1. Primary stability model (non-osseointegrated model).
2. Secondary stability model (partial or full osseointegration model).
3. Compromised osseointegration model.

It was not practical to use real bone for either of the osseointegrated models (2 and 3) as discussed further in Section 6.1.2. Such models would require a large animal study which is only justified when there is sufficient evidence to make this worthwhile.

The secondary stability (full osseointegration) and compromised models were made by drilling an oversized hole in the bone and filling it with glass ionomer cement (GIC) and then casting the implant into the cement.
This protocol was used because:

1. Glass ionomer cement has been established as having a good acoustic impedance match with bone (Ossi et al., 2013), and also has good integration with bone (Nicholson, 1998).
2. The drilling of the oversized hole means that the trabecular bone around the implant is not being repaired but is replaced with a model of solid bone.

Some researchers have used materials such as polymethyl methacrylate resin to simulate human bones for testing stability monitoring techniques such as Periotest and resonance frequency analysis (Cavusoglu et al., 2012, Choi et al., 2014, Veltri et al., 2014). However, such models are simply used to offer fixity, and are not designed to integrate with the bone and /or with the implant in the way that used in this study where acoustic coupling is important as is onward transmission in the bone.

Primary stability model

The primary stability model served three distinct purposes for the study:

- to provide a connection with earlier work (Ossi, 2013) which was confined to primary stability,
- to provide a real baseline bone-implant interface (albeit *in vitro* and on an animal model),
- to provide data on the transmission of AE in bones which might prove useful in a clinical setting to assess patient bone density at installation.

In this model the mechanical integration of the implant was simulated by screwing it tightly into the bovine bone as follows. The implant sites were prepared to the manufacturer's recommended dimensions (Straumann). Next, the implants were screwed in tightly according to the manufacturer's surgical guidelines, but in the presence of water to obtain a better acoustic transmission.

Secondary stability model

Designing and developing a configuration to simulate the biological fixation of the implant was essential in this work in order to allow the assessment of any changes in the bone-implant interface using the transmitted acoustic energy. Therefore, two models for varying the amount of simulated bone-implant contact (partial or full integration) were developed from the primary stability model using glass ionomer cement.

Two different drilling and implant placement protocols were applied for these models as follows:

a) Secondary stability type-1: implants were tightly screwed into holes of manufacturer's recommended dimensions filled with a luting glass ionomer cement.
b) Secondary stability type-2: implants were installed into oversized holes filled with a restorative glass ionomer material.

On sectioning, as shown in Figure 3.3, it is apparent that type-1 presented incomplete contact between the implant and surrounding bone contrary to the expectation that at least some of the cement would be extruded into the inter-trabecular spaces. However, it was considered that this would serve as a partial osseointegration model, although it was accepted that the degree of partial integration would have to be determined *post hoc*. On the other hand, the type-2 models exhibited a continuous layer of the cement formed into the interface between the implant and surrounding bone and was therefore regarded as a suitable model for full osseointegration. For this model, the hole was enlarged in order to allocate the extra space for the cement to be injected around the implant to mimic the manner into which a layer of new bone is deposited on the implant surface during osseointegration.

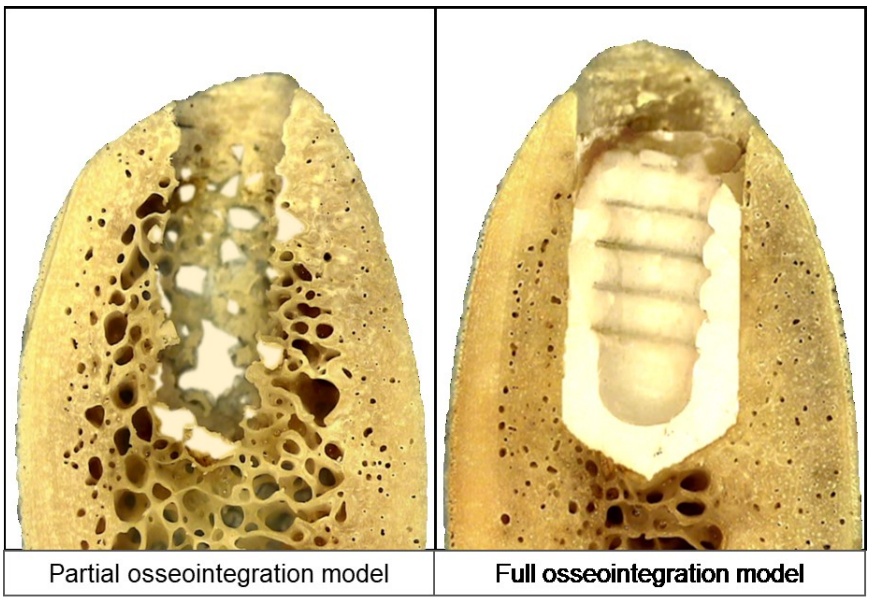

Figure 3.3: Types of simulated osseointegration models

Compromised osseointegrated model.

Following establishment of the simulated osseointegration of dental implant in bovine bone and determining its AE characteristics, further investigations were carried out to modify the fully osseointegrated model in order to create compromised versions of the interface in bovine bone models. The compromised model was developed to simulate various changes in the boundary of the established bone-implant interface, and to assess whether any of these changes can be detected by the transmitted acoustic energy.

In order to do this, it was necessary first to search for a material that can act as an acoustic attenuator to simulate bone loss in the cervical peri-implant area. Results from a basic AE transmission test showed that adhesive foam pads were the most suitable of the materials tested.

Figure 3.4 summarises schematically the various model configurations developed for the study.

Figure 3.4: Drilling and placement protocol for the different implant stability and compromised configurations

Experimental models	Primary stability	Partial osseointegration	Full osseointegration	Compromised osseointegration
Illustrations	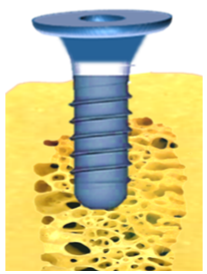	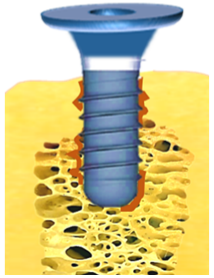	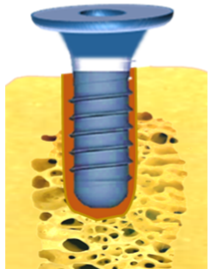	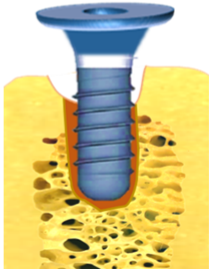
Drilling protocol	Pilot drill ø 2.5mm Final drill ø 3.5mm	Pilot drill ø 2.5mm Final drill ø 3.5mm	Pilot drill ø 2.5mm Final drill ø 5.3mm	Pilot drill ø 2.5mm Final drill ø 5.3mm
Implant placement protocol	Implants were tightly screwed into holes of manufacturer's recommended dimensions filled with water	Implants were tightly screwed into holes of manufacturer's recommended dimensions filled with luting GIC	Implants were embedded in oversized holes filled with restorative GIC	Peri-implant defect Implants were embedded in oversized holes filled with restorative glass ionomer material

3.1.2 Acoustic emission measurement methods

Acoustic emission (AE) is a term used in engineering to describe self-generated ultrasound, such as that made, for example by a leak in a pipeline. It is detected by placing a sensor on the structure which carries the ultrasound (e.g. the pipeline) and, in metals, there is relatively little loss of sound energy over quite long distances. In the current work, the AE is generated by an artificial source (a pencil lead break) and the structure carrying the sound energy is initially the implant. The basic principle of the measurement is that the condition of the interface will determine how much of the pencil lead energy is transmitted to the sensor placed on the bone, although it needs to be acknowledged that some energy is lost in transmission from the interface to the outer surface of the bone where the sensor is mounted.

Both the AE equipment and the pencil lead break are well established for engineering use and are described in turn below.

3.1.2.1 *Acoustic emission system*

An acoustic emission (AE) system generally consists of sensors, preamplifiers, signal conditioning unit, data acquisition cards and computer with software for controlling the acquisition and storage of the data, as shown schematically, in Figure 3.5.

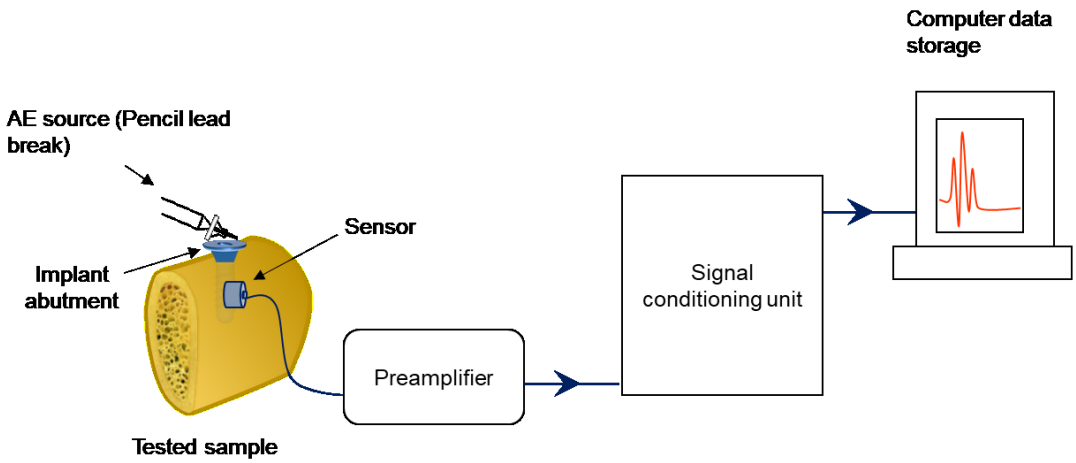

Figure 3.5: Schematic diagram of AE system and experimental set-up

The sensors used (Micro-80D from Physical Acoustic Corporation, New Jersey, USA) operate on the piezoelectric effect using a Lead Zirconate Titanate (PZT) crystal. The crystal detects ultrasonic waves on the surface and responds in the frequency range of 0.1 – 1 MHz with resonances at 325 KHz and 650 KHz. The sensors are 10 mm in diameter and 12 mm high. The sensors convert the waves detected under their footprint into a time varying voltage signal, which is sampled at a rate of 5 million samples per second.

The surface of the bone specimen was cleaned and lightly smoothed at the sensor positions using a large round burr. A water-based ultrasonic transmission gel was used as a couplant between the sensor and bone surface to eliminate air between bone and sensor which otherwise would affect AE transmission. It was found that best results were achieved using a thin layer of the couplant with the sensor being secured using elastic bands and an in-house designed clamps. As described later, careful placement of the sensor was essential for reproducible AE readings. Figure 3.6 illustrates the sensor placement on the bone surface.

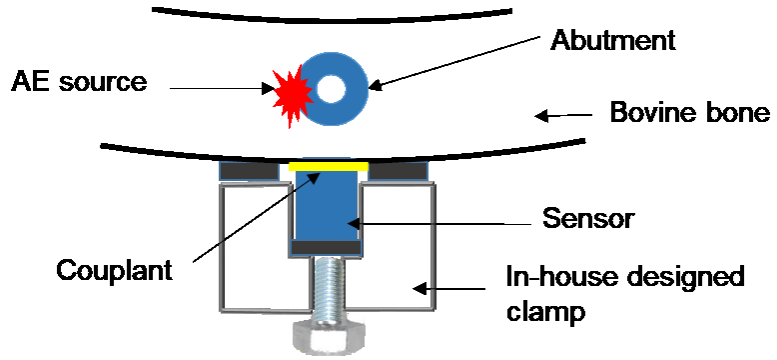

(a)

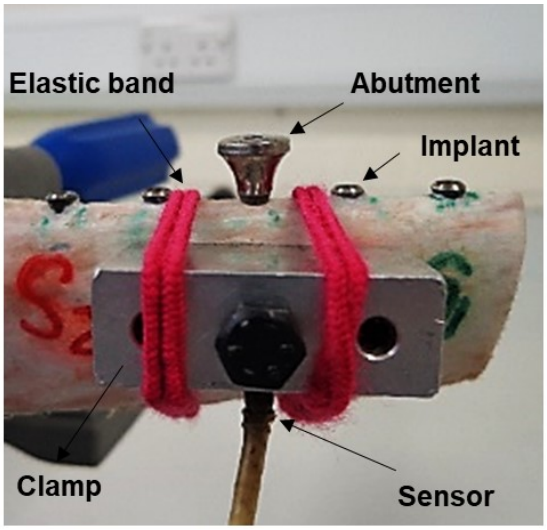

(b)

Figure 3.6: AE sensor placement on bone (a) schematic plan view, (b) photograph of actual placement

The raw voltage from the piezoelectric crystal is very small and needs to be amplified substantially before it can be fed to a coaxial cable and hence to a data acquisition system. To do this, Physical Acoustic Corporation 1220A pre-amplifiers were used. The pre-amplifiers incorporate a switchable gain of either 40 or 60 dB and a band-pass filter of 0.1- 1 MHz, and are powered by a 28 V power supply via the signal conditioning unit, with capacity for up to 4 channels.

All AE data were acquired at full bandwidth using an in-house built desktop PC with a 12 bit, National Instruments (NI), PCI-6115 board capable of acquiring data from 4 channels simultaneously at 10 M samples per second. In this work, a sampling rate of 5 M samples per second was used (sufficient to reveal waves of frequency up to 1 MHz) and a maximum of 2 channels was used, more often one.

A Lab-View126 script was used to control data acquisition and a MATLAB programme was used for processing the raw AE data to provide a measure of the wave energy. The relevant codes used here had already been developed (Nivesrangsan, 2005).

3.1.2.2 *Hsu-Nielsen source*

The Hsu-Nielsen source is recognised as a reproducible source of acoustic emission (AE) (Hellier, 2003). The technique uses a mechanical pencil supported by a guide ring, to generate a burst of AE by breaking a pencil lead on the surface of the test specimen. In this study, an HB pencil lead with a diameter of 0.5 mm and 2-3 mm length tip protruding was used throughout as a simulated AE source, Figure 3.7a. The tip of the lead was pressed firmly against the surface of the abutment until the lead broke, as shown in Figure 3.7b. A total of 20 AE measurements were taken for each implant in all of the systematic experiments.

This source was chosen for the following reasons:

1. It is regarded as a consistent and reproducible source of acoustic emission.
2. It is very easy to deploy and inexpensive.
3. It is an impulsive source.

However, it is recognised that this type of source would not be deployable in the patient's mouth and that an alternative impulsive source would need to be developed for any commercial instrument. The most likely source would be a dental air jet, but this has the disadvantage that it is not truly impulsive and would need to be calibrated for clinical practice. Alternatively, it might be possible to develop a standard, non-food "friable bite" source, based on early experiments by Ossi (2013) recording signals generated by subjects biting almonds and other hard foods.

The breaking of the lead on surfaces generates a short duration and localised impulse resulting from the rapid unloading of the surface when the lead breaks. ASTM standard (E976–99) recommends that the pencil lead should be consistent (HB or 2H, 0.3 or 0.5 mm diameter) with a 2-3 mm length tip protruding. The guide ring helps to provide reproducible breaks (aids in breaking the lead consistently) offering leverage and avoiding scratching or scuffing. Although the AE signal obtained from a pencil lead break test is well reproducible, variations in test handling can cause differences in the signal

(Sause, 2011). Therefore, care was taken to break the same length of the pencil lead on the same spot on the abutment surface with the same angle and orientation.

At the research stage, an impulsive source is preferable to a continuous source when carrying out a transmission test, as the propagation of the signal can be easily tracked and characterised due to there being a fixed start and end-time as the wave packet passes the relevant sensor. It would have been possible to use an ultrasonic transducer to provide controlled impulsive source, but that would have necessitated a choice of the relevant frequency range for best visibility of the interface, which is not known *a priori.* The use of such a transducer in a practical application remains an option, although this would make the equipment more expensive and more difficult to deploy in the patient's mouth.

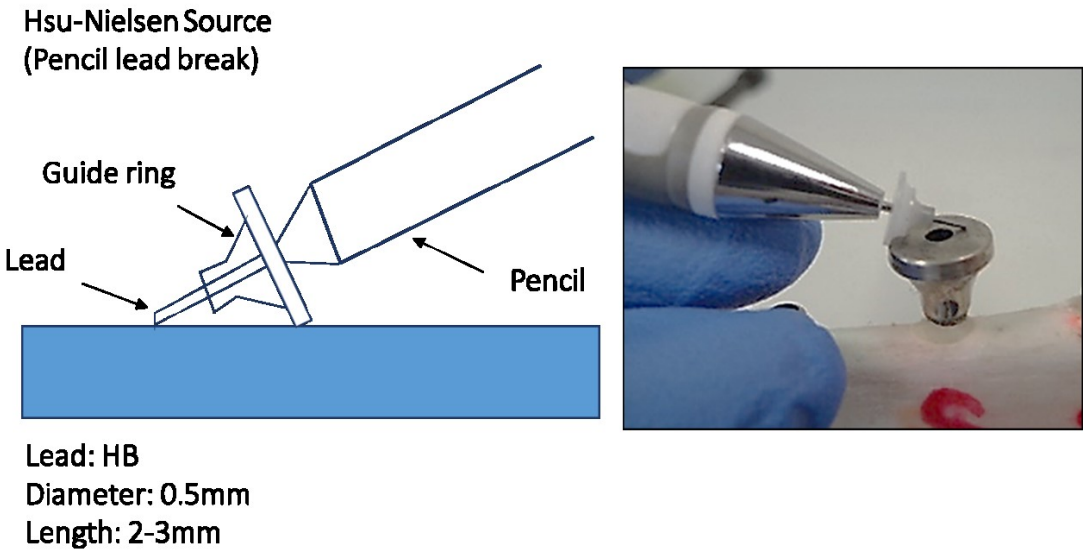

Figure 3.7: Hsu-Nielsen source: (a) Schematic diagram, lead diameter and guide ring. (b) Lead break on the customized abutment

3.1.3 Histological Examination

To better understand the effect of bone on acoustic transmission, it was essential to characterise the bone microstructure. Therefore, an extensive histological analysis was conducted to derive a set of quantitative data for cortical and trabecular bone parameters and to correlate these data with the transmission as a function of implant stability. The components of bone which are of interest from point of view of transmission are solid (cortical and trabecular bone) and non-solid (bone marrow) components where the latter appear as voids in the prepared sections.

3.1.3.1 *Preparation of histological sections*

After completing the AE measurements, bone samples from the first and second systematic experiments (Section 3.2.2.1 and Section 3.2.2.2, respectively) were processed for histologic preparation which was performed by the investigator. Before sectioning, implants were retrieved from their beds and the midline of their corresponding holes was determined. The empty implant sites were then sectioned along their longitudinal axis using a high precision diamond disc (IsoMet® 1000 Precision Saw, Buehler USA) to produce approximately 5 mm thick transverse sections. In the case of the osseointegration models, empty implant sites were filled with a wax to reinforce the glass ionomer cement during sectioning. The sectioned samples were then cleaned of marrow tissue remnants by immersing them into warm sodium hypochlorite solution NaOCl (5.25 %) and then rinsed in normal saline.

In the first systematic experiment (studying the effect of bone on the transmission, Section 3.2.2.1), transverse sections were obtained for the primary stability model after implant removal (at the reference sensor position), and for the other three sensor positions on the bone (B1). In addition, longitudinal sections were cut through the remaining bone segments between sensor positions along the bone (Figure 3.8a).

In the second systematic experiment (studying the effect of simulated osseointegration on the transmission, Section 3.2.2.2), only transverse

sections were obtained for primary and osseointegrated models along the bone (B2 and B3), as illustrated in Figure 3.8 (b, c).

3.1.3.2 *Imaging*

Sections were examined and imaged using a digital camera connected to a stereomicroscope (Leica MZ6) capable of magnification from 5 to 50 diameters. For each section, the acquired digital images were imported into Photoshop CC (Adobe System Inc., San, CA, USA) to be stitched into a panoramic view using a photo-merging tool. The measurement scale was set to correspond with the actual sample using a grid. Figure 3.8d shows typical stitched images, each consisting of 12-20 micrograph frames.

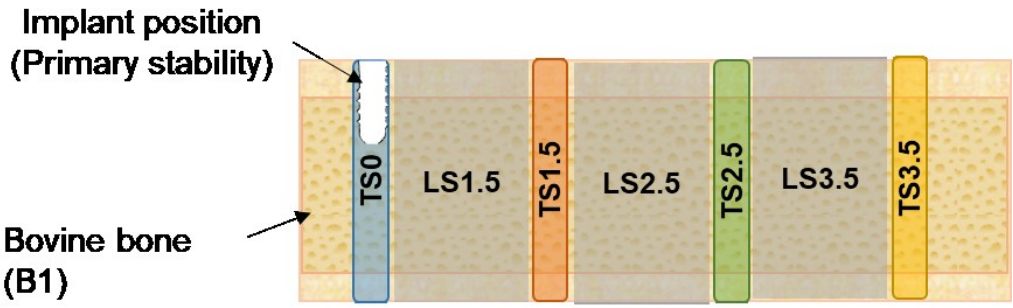

(a)

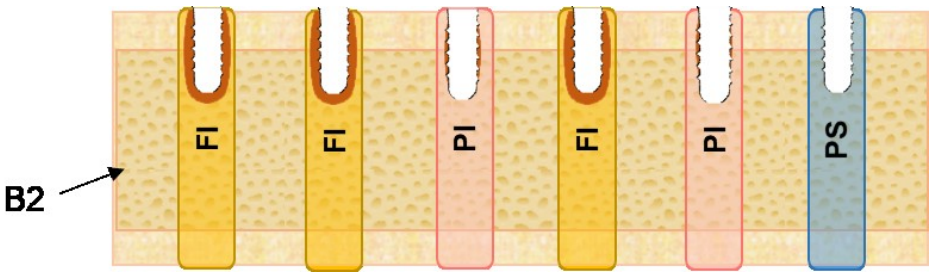

(b)

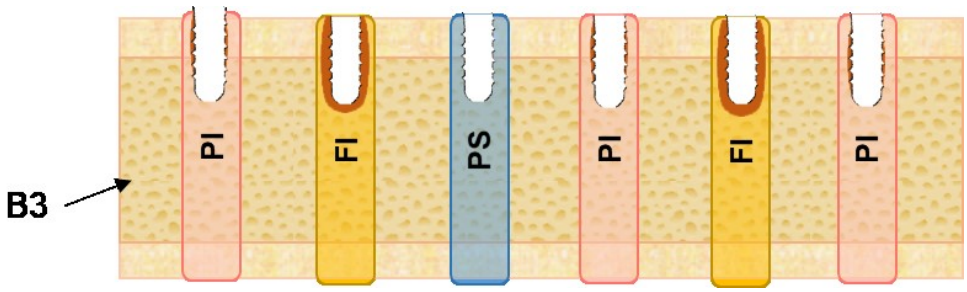

(c)

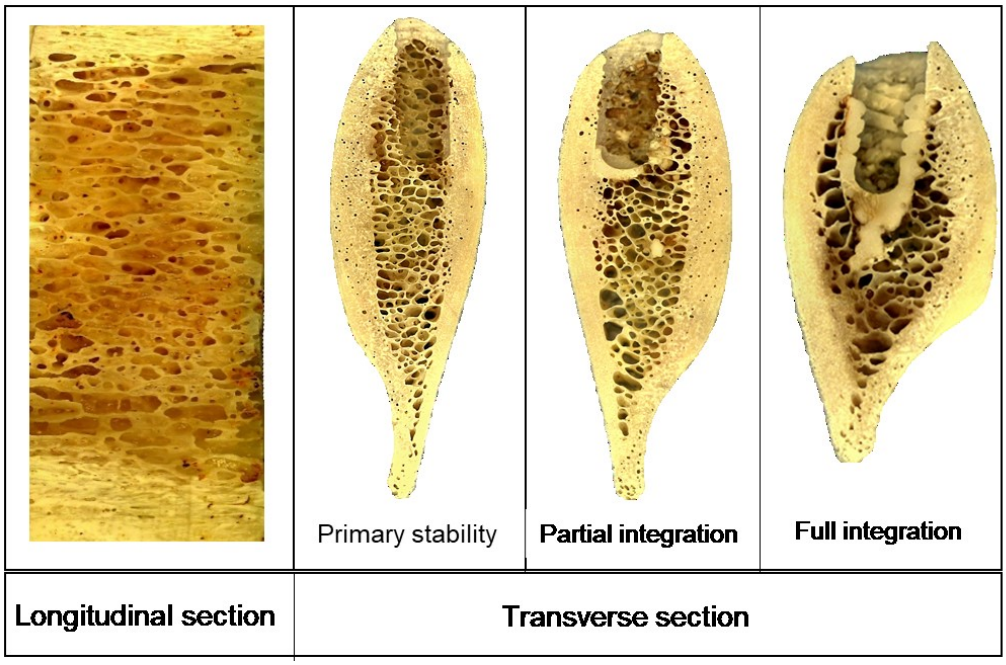

(d)

Figure 3.8: Schematic view for (a) Longitudinal section (LS) and Transverse section (TS) along bone (B1); numbers refer to distance from implant in (cm), (b) Transverse section along B2 and (c) Transverse sections along B3; PS: Primary stability, PI: Partial integration, FI: Full integration. (d) Examples of longitudinal and transverse sections of bone and different stability configurations.

3.2 Experimental procedures

This section describes the procedures for all experiments. First, a set of preliminary assessments is described, followed by details of the rationale and protocols for the systematic experiments.

3.2.1 Preliminary assessments

A set of preliminary tests was performed in order to decide how to configure the systematic investigations. These tests included the effect of ageing and hydration of the bone on transmission, calibration of AE sensors and source, the effect of bone surface curvature, and also interface masking and implant reuse.

3.2.1.1 *Effect of ageing and hydration on AE transmission*

The aim of these tests was, first, to examine the influence of moisture on the AE transmission and, second, to study the effect of ageing in order to establish an appropriate time frame for testing.

Application of water to the implant site

It was observed early in the study that some primary stability installations showed weak transmission despite the use of saline soaked gauze to retain moisture. Given that no irrigation or coolant was applied during preparation of the implant sites, this experiment was designed to determine whether the transmission would be improved by applying water to the implant bed after completing the preparation. A titanium implant was inserted in a hole without any sort of hydration during or after the preparation. After completing AE measurements, the implant was retrieved and the hole was filled with tap water in order to rehydrate the bed before reinserting the implant so that water is squeezed into the adjacent trabecular bone, Figure 3.9 (a, b). At each condition, 15 AE recordings (pencil lead breaks) were taken from each of two sensors mounted on the surface of the bone: one at the position of the implant (measuring only through-bone transmission), and one at 2 cm along the bone from the position of the implant (measuring through-bone and along-bone transmission). The results are presented in Chapter 4, Section 4.1.1.

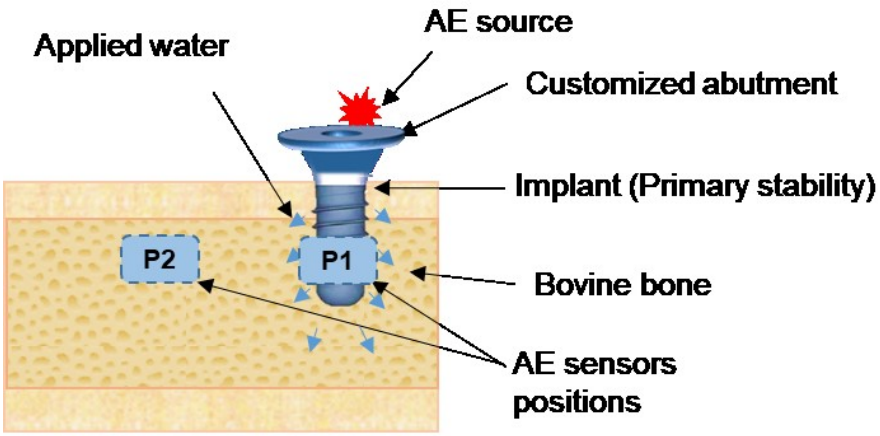

(a)

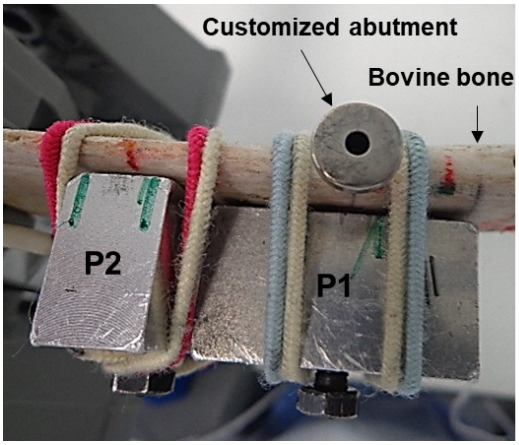

(b)

Figure 3.9 (a, b): Schematic view and experimental set-up for the effect of water on AE transmission. Sensors: S_1 at P1 and S_2 at P2

Effect of ageing on AE transmission

In order to establish a protocol for acquisition, storing and testing bovine bone samples, this simple transmission test was conducted to examine the influence of ageing on the transmission and to select the appropriate time frame for testing. A titanium dental implant was inserted in a fresh bovine bone, in primary stability condition, as described in Section 3.1.1, and hydrated as above with sensors placed as in Figure 3.9. A total of 10 AE recordings were taken for each sensor position immediately after implant installation, and again after one hour. The results are presented in Chapter 4, Section 4.1.2.

3.2.1.2 *Reference tests for variability of the source and coupling, and back-to-back calibration of sensors*

As mentioned above, AE sensors are normally used on metal surfaces, so these tests were conducted on a metal surface to cross-calibrate the two sensors used and to isolate the random variations due to pencil lead breaks and sensor coupling from those in the actual experiments with a bone surface and with the pencil-lead being broken on the abutment.

First, the two Micro-80D sensors, S_1 (127) and S_2 (93), were calibrated back-to-back by positioning them with vacuum grease coupling on the end face of a large cylindrical steel block (38 cm diameter, 20 cm height) equidistant from a pencil lead source on the same surface, Figure 3.10. A total of 10 breaks were recorded at each of the two sensors.

Next, the reproducibility of the pencil lead breaks was assessed by mounting S_1 on the steel cylinder with vacuum grease couplant at a distance of 8 cm from the source and acquiring a total of 50 lead breaks. To analyse the effect of recoupling of the sensor on the reproducibility of the source, the sensor was removed and remounted at the same position and another 50 breaks were acquired. The results are presented in Chapter 4, Section 4.2.

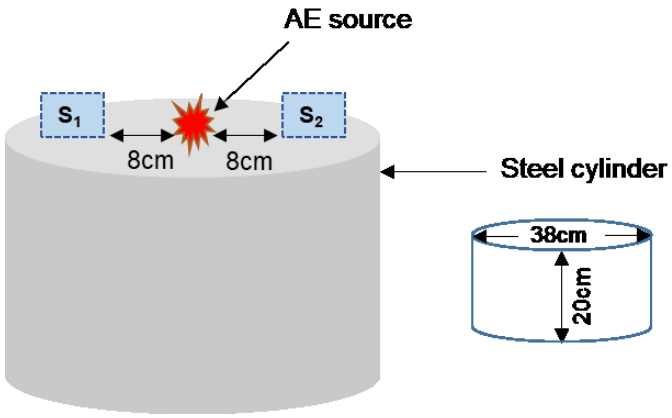

Figure 3.10: AE sensor calibration on cylindrical steel block

3.2.1.3 *Consistency of AE sensor coupling and source in bone configuration*

One of the problems associated with AE measurements in a given practical application is the consistency of the source and the coupling between the

structure and the sensors. Figure 3.11 illustrates the potential inconsistencies involved in the systematic experiments. First of all, breaking a pencil lead on the abutment is different to a set-up on a calibration block and so may not always be as consistent. In addition, bone samples have irregularities of surface form which may complicate coupling of sensors to the surface. Accordingly, this test was undertaken to quantify the reproducibility of placement and coupling of the sensors to the bone surface and also of the AE source. A total of 10 AE recordings were taken with the set-up shown in Figure 3.9, at each position of the sensor. Then, the sensors were removed and remounted three times at the same locations on the bone with fresh ultrasound gel applied, with 3 recordings being taken for each remount. The results are presented in Chapter 4, Section 4.3.

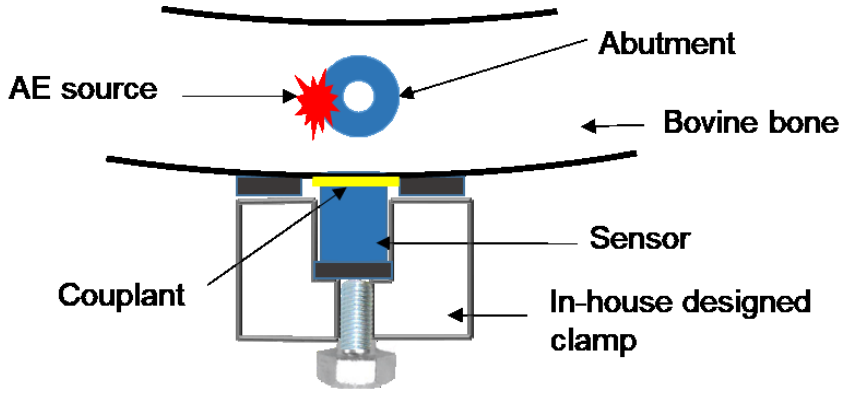

Figure 3.11: AE sensor placement on the bone surface

3.2.1.4 *Effect of bone surface curvature on AE transmission*

The bovine rib model used in this work, like the jaw bone it represents, has a pronounced curvature in that the “buccal” face is convex, whereas the “lingual” surface is concave, Figure 3.12. Accordingly, it was necessary to investigate whether the curvature of the bone sample would significantly influence the signal transmission on either side of the rib. A total of 12 experimental models (primary stability, partial osseointegration and full osseointegration) were prepared randomly in two fresh bovine ribs as described in Section 3.1.1. A total of 20 AE recordings were taken for each installation and collected by a

sensor placed on the buccal surface of the rib at the position of the implant, followed by another 20 recordings taken for the same sensor but placed on the opposite (lingual) surface. The results are presented in Chapter 4, Section 4.4.

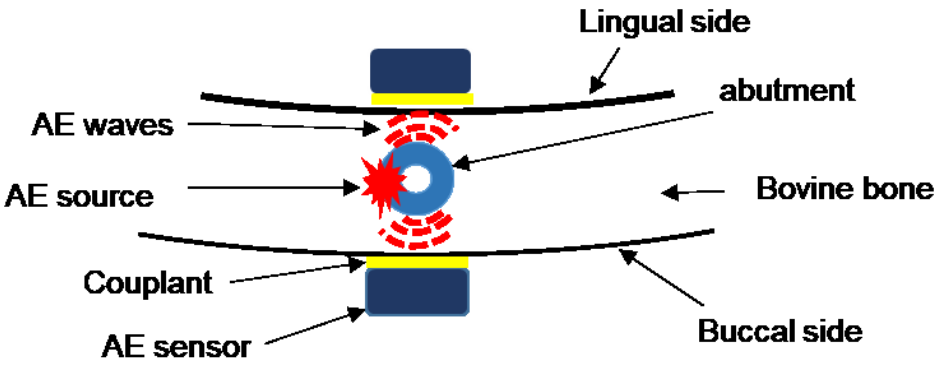

(a)

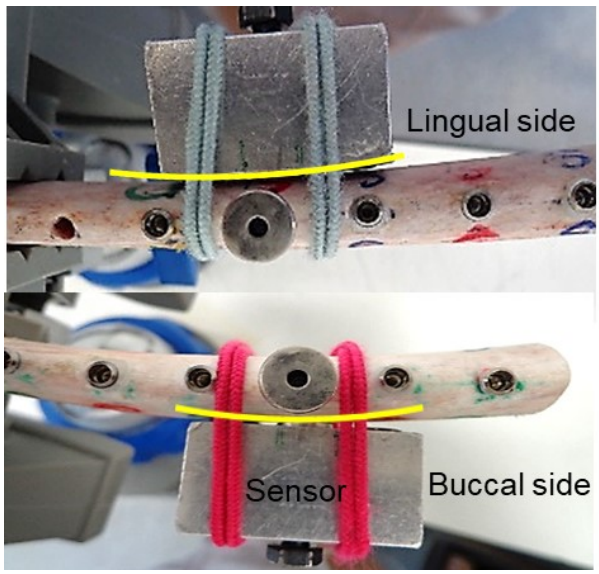

(b)

Figure 3.12: (a) Schematic view of AE sensor coupling on bone surface; (b) Sensor coupling on the simulated buccal and lingual sides of bone

3.2.1.5 *Choice of interface masking material*

Following establishment of the simulated osseointegration model, the next step was to modify this model in order to replicate marginal bone changes

around the osseointegrated implant. A series of tests were conducted to develop a compromised model of osseointegration, by “stopping off” some parts of the transmission path.

Materials with various structures; paraffin wax, impression material (polyvinyl siloxane) and adhesive foam pads were tested for their acoustic attenuation properties. The best candidate (adhesive foam pads) was tested 3 times in total to assess the reproducibility of its application. For creating a compromised bone-implant interface in the fully osseointegration model, a 3 mm length of the cervical surface of the implants (junction between the roughened surface and polished collar of the implant) was coated circumferentially with one of the above materials before embedding into the glass ionomer cement (see Figure 3.13). A fully integrated model was included as a control. For each model, 10 AE recordings which were collected from a sensor placed on the buccal surface adjacent to the model. The results are presented in Chapter 4, Section 4.5.

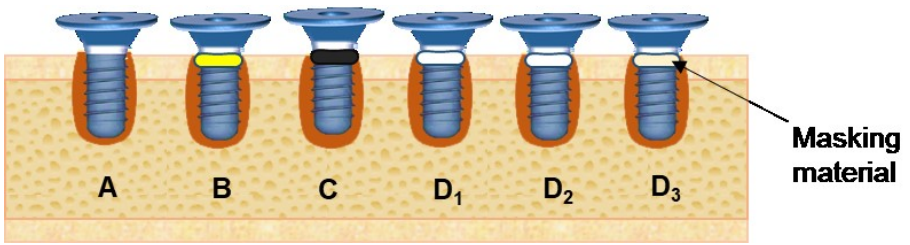

Figure 3.13: Masking implants with wax, impression material or adhesive foam pads A: Full osseointegrated model, B-D: Compromised integration models using: (B) Wax, (C) Impression material, (D) Adhesive foam pads

3.2.1.6 *Re-use of implants*

A limited number of implants had been allocated for the experimental work. Although the preference was to use new implants for each test, it was necessary to know the consequences of reuse. For this test, randomly selected implants from Section 3.2.1.4 were reused to prepare primary stability, partial and full osseointegration models in a fresh bovine rib as per Section 3.1.1. A total of 20 AE recordings were taken for each implant and

collected by a sensor mounted on the surface of the bone, at the position of the implant. The results are later compared with those from Section 3.2.1.4 produced by the same implants, and presented in Chapter 4 Section 4.6.

3.2.2 Systematic experiments

The aim of these experiments was to study the characteristics of AE transmission in bone and through the bone-implant interface, in order to assess to what extent, the quality of the interface affects the transmission. It was therefore necessary to set up a systematic series of experiments to measure the effects of an interface in primary stability, the development of secondary stability (osseointegration) and, ultimately, the degradation of secondary stability. In addition, a separate set of systematic experiments was carried out to measure the influence of bone microstructure on AE transmission, and this is dealt with first.

3.2.2.1 *Effect of bone microstructure on AE transmission through primary stability model*

The aim of this experiment was to investigate the correlation between bone microstructure, bone-implant interface and acoustic transmission. A titanium dental implant was tightly screwed in a fresh bovine rib bone (B1), in primary stability configuration, as per Section 3.1.1. Pulses of acoustic energy were generated on the abutment and collected by two sensors mounted on the bone surface; one adjacent to the implant (measuring only through-bone transmission) and one placed at various axial positions along the bone at distances of 1.5, 2.5 and 3.5 cm from the position of the implant (measuring through-bone and along-bone transmission). Figure 3.14 shows sensors positions on the bone surface. A total of 20 AE recordings were taken at both sensors for each position of the second sensor. Transverse sections at each of the sensor positions and longitudinal sections between the positions were prepared in order to assess the structure of the bone both across and along the bone sample as described in Section 3.3.2.1. The results are presented in Chapter 5, Section 5.1.

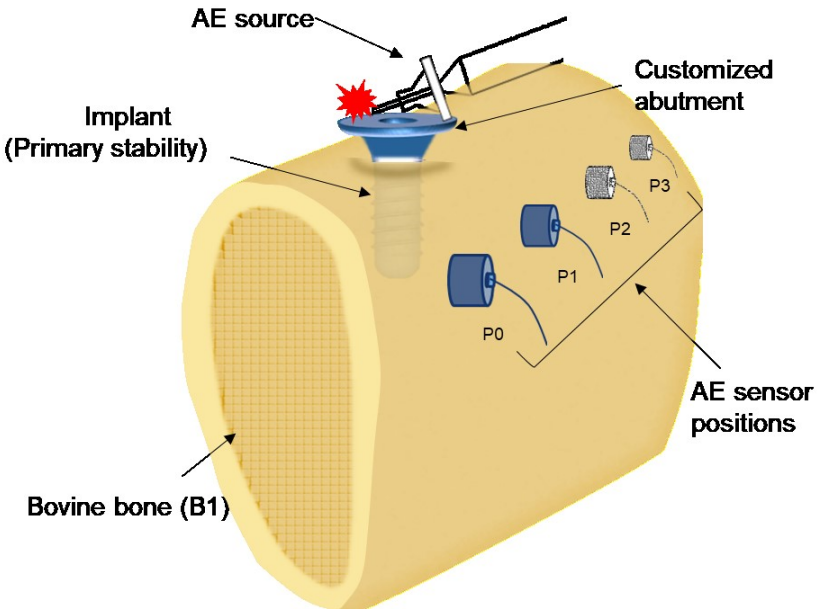

Figure 3.14: Schematic view for arrangement of source and sensor positions on bone. P0: Adjacent sensor position, P1-3: Distant sensor positions; P1: 1.5cm, P2: 2.5cm, P3: 3.5cm

3.2.2.2 *Influence of simulated osseointegration and secondary stability on acoustic transmission*

The objective of this experiment was to assess the potential of AE to monitor the development of secondary stability in implants. To this end, two simulated osseointegration configurations were developed using two different glass ionomer cements (luting and filling GIC). The luting cement was used in the normal-sized implant bed and served as a partial osseointegration model. The filling cement was used in an oversized bed and the implant was effectively cast into place, giving the full integration model. The primary stability configuration (non-osseointegrated) was included in this series of tests as a control. Figure 3.15 is a schematic comparison for the different stability configurations.

A total of 12 new titanium implants were inserted randomly into two fresh bovine ribs (B2, B3) according to the protocol described in Section 3.1.1. Three more primary stability models from different series on different bones (one in B1, two in B4) were also included in the analysis to give a total of 15 experimental models, five models for each stability class. Pulses of acoustic

energy were generated on the surface of the customized abutment using 20 pencil lead breaks for each model, and collected by a sensor placed on the side of the bone, adjacent to the implant position. Histological examination for a series of transverse sections of the different stability configurations was performed as described in Section 3.3.2.2 to obtain the following measurements: average distance between the interface and bone surface, bone porosity, and average width of the simulated osseointegration layer around the implant. The results are presented in Chapter 5, Section 5.2.

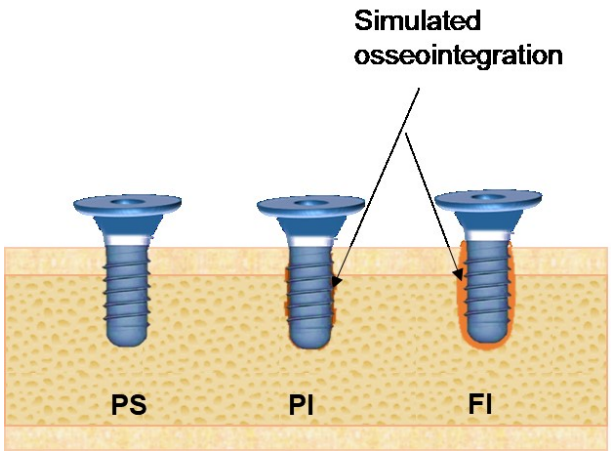

Figure 3.15: Simulated stability configurations, PS: Primary stability, PI: Partial integration, FI: Full integration

3.2.2.3 *Potential of AE energy for diagnosing peri-implant bone loss*

The aim in this set of tests was to assess whether AE transmission could be used to monitor marginal bone loss around an implant which was originally fully integrated. Two types of model were used, simulating circumferential and vertical bone loss, respectively.

Effect of simulated circumferential bone loss on AE transmission

For this experiment, a total of 20 experimental models were prepared in 5 blocks of fresh bovine rib (B5, B6, B7, B8, and B9), 4 models on each bone. Models were distributed randomly on two of the rib blocks using 8 new

implants. The implants were recovered after testing and then re-used randomly again on the other three blocks.

Circumferential defects were created by coating the cervical portion of the implant with strips of adhesive foam pads which increased in depth by 2 mm increments ranging from 1 to 5 mm, as shown in Figure 3.16. Thus, three different compromised interfaces were created to simulate circumferential horizontal marginal bone loss around the implants to three different depths: 1, 3 and 5 mm. An intact fully integrated interface was included for comparison. A total of 20 AE recordings were taken for each implant, collected by a sensor mounted on the side of the bone, adjacent to the implant position. The results are presented in Chapter 5, Section 5.3.1.

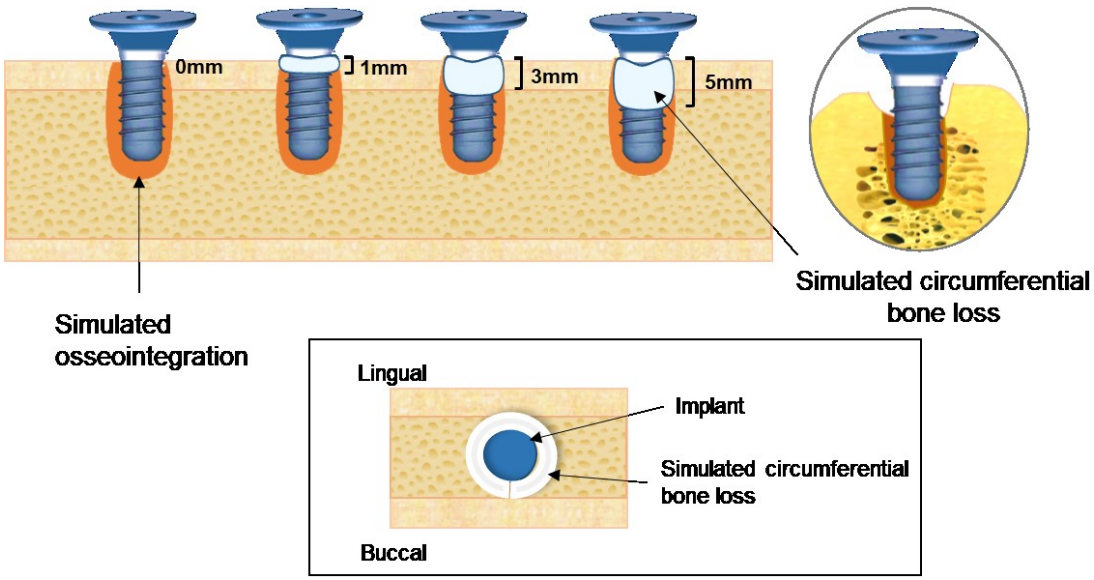

Figure 3.16: Models used to investigate effect of severity of circumferential bone loss on AE transmission

Effect of simulated vertical peri-implant bone loss on AE transmission

The objective of this test was to examine the capacity of transmitted acoustic energy to recognise changes in the circumferential extent (from buccal or lingual sides of the implant) of a vertical bony defect of apical depth of 1 mm. A similar setup to the previous experiment was followed where a total of 25

models were prepared in 5 blocks of fresh bovine rib (B10, B11, B12, B13 and B14), 5 models to each block. Again, 10 new implants were inserted randomly in two of the rib blocks, and then reused randomly for the other three blocks.

For each bone sample, 4 compromised interfaces were prepared with partial vertical defects of different circumferential extents: quarter implant circumference (25% defect), half implant circumference (50% defect), full implant circumference (100% defect), with an intact interface being included as a control. A 50% defect was installed on both buccal and lingual sides of the implant but the recording sensor was placed only on the buccal side, adjacent to the model. Accordingly, the experimental defect models were grouped as shown in Figure 3.17. Again, 20 AE recordings were collected for each model. The results are presented in Chapter 5, Section 5.3.2.

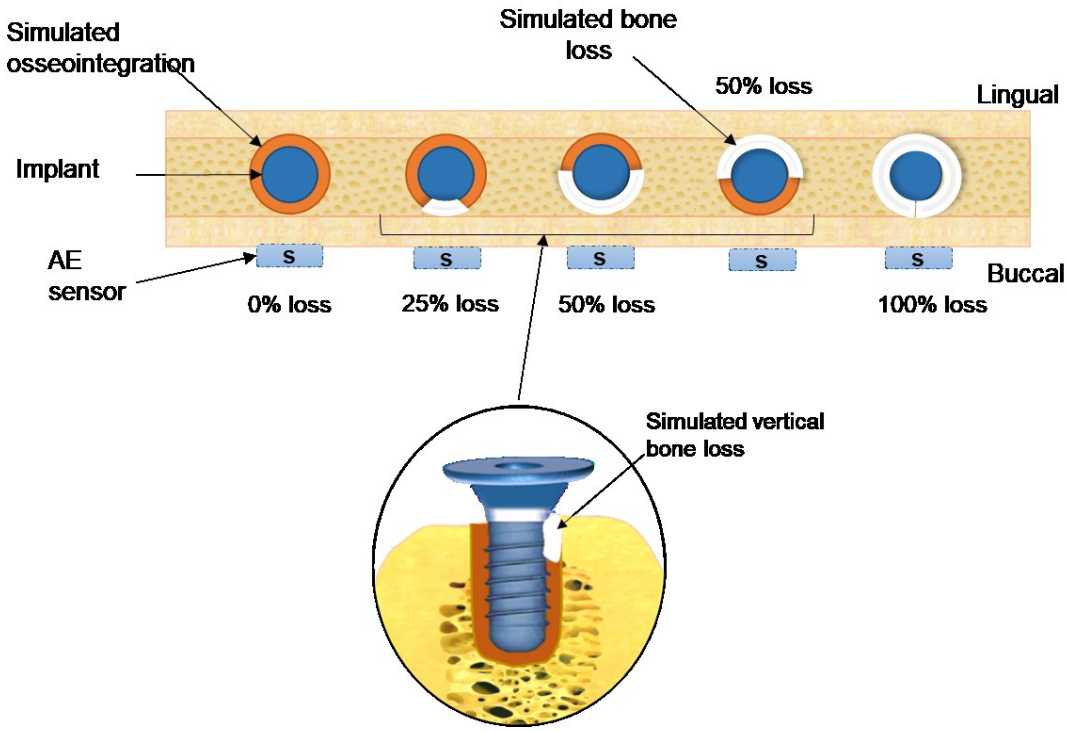

Figure 3.17: Experimental set-up for the effect of vertical bone loss on AE transmission

3.3 Analytical methods

This section describes the techniques used to process the AE and micro-graphical data and to examine the relationship between the systematic parameters.

3.3.1 Acoustic emission signals

AE signals consist of a large number of voltage values sampled at very high frequency (5 million samples per second in this work). Plotted as time series, they can be described as burst-signals or continuous signals, Figure 3.18 (Grosse and Ohtsu, 2008). Burst emissions are discrete signals generated by an individual event (such as a pencil lead break) and continuous emissions are generated by successive emission events from one or many sources, such as a gas jet playing on the surface. The technique used here will relies on propagating a single burst from the pencil lead break to the receiver sensor.

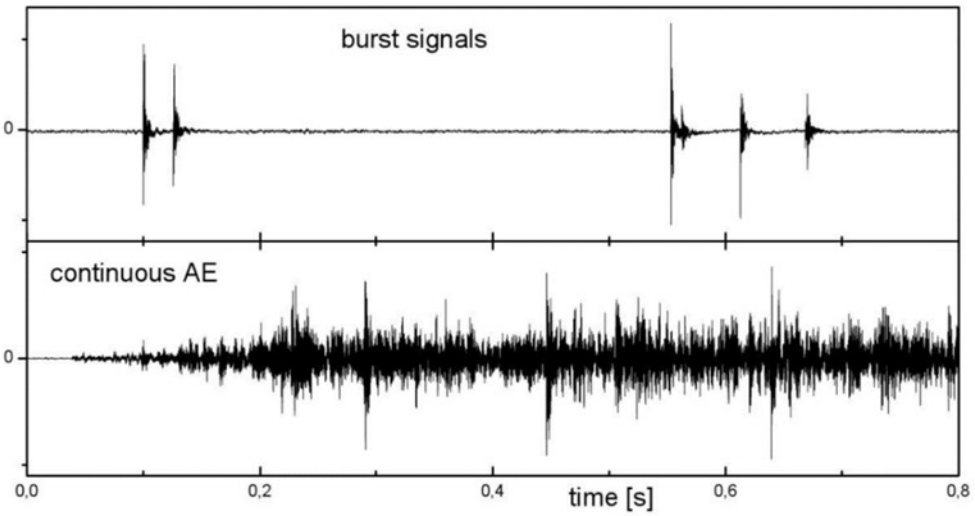

Figure 3.18: AE signal types (Grosse and Ohtsu, 2008)

Figure 3.19a shows a typical time-series of the AE signal emanating from a pencil lead broken on the abutment and recorded by an AE sensor mounted on the surface of bovine bone. As can bee seen, the burst recorded at the sensor decays over a period of around 1 millisecond. In all experiments, the

AE data were acquired at a sampling rate of 5 MHz for 0.1 second, 100 times the scale shown in Figure 3.19a, which is enough to capture all of the wave and to exclude any reflections after the disturbance has crossed the interface (which are not likely to happen in this experiment). It is likely that a certain amount of “riniging” occurs within the implant leading to a series of packets crossing the interface with a slight phase delay and this may be the source of the pulsations with period around 5×10^{-5} sec seen in Figure 3.19a.

All records were analysed by determining the total energy of the voltage-time signal for the entire 0.1 second duration which allows capture of all of the input energy, including that from ringing in the implant. Given that the time duration is constant, the total energy is directly proportional to the area under the curve of the amplitude squared versus time. It is recognised that this procedure will result in some noise being added to the energy from times above about 1.5×10^{-3}sec.

Therefore, the energy for a recorded AE signal was obtained by integrating the square of the amplitude over the fixed time chosen of 0.1 sec as follows (Harris and Bell, 1977):

$$E = \int_0^t V(t)^2 dt$$

E = Acoustic energy in V.s,
V (t) = Amplitude of the AE waveform in volts (V),
t = time in seconds (s)

In practical terms, the total energy of an AE signal was calculated by adding the squared values of each of the 500000 points in each record for each channel. This process was encapsulated in a pre-written algorithm, which was applied to all acquired data yielding a value of AE energy in V.s used throughout this thesis as the measure of transmitted energy, assuming that the input energy (from the pencil lead break and associated implant ringing) is constant.

Figure 3.19 (b and c) shows the segment of AE signal highlighted in Figure 3.19a to illustrate the squaring and integration process of the amplitude at a magnification that allows the individual points to be seen. The energy of this segment is calculated from the area under the curve (the shaded area) which is tantamount to a numerical integration.

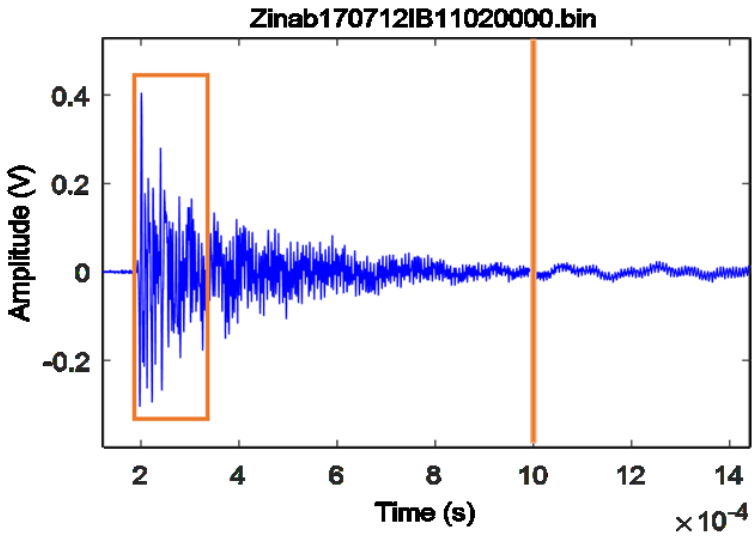

(a)

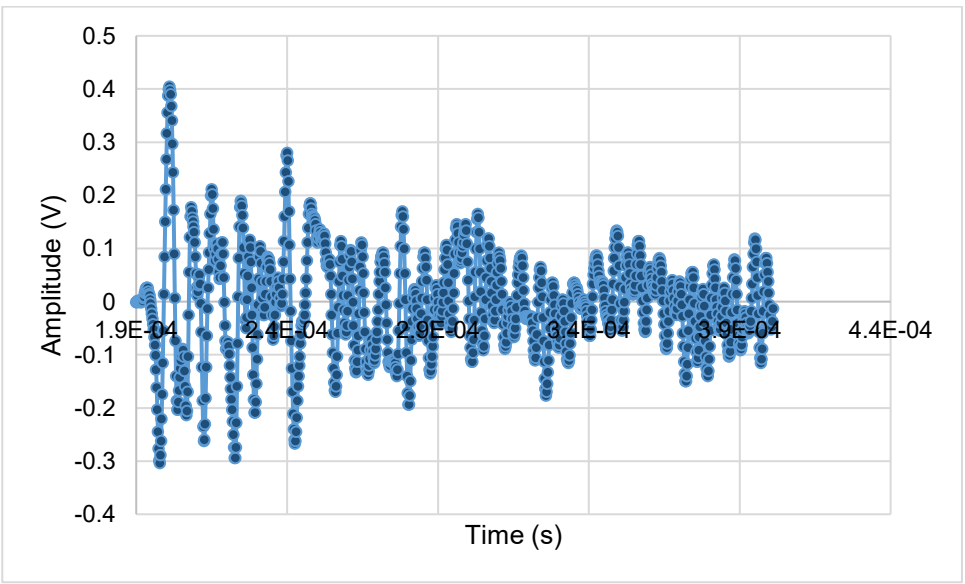

(b)

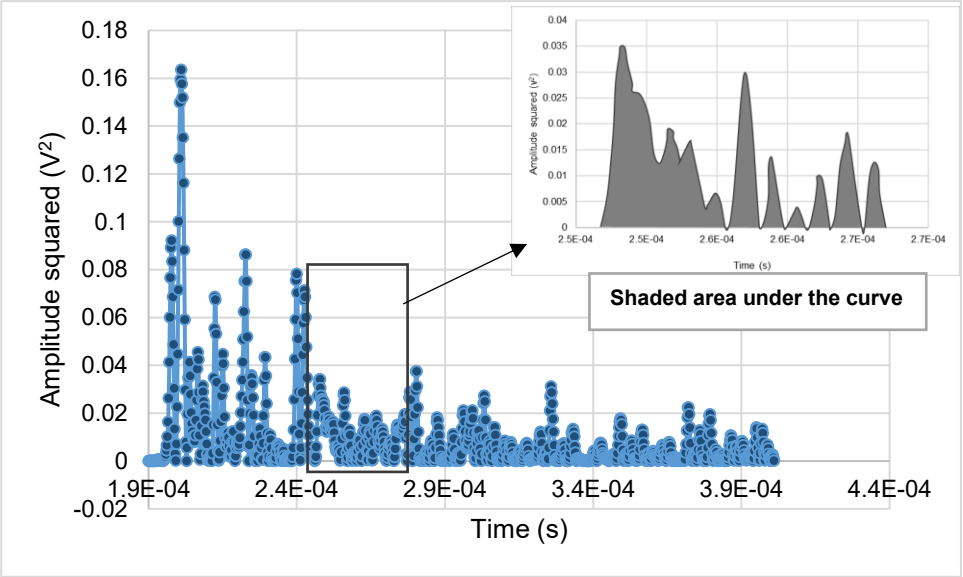

(c)

Figure 3.19: (a) Typical recorded AE signal in bone
(b) The segment of AE signal highlighted in Figure 3.19a
(c): Signal processing; squaring and integrating the amplitudes & the shaded area under the curve

3.3.2 Histological analysis

The microstructural analysis was performed manually on photographic images for the regions of interest (bone and bone-implant interface) as follows:

3.3.2.1 *Bone*

The histological structure revealed in the sections from the first (all sections) and second (those including primary stability models) systematic experiments, Figure 3.8, was examined. A panel of features was measured in order to assess which aspect of microstructure affected the transmission rate. As many features as possible were generated (adapted from various sources see below) in order to describe the distribution of solid and spongy bone as well as the interface between them and to find which are the best indicators of transmission. These include: cortical bone width, the interface between solid and spongy bone assessed by fractal dimension, cancellous and trabecular bone volume fraction, mean free distance in bone, aspect ratio of bone marrow spaces and cross-sectional area of bone.

Cortical width (Cort W)

Cortical bone width is considered the most important feature in this analysis as it is expected to be the main transmission path along the bone, particularly in the primary stability model of bone-implant interface. The width of cortical bone for each transverse section was measured. The widths were measured at points, 2 cm apart, distributed around the entire cortex as illustrated in Figure 3.20a. The mean value in millimetres, was recorded as the cortical width of the section.

Fractal dimension (FD)

The cortical-cancellous interface is one of the boundaries that AE waves would encounter on their path of transmission from source to sensor which may have an effect on the transmitted energy. The interface between the solid (cortex) and spongy (cancellous) bones was expected to be important for through-bone transmission (from implant interface to surface) and not so much for along bone transmission. In a simplified model of transmission, one might expect the AE emanating from the interface to propagate along the cortex and the cancellous bone with a certain amount of leakage from one to another conditioned by the complexity (tortuosity) of the interface. Therefore, in this analysis the fractal dimension of the cortex-core interface was measured from transverse sections of bone at each of the sensor positions, to assess its effect on AE transmission, with an expectation that increasing the tortuosity of this interface would have a positive correlation with the transmission.

Fractal dimension is a geometric parameter used to measure a tortuosity of a perimeter and complexity of microstructures (Mandelbrot, 1967). Box-counting is the most common method for measuring the fractal dimension, and the method has been used previously for fractal analysis of trabecular bone (Fazzalari and Parkinson, 1996). The region of interest was outlined on the photographic image of the transverse section to identify the trabecular perimeter (cortical–trabecular bone interface) as illustrated in Figure 3.20a. Different sized square grids (of side x) were superimposed on the interface along the section and the number of boxes, N(x) landing on the interface was counted, Figure 3.20b. The total number (N) of boxes of side length of (x)

required to completely cover the interface was recorded for (x) varying from 0.4 to 1.25 cm. Next, the total number of counted boxes (N) was plotted against the box size (x) on a double logarithmic scale. Finally, the fractal dimension was calculated from the slope of the line of the log-log plot of data (i.e. log (N) against log(x)).

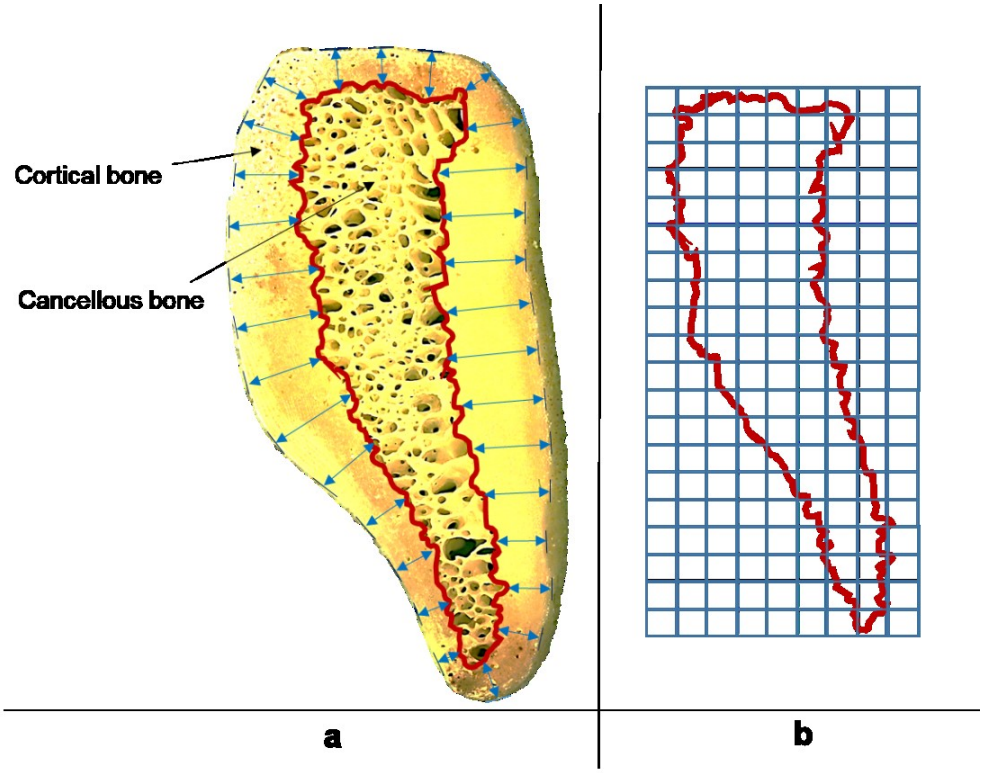

Figure 3.20: Illustration of measurement of (a) width of cortical bone, (b) fractal dimension of cortex-cancellous interface

Cancellous bone volume fraction (Canc VF)

Cancellous bone volume fraction (Canc VF) is the proportion of the whole of a bone section that is cancellous. It was determined using a point counting method (Revell, 1983), by superimposing a 0.5 cm square grid over the bone section image as illustrated in Figure 3.21a. The number of points hitting the cancellous structures (trabeculae and marrow spaces) were counted and related to the total bone tissue grid.

Canc. bone volume fraction = Canc. bone volume / Total bone volume

Trabecular Volume Fraction (Tb VF)

The trabecular volume fraction (Tb VF) was calculated relative to the total cancellous bone volume (trabeculae and marrow) and is therefore a measure of the cancellous bone density. It was also determined by the point counting method (Revell, 1983) using a square grid for each section as illustrated in Figure 3.21b.

Trabecular volume fraction = Trabecular volume / Canc. bone volume

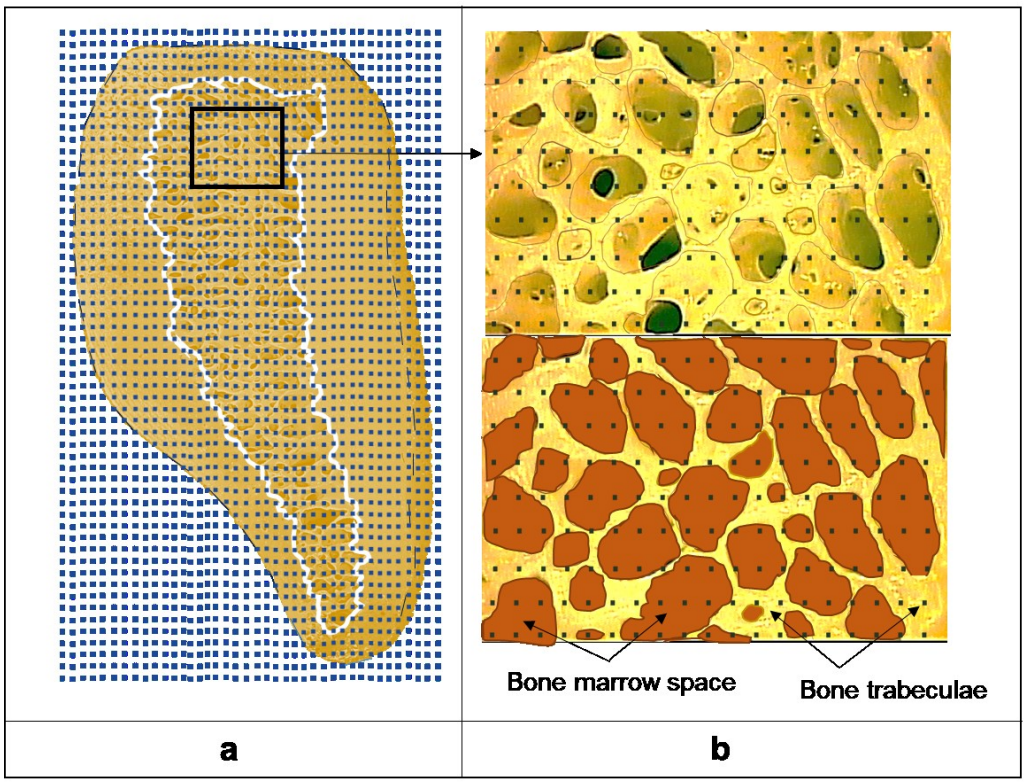

Figure 3.21: Diagram to show the principle of point counting method to calculate: (a) cancellous bone volume fraction (Canc VF). (b) Trabecular volume fraction (Tb VF), the dark brown islands are bone marrow spaces and the matrix (yellow) areas are bone trabeculae. In this section 53 out of the 171 points fall in trabecular areas, so the Tb VF is 31% of the total cancellous bone tissue.

Mean Free Distance in bone (MFD)

Mean free distance of bone is the average straight-line distance through solid components of the bone (cortical and trabecular bone) in a section. It can be regarded as the average distance travelled by an AE wave before it encounters

an interface and may be related to attenuation in porous bone. The method of intercept or cord length estimation (Underwood, 1979) was used in this work to estimate the mean free distance of the trabecular bone (Tb MFD). A set of test straight lines were drawn 1 cm apart along the trabecular bone in horizontal and vertical directions as illustrated in Figure 3.22a. Only the lengths of straight (blue) line intercepts along the trabeculae were measured as shown in Figure 3.22(b, c). The mean length of intercepts for test straight lines, in the horizontal and vertical directions, were calculated and then averaged for the mean free distance of trabeculae. The same procedure was followed to calculate the mean free distance of cortical bone (Cort MFD) in both horizontal and vertical directions.

Aspect ratio of bone marrow spaces (AR)

Aspect ratio of bone marrow spaces is the average ratio of width to height. It was also determined by the method of intercept or cord length estimation (Underwood, 1979). A set of test straight lines were drawn 1 cm apart along the cancellous bone in horizontal and vertical directions, Figure 3.22. The ratio of average width to average height of the marrow spaces that are crossed by the test lines (red) were calculated for the aspect ratio of the bone section.

Aspect ratio of bone marrow space = Average width / average height

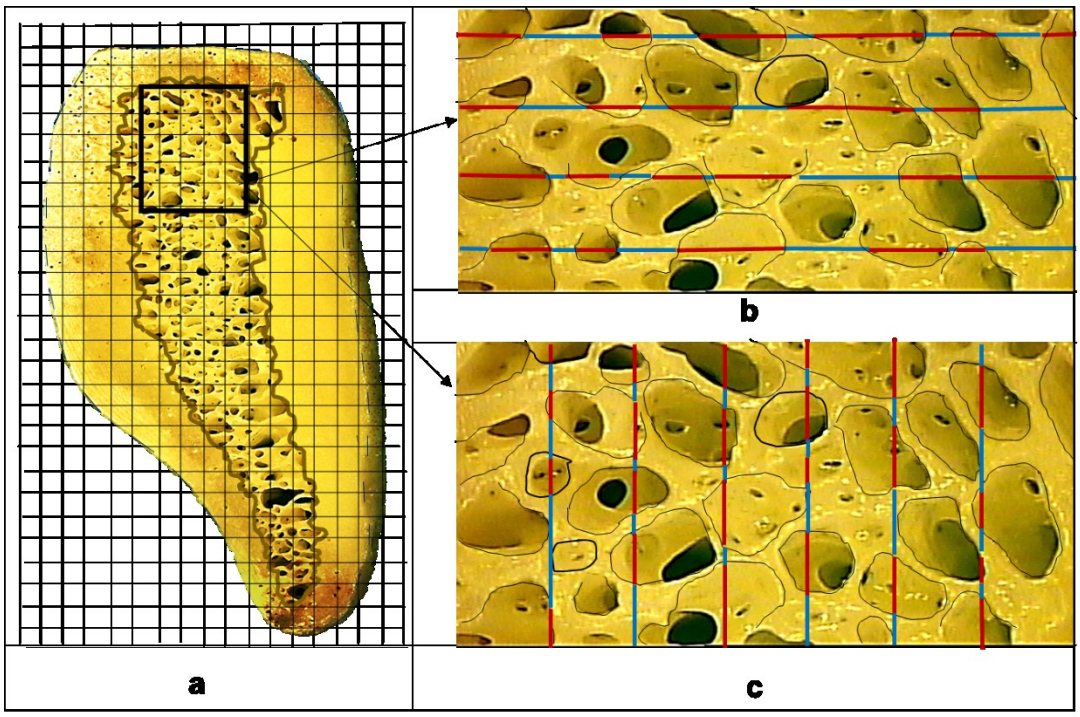

Figure 3.22: (a) Superimposition of line grid on bone section to measure: (1) Mean free distances (MFD): (b) blue horizontal lines to measure Tb HMFD and (c) blue vertical lines to measure Tb VMFD. (2) Aspect ratio (AR): (b) red horizontal lines to measure width of the marrow spaces and (c) red vertical lines to measure height of the marrow spaces.

Cross-sectional area of bone section

The cross-sectional area of the transverse sections of bone was calculated using the Ellipse Model Method (O'Neill and Ruff, 2004). In this method, sub-periosteal (AP) and medullary (ML) breadths were measured from the photographic image as illustrated in Figure 3.23, then the total cross-sectional area (TA) of bone section was calculated using the equation:

$$TA = \pi \times [(AP \times ML) / 4]$$

Subsequently, the cross-sectional area of the solid components of bone tissue, the cortical and trabecular bone, was extracted from the total area using bone volume fractions measured previously as follows:

Area of solid components of bone = Area of trabecular bone + Area of cortical bone

Area of trabecular bone = Total cross-sectional area of bone × Canc. VF × Tb VF

Area of Cortical bone = Total cross-sectional area of bone × (1 – Canc. VF)

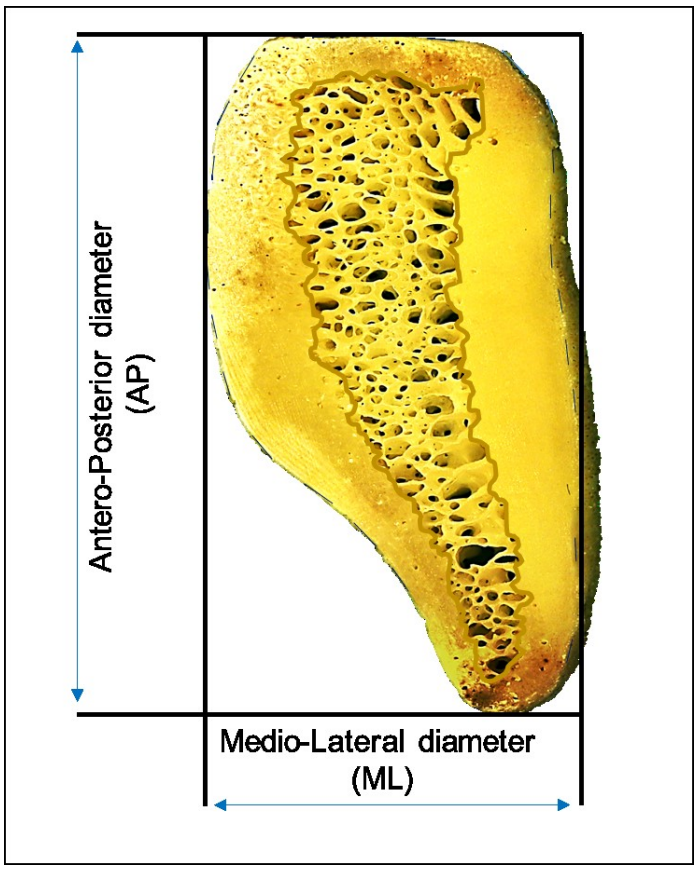

Figure 3.23: Diagram showing the principle of the Ellipse Model Method to calculate the cross-sectional area of bone

3.3.2.2 *Bone-implant interface*

Set of quantitative measurements for interface parameters were obtained from the histological sections of primary stability and osseointegration models.

The following parameters were measured at the region of interest (RoI) for the primary stability and osseointegration models , which includes the peri-implant bone tissues at the side of the adjacent sensor (Figure 3.24), using the same methods described earlier in this section:

1. Average distance between bone-implant interface and bone surface.
2. Bone porosity, estimated by point counting method described in the previous section.

In addition, the width of the simulated osseointegration layer around the implant (simulated bone-implant contact) was measured by calculating the average for the cement widths measured every 2 cm all around the implant.

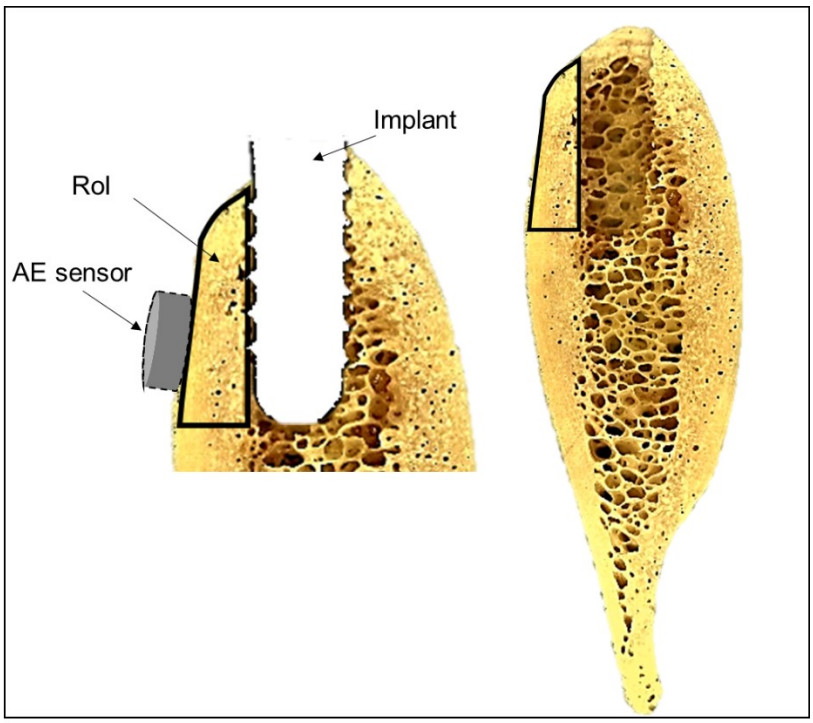

Figure 3.24: Bone-implant interface and adjacent sensor

3.3.3 Statistics

Because this work does not involve patients, all of the statistical methods used were those suitable for physical measurements. All methods used are well-established and relatively straightforward.

For preliminary assessments of the effect of systematic changes, a one-way analysis of variance (ANOVA) was used. For the systematic investigations, one-way or two-way analysis of variance (ANOVA) and Tukey's post-hoc test were performed where indicated to find the effect of individual bones (animal specificity), degree of osseointegration and peri-implant bone loss (circumferential or vertical) on the AE transmission.

Finally, for the effect of continuous variables such as bone density, degree of osseointegration and amount of peri-implant bone loss, regression analysis was performed to evaluate the strength of correlation and provide a quantitative equation. All analysis conducted with the level of statistical significance set at $P \leq 0.05$.

Chapter 4

Results-Ⅰ: Preliminary assessments

This chapter presents and analyses the results of the preliminary measurements. These were carried out to inform and configure the systematic experiments and to establish a number of practical issues with the overall aim of quantifying the random variability in the systematic experiments.

Areas where preliminary assessments were carried out included:

- the effect of ageing and hydration of the bone on AE transmission,
- reference tests for variability of the source and coupling, and back-to-back calibration of sensors,
- variability of AE sensor coupling on bone surface and source onto abutment,
- effect of bone surface curvature on AE transmission,
- choice of interface masking material,
- re-use of implants.

These are presented in following sections and are followed by a summary of findings.

4.1 Effect of ageing and hydration on AE transmission

Bones were acquired in small quantities and it was necessary to establish, as far as possible, the effect of time since removal from the carcase on AE transmission in nominally identical tests.

4.1.1 Application of water to the implant site

Since installation of the implant was carried out *ex vivo*, this test (described in Chapter 3 Section 3.2.1.1) was designed to determine whether the transmission would be improved by applying water to the implant bed during installation. Figure 4.1 compares the average of 15 breaks for the energy transmitted through dry and wet implant beds measured at two sensor

positions (one adjacent to the implant, and one 2 cm along the bone from the implant) for a single implant installation. There is a substantial increase in average energy, by a factor of around two, for transmission to the adjacent sensor, and around three for transmission to the more distant sensor. To test for statistical significance of this, ANOVA was carried out for the two groups of data with and without hydration for each of the sensor positions. The resulting P-values (at 5% significance level), Table 4.1, shows that the differences observed in Figure 4.1 are statistically significant. Accordingly, water was applied to the prepared implant site for all primary stability models throughout the study.

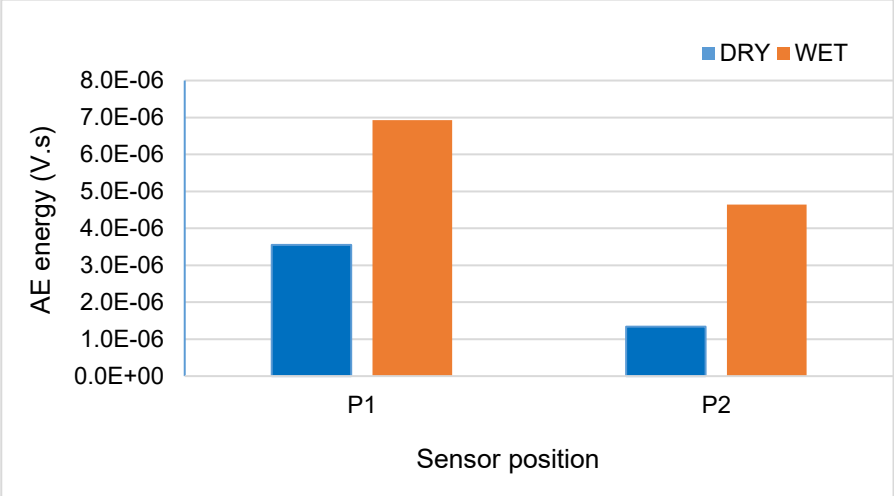

Figure 4.1: Average transmitted AE energy through dry and wet implant beds for sensor positions P1 and P2

	P1	P2
P-value	4.56×10^{-5}	1.7×10^{-8}

Table 4.1: ANOVA significance summary for dry and wet implant beds for sensor positions P1 and P2

4.1.2 Effect of ageing on AE transmission

The objective of this test (described in Chapter 3, Section 3.2.1.1) was to examine the influence of ageing (effectively drying out of the bone) on the

transmission and to select the appropriate time frame for testing. Table 4.2 shows ANOVA results for the influence of sample ageing on the transmission through the interface for the two sensor positions P1 and P2 described above for 10 pencil breaks per observation on a single installation on a single bone. As can be seen, the mean energy decreases by about 10% / hr at the sensor position adjacent to the implant (P1) and by about 50% / hr at the sensor position along the bone (P2). The P-values indicate that this difference is significant at position P2, but not at position P1. In view of these results, it was decided to ensure that all primary stability tests were completed within an hour of implant placement and, even then, it must be acknowledged that there could be around 10% reduction in recorded energy when the sensor is adjacent to the implant and more if it is not.

Sensor position	**Mean**		**Standard deviation**		**P- value**
	Immediately	**After 1 hr.**	**Immediately**	**After 1 hr.**	
P1	4.08×10^{-5}	3.66×10^{-5}	6.50×10^{-6}	8.42×10^{-6}	0.224
P2	2.95×10^{-5}	1.46×10^{-5}	8.91×10^{-6}	2.68×10^{-6}	7.75×10^{-5}

Table 4.2: Summary of ANOVA for the effect of sample ageing on AE transmission

4.2 Reference tests for variability of the source and coupling, and back-to-back calibration of sensors

This reference test, described in Chapter 3 Section 3.2.1.2, allowed an assessment of the uncontrolled variations in the recorded AE data due to: (1) sensor sensitivity, (2) pencil lead breaks and (3) sensor coupling. First, two well-studied Micro-80D sensors, S_1 (127) and S_2 (93), were tested back-to-back by positioning them on the end face of a large cylindrical steel block equidistant from a pencil lead source on the same surface. Figure 4.2 shows the averages of 10 pencil lead breaks and the associated standard deviations of AE energy recorded by the two sensors.

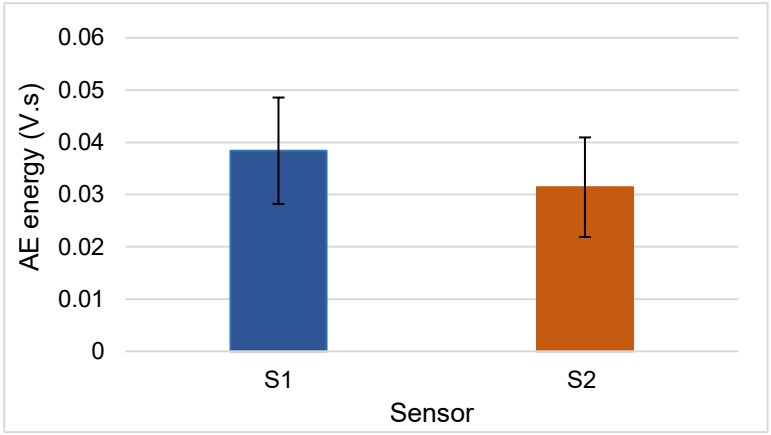

Figure 4.2: Box plots of AE energy for calibration of two sensors on steel block

Although it appears from Figure 4.2 that S_2 is less sensitive than S_1, an ANOVA test (Table 4.3) shows that the P-value (around 0.1) is greater than the 0.05 confidence level used for all other variance tests. This means that the individual sensor sensitivity is not significant in the face of the other potential sources of uncontrolled error. Most of the systematic tests are carried out using one sensor (S_1:127) so this finding is only of importance when considering the transmission tests along the bone where two sensors are used (see Section 5.1.1).

ANOVA: Single Factor

Summary

Groups	*Count*	*Sum*	*Average*	*Variance*	*SD/Mean (%)*
S_1	10	0.384	0.038	1.04×10^{-4}	27
S_2	10	0.314	0.031	9.07×10^{-5}	30

ANOVA

Source of variation	*SS*	*df*	*MS*	*F*	*P-value*	*F crit*
Between groups	2.44×10^{-4}	1	2.44×10^{-4}	2.51	0.13	4.41
Within Groups	1.75×10^{-3}	18	9.72×10^{-5}			
Total	1.99×10^{-3}	19				

Table 4.3 ANOVA for S_1 and S_2 data calibration on steel block

Next the reproducibility of the pencil lead breaks was assessed by mounting one of the sensors (S_1) on the end face of the steel cylinder and acquiring a total of 50 lead breaks without moving the sensor. Figure 4.3 shows a histogram of the AE energy, which looks reasonably Gaussian. The ratio of the standard deviation to the mean for the 50 breaks showed that the energy recorded for this installation varies by about 30%.

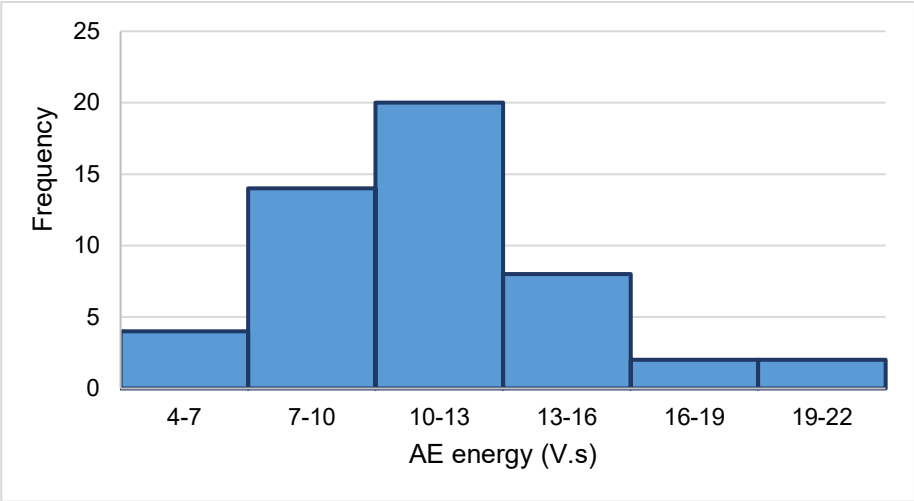

Figure 4.3: Histogram of AE energy values

Finally, to assess the effect of coupling of the sensor, it was removed and remounted at the same position and another 50 breaks were acquired. Figure 4.4 shows the averages and standard deviations of AE recorded for each set.

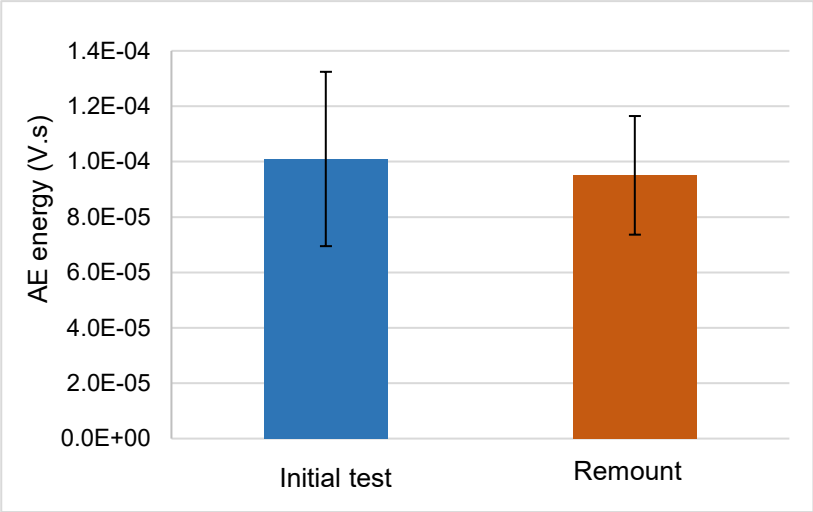

Figure 4.4: Box plots of AE energy when sensor is remounted

To examine the effect of recoupling *vs* pencil lead break variability, an ANOVA was carried out to compare the variation due to coupling (between-groups) with that due to pencil lead breaks (within-groups). As can be seen from Table 4.4, P-value is 0.275 at 5% confidence level, indicating that the variability due to pencil lead breaks is greater than that due to sensor coupling on the steel block (although see later for coupling on a bone). The mean is about 5% lower for the remounted set and the ratio of the standard deviation to mean is also lower (around 20% *vs* 30%).

ANOVA: Single Factor

Summary

Groups	*Count*	*Sum*	*Average*	*Variance*	*SD/Mean (%)*
Initial test	50	5.05×10^{-3}	1.01×10^{-4}	9.91×10^{-10}	31
Remount	50	4.75×10^{-3}	9.51×10^{-5}	4.59×10^{-10}	23

ANOVA

Source of variation	*SS*	*df*	*MS*	*F*	*P-value*	*F crit*
Between Groups	8.73×10^{-10}	1	8.73×10^{-10}	1.2	0.275	3.94
Within Groups	7.1×10^{-8}	98	7.25×10^{-10}			
Total	7.19×10^{-8}	99				

Table 4.4: ANOVA for consistency of AE sensor coupling and source

This set of tests shows that, on a flat metal surface, the variability due to the pencil lead break is more significant than either sensor coupling or sensor. The ratio of standard deviation to mean for each set of pencil lead breaks is between 20 and 30%. Sensor coupling on typical actual bone surface used in the experiments is assessed in the following section as is the reproducibility of the source on the actual configuration used in the systematic experiments.

It was not necessary to carry out tests on sensor coupling by mounting and remounting of the sensor on the steel block. Instead, a previous published study (El-Shaib, 2013) using the same sensors and amplifiers as used here was adopted, which has shown that removal and installation of the sensor results in a variability in the AE energy of about 20%.

4.3 Consistency of AE sensor coupling and source in bone configuration

This test, described in Chapter 3 Section 3.2.1.3, was conducted to assess the reproducibility of placement and coupling of the sensors to the bone surface and also of the AE source in the actual configurations used in the experiments. Table 4.5 shows a summary of ANOVA comparing the variability due to sensor coupling with variability of the pencil lead break source for the two sensors placed adjacent to the implant (S_1) and 1.5 mm along the bone from the implant (S_2). Tested at the 5% confidence level, the P- values were 10^{-5} and 0.004 for S_1 and S_2, respectively, indicating that the variability in coupling of the sensors on the bone surface is greater than that due to the pencil lead fracture. The average ratio of standard deviation to mean of the transmitted energy due to the source is in the region of 10, meaning that there is an inherent variability of ±10% due to the source, compared with ±20-30% for pencil lead breaks on the calibration block.

Table 4.5: ANOVA summary for consistency of AE sensor coupling and source

(a) Position S_1

Groups	*Count*	*Average*	*Variance*	*SD/Mean (%)*
Initial installation	10	4.08×10^{-5}	4.22×10^{-11}	16
Remount-1	3	3.38×10^{-5}	1.27×10^{-10}	33
Remount-2	3	4.22×10^{-5}	2.12×10^{-11}	11
Remount-3	3	6.87×10^{-5}	1.33×10^{-11}	5

ANOVA

Source of variation	*SS*	*df*	*MS*	*F*	*P-value*	*F crit*
Between Groups	2.25×10^{-9}	3	7.5×10^{-10}	16	6.09×10^{-5}	3.29
Within Groups	7.03×10^{-10}	15	4.69×10^{-11}			
Total	2.95×10^{-9}	18				

(b) Position S_2

Groups	*Count*	*Average*	*Variance*	*SD/M (%)*
Initial installation	10	2.95×10^{-5}	7.94×10^{-11}	30
Remount-1	3	1.57×10^{-5}	1.04×10^{-12}	6
Remount-2	3	4.04×10^{-5}	4.07×10^{-11}	16
Remount-3	3	3.75×10^{-5}	6.21×10^{-12}	7

ANOVA

Source of variation	*SS*	*df*	*MS*	*F*	*P-value*	*F crit*
Between Groups	1.11×10^{-9}	3	3.69×10^{-10}	6.82	0.004	3.29
Within Groups	8.11×10^{-10}	15	5.41×10^{-11}			
Total	1.92×10^{-9}	18				

4.4 Effect of bone surface curvature on AE transmission

Table 4.6 shows summary results of ANOVA for the effect of bone curvature on AE transmission (the test is described in chapter 3 Section 3.2.1.4). The 20 AE energies for each configuration for each bone were grouped according to whether they were recorded on the buccal or lingual side and tested at the 5%

confidence level. As well as the P-values, the ratio of average energy recorded at the buccal side to that recorded at the lingual side (Eb/El) is also shown for each of the models tested. As can be seen, the difference in recorded energy is only significant in 8 of the 12 models tested and the energy is higher on the buccal side in (a different) 7 of the 12 models. This suggests that the curvature is not the most significant source of variation, and other factors, such as the asymmetry of the bone structure and the reproducibility of placement (see above), are more likely to account for the changes. Nevertheless, it was decided to concentrate systematic measurements on the buccal side, as this is more clinically practicable.

Bone-2 / Buccal *vs* Lingual						
	Full integration	Full integration	Primary stability	Partial integration	Full integration	Partial integration
P-value	0.862	6×10^{-4}	0.018	0.628	0.324	2.47×10^{-9}
Eb/El	2.75	1.30	0.908	1.03	0.913	3.63
Bone-3 / Buccal *vs* Lingual						
	Partial integration	Full integration	Primary stability	Partial integration	Full integration	Partial integration
P-value	1.03×10^{-7}	6.26×10^{-6}	0.023	0.222	7.45×10^{-9}	8.76×10^{-9}
Eb/El	0.58	1.76	0.88	0.96	2.63	2.29

Table 4.6: Summary of ANOVA analysis and buccal /lingual AE ratio for effect of bone curvature

4.5 Choice of interface masking material

The aim of this simple transmission test (described in Chapter 3 Section 3.2.1.5) was to search for a model which can be used to simulate bone loss around the implant. Paraffin wax, impression material (polyvinyl siloxane) and adhesive foam pads were tested for their acoustic attenuation properties and reproducible application. As shown in Figure 4.5, the adhesive pads transmitted the lowest energy, which indicates that they would be the best

material to use to inhibit AE transmission and hence model an integration defect.

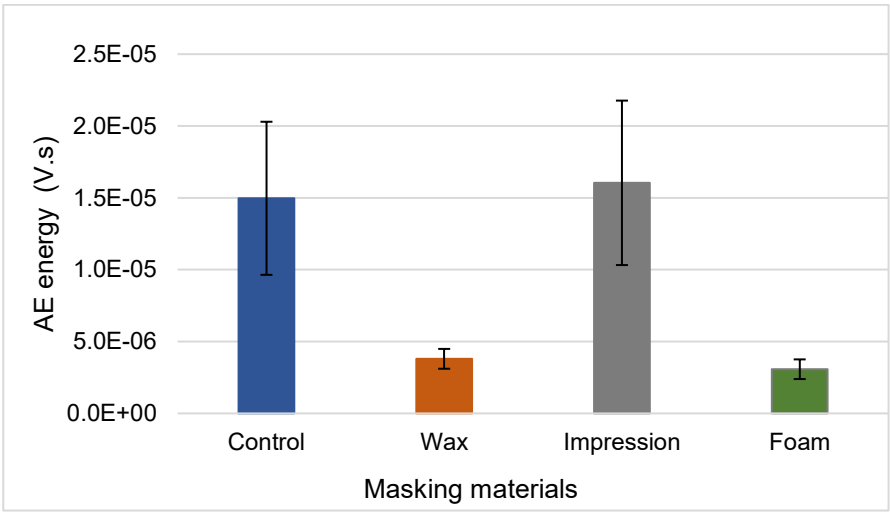

Figure 4.5: Comparison of transmitted energy for candidate masking materials

To develop the defect model, another test was required to examine the reproducibility with which the adhesive foam could be used to simulate a given peri-implant bone defect. Accordingly, two additional samples, using the adhesive foam pads, were prepared and tested the same way as above. The ANOVA of the three samples indicated a P-value larger than 0.05 (Table 4.7) which indicates that the models are reproducible, in the face of the other potential sources of variation.

Foam pad models

Groups	*Count*	*Sum*	*Average*	*Variance*
Foam-1	10	3.08×10^{-5}	3.08×10^{-6}	4.69×10^{-13}
Foam-2	10	3.91×10^{-5}	3.91×10^{-6}	3.56×10^{-12}
Foam-3	10	4.56×10^{-5}	4.56×10^{-6}	1.52×10^{-12}

ANOVA

Source of Variation	*SS*	*df*	*MS*	*F*	*P-value*	*F crit*
Between Groups	1.1×10^{-11}	2	5.52×10^{-12}	2.98	0.067	3.35
Within Groups	4.99×10^{-11}	27	1.85×10^{-12}			
Total	6.1×10^{-11}	29				

Table 4.7: ANOVA for the reproducibility of foam pads defect models

4.6 Reuse of implants

A limited number of implants had been allocated for the experimental work. Although the preference was to use new implants for each test, it was necessary to conduct this test (described in Chapter 3 Section 3.2.1.6) to know the consequences of reuse. ANOVA was carried out to determine whether there is any difference in transmission between models using new or reused implants. For each different stability model, the 20 pencil lead breaks were grouped into new or reused and tested at 5% confidence level. P-values are shown in Table 4.8, all are higher than 0.05 confidence level, indicating no significant differences in the signal transmitted when the implant is re-used for the same model.

	Full integration	Partial integration	Primary stability
P-value	0.521	0.403	0.459

Table 4.8: Summary of ANOVA for the effect of reusing the implants on AE

4.7 Summary of preliminary results

The preliminary assessments have resulted in / suggested the following actions for systematic measurements:

- AE energy has been shown to be affected by the moisture level at the bone-implant interface. If water is applied to the implant bed during installation, transmission from a primary stability model to sensors placed adjacent and some way along the bone increases by a factor of about 2 or 3 times, respectively. In addition, the transmission for these models through and along bone fell by 10% and 50%, respectively, one hour after installation. Accordingly, it was decided to apply water in all primary stability models and to perform the transmission tests within one hour of installation.

- The energy recorded for a given installation can vary due to the pencil lead breaks on the implant abutment by about 10%, whereas sensor remounting increases the variability in the energy to 30% (including the pencil lead break).
- Neither the curvature of the bone samples or reuse of the implants resulted in any significant changes in the transmission in the face of other factors, such as asymmetry of bone structure and reproducibility of sensor and implant placement. Nevertheless, it was decided to make the systematic measurements on the “buccal” side of the rib as they would be in the real situation.
- Adhesive foam pads were good enough to model a peri-implant bone defect due to their acoustic attenuation and reproducible application.

Chapter 5

Results-Ⅱ: Systematic experiments

This chapter presents and analyses the results of the systematic experiments.

Three sets of systematic experiments were carried out to investigate:

- The influence of bone microstructure on AE transmission through primary stability model.
- The effect of simulated osseointegration and secondary stability on AE transmission.
- Potential of acoustic energy for diagnosing peri-implant bone loss.

The results of these experiments are presented below, followed by a summary of the key findings.

5.1 Influence of bone microstructure on AE transmission through primary stability model

This part of the study, described in Chapter 3 Section 3.2.2.1, was designed to examine the influence of bone microstructure on the transmission of AE signals through and along bone. The effect of transmission through the bone-implant interface was not varied from a fixed level of primary stability, and a single bone (B1) and a single implant installation were used. Two sets of tests were performed, aimed at transmission along the bone and through the bone, respectively and these are discussed in turn below.

5.1.1 AE transmission along bone

This test (summarised in Figure 5.1) was intended to characterise AE attenuation by the bone material itself. A single (primary stability) installation of implant in a single bone (B1) was used to inject the AE wave so that the only uncontrolled variable was the pencil lead break. Sensor S_2 was placed at positions P1, P2 and P3 in order to record the attenuation relative to the sensor S_1 at P0 which was not moved during the test, thus avoiding any variation in

the reference signal due to coupling. The bone microstructure was first measured in detail to find which features correlated best with attenuation, prior to developing an attenuation model.

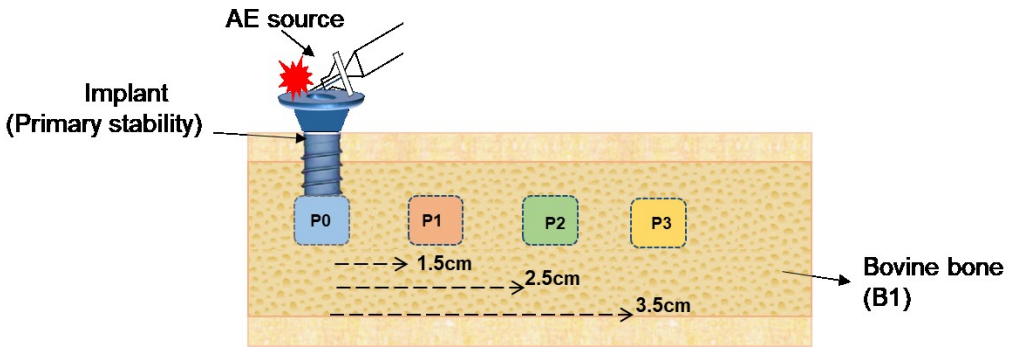

Figure 5.1: Schematic view for AE source and sensor positions (P0-3) on the bone

5.1.1.1 Microstructural parameters of bone

Detailed measurements of selected microstructural parameters of bone tissues were obtained from the transverse sections (at each sensor position, TS) and longitudinal sections (between sensors positions, LS) of the bone sample, as illustrated in Figure 5.2 (adapted from Figure 3.8 for clarity).

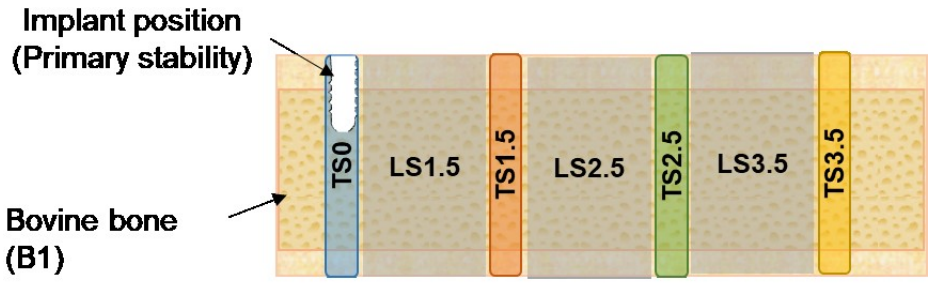

Figure 5.2: Labelling scheme for the transverse and longitudinal sections in bone (B1)

Figure 5.3 shows the variation of the various microstructural parameters along bone B1 alongside the AE energy. The AE energy recorded at each of the

sections would be expected to decrease, even if the microstructure remained constant along the bone, so the microstructural analysis is a conditioning factor only. As can be seen, all of the microstructural parameters vary systematically along the bone, some, such as the fraction of the cross-section which is cancellous (Canc VF) and the proportion of the trabeculae (i.e. density) of the cancellous bone (Tb VF) reinforcing the gradient in AE and some, such as the width of the cortex (Cort W) reducing the gradient. The remaining microstructural measurements are of secondary interest; the fractal dimension of the boundary between the cortical and cancellous bone gives an assessment of the transmissibility between the cortex and the core; the horizontal and vertical mean free distances give an assessment of the asymmetry of the connectivity of the bone in the vertical and horizontal directions.

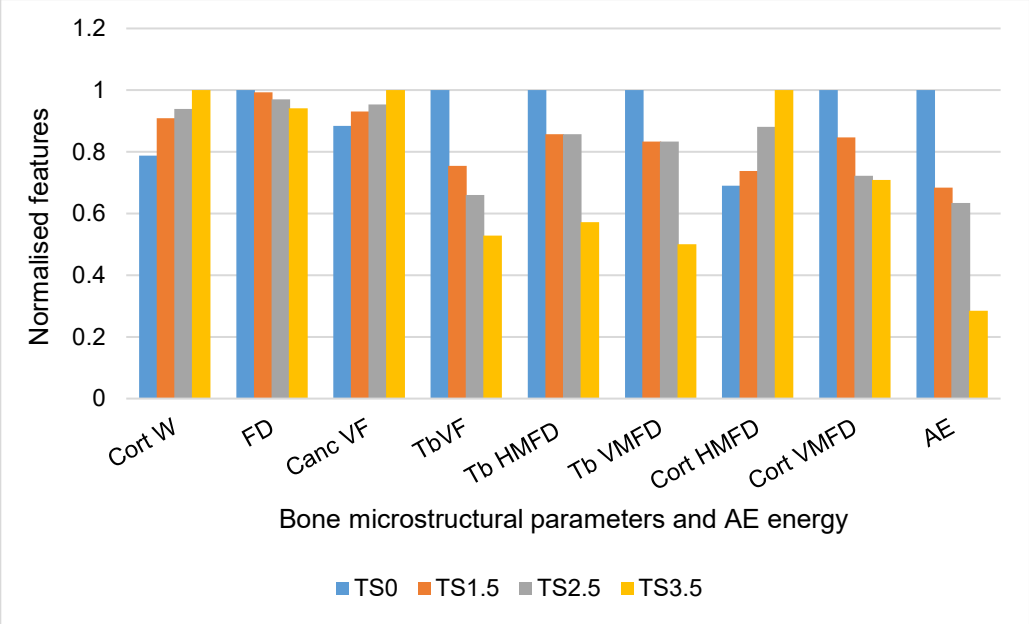

Figure 5.3: Relative AE energy and normalised bone microstructural parameters for transverse sections of bone (TS): Cortical width (Cort W), Fractal dimension (FD), Cancellous volume fraction (Canc VF), Trabeculae volume fraction (Tb VF), Trabecular horizontal and vertical mean free distances (Tb HMFD, Tb VMFD) and Cortical horizontal and vertical mean free distances (Cort HMFD, Cort VMFD).

Figure 5.4 shows the microstructural parameters obtained from the longitudinal sections of the bone between the positions of the sensors, along with the associated AE energies. As would be expected, the cancellous and trabecular volume fractions show a similar (although weaker) variation along the length between sections. Of additional interest are the trabecular and cortical horizontal mean free distances, since the horizontal dimension in these sections is along, rather than across the bone.

Figure 5.5 compares the absolute values of trabecular and cortical horizontal mean free distances between the transverse and longitudinal sections. As it can be seen, both distances are longer along the bone in the longitudinal sections than across the bone in the transverse sections, which allow more transmission. This asymmetry of microstructure, whilst interesting, is not of great significance for the current study as transverse transmission had little effect on the experiments reported. However, it will be of significance when developing a system for clinical use where individual patients may have very different bone densities.

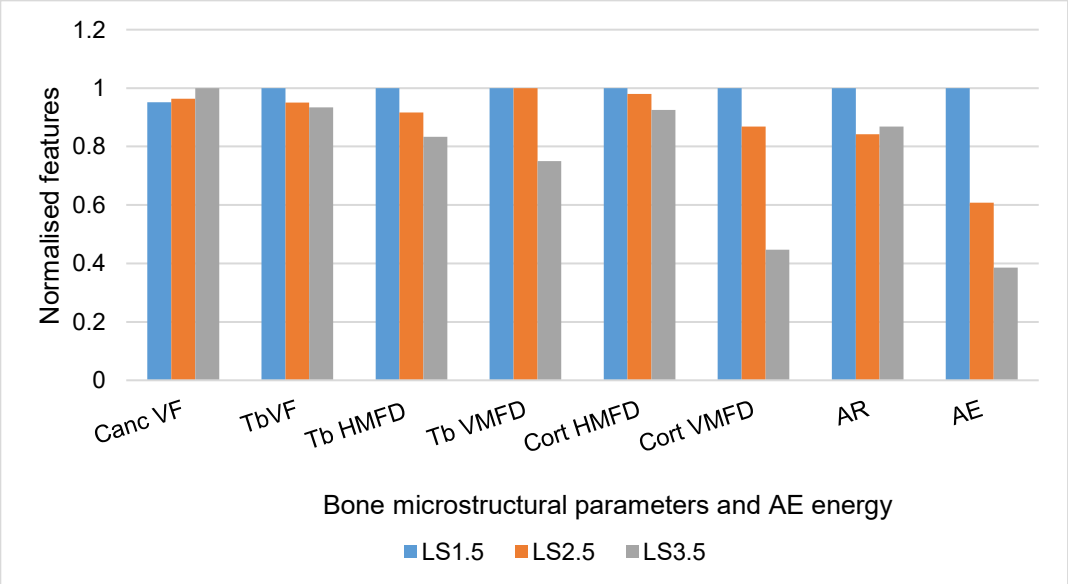

Figure 5.4: Relative AE energy and normalised bone microstructural parameters for longitudinal sections of bone (LS): Cancellous volume fraction (Canc VF), Trabeculae volume fraction (Tb VF), Trabecular horizontal and vertical mean free distances (Tb HMFD, Tb VMFD), Cortical horizontal and vertical mean free distances (Cort HMFD, Cort VMFD) and Aspect ratio of marrow cavities (AR).

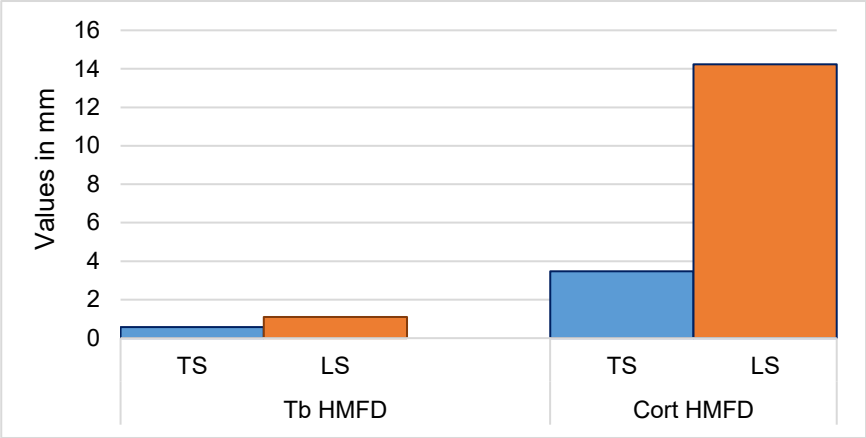

Figure 5.5: Comparison of Tb HMFD and Cort HMFD between transverse sections (TS) and longitudinal sections (LS)

5.1.1.2 AE attenuation measurements along bone

In order to quantify the attenuation of AE energy along the bone, the relative AE energy is plotted against source-sensor distance in Figure 5.6 (a, b). As illustrated in Figure 5.1, the first position (the closest to the PLB source) is used as a reference so that the attenuated energy at each subsequent position is given by (E_i / E_0), where (E_0) is the AE measured at the reference position (P0), and (E_i) is the AE collected at the positions 1, 2 and 3. The Error bars for P1, P2 and P3 represent the uncontrolled variations due to pencil lead breaks and due to the fact that the sensor (S_2) was removed and replaced for each of the positions. For P0, the sensor was not removed and replaced, so the error is entirely due to the pencil lead breaks. Overall, the measurements suggest that the energy attenuation of this bone is around 20% per cm.

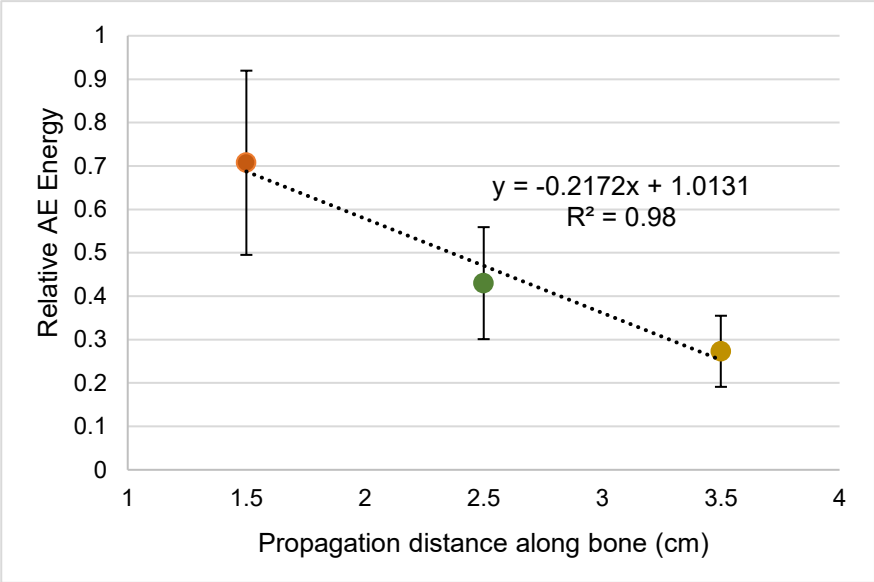

(a)

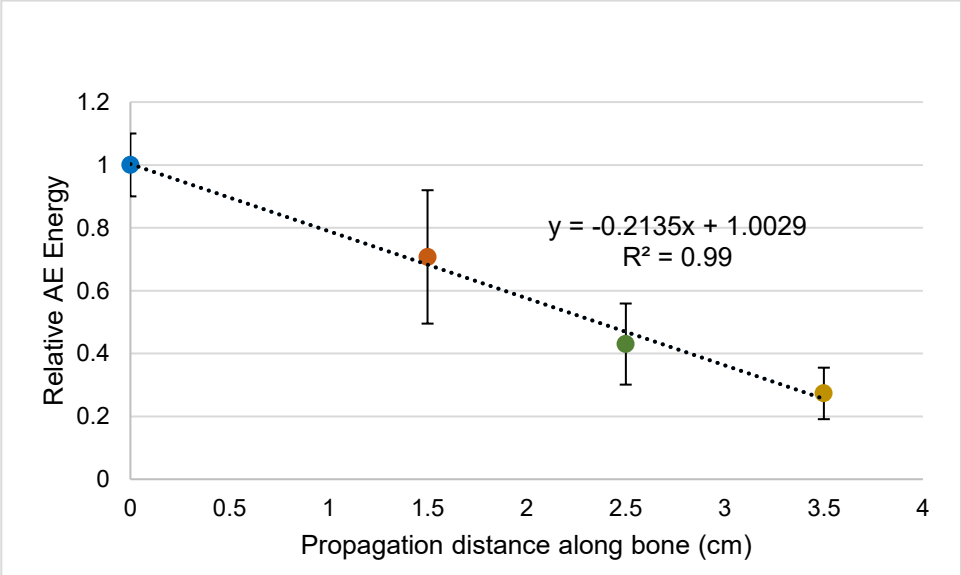

(b)

Figure 5.6 (a, b): AE transmission per unit distance along bone

As can be seen from Figures 5.6 (a) and (b), the AE attenuation function is very similar whether or not the reference position is used. To take into account the effect of cross-sectional area of bone on propagation of the AE, the AE energy is plotted (Figure 5.7) against the propagation distance per cross-sectional area of the solid components of bone tissue (cortex and trabeculae)

where most of the energy is expected to be transmitted. As can be seen, the relationship is still linear with a negative slope but, comparing with Figure 5.6(a), the correlation is considerably stronger (from a very strong baseline). This indicates that, whilst the propagation distance is the main influence on the attenuation, the bone microstructure (the animal-specific aspect) has a significant effect.

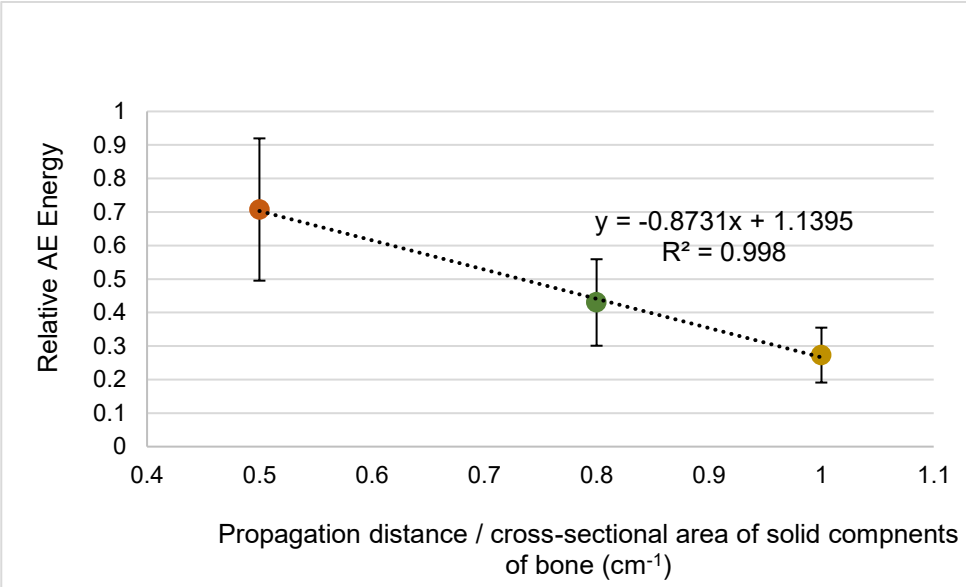

Figure 5.7: AE transmission per propagation distance per unit cross-sectional area of solid components of bone (cortex and trabeculae)

Based on the above observation, the loss of energy can be determined using the attenuation coefficient, which is the slope of the best-fit line for the measured AE as a linear function of distance travelled per unit cross-sectional area of bone.

Rate of energy loss = 0.87 × propagation distance (cm) / cross-sectional area of bone (cm²).

5.1.2 AE transmission through bone

Examining the transmission through the bone to the nearest surface is more difficult since it requires multiple primary stability exemplars and different bones (B1, B2, B3), with the associated uncontrolled variations in source energy entering the bone-implant interface. Figure 5.8 illustrates the

experimental set-up and the associated microstructural regions of interest (RoIs). The AE energy values for three primary stability models were compared to their corresponding bone microstructural parameters measured from transverse sections of the samples. In addition, the propagation distance and porosity of bone were measured for the RoI which includes the area of bone between the interface and the surface of the bone at the position of the adjacent sensor, as shown in Figure 5.8.

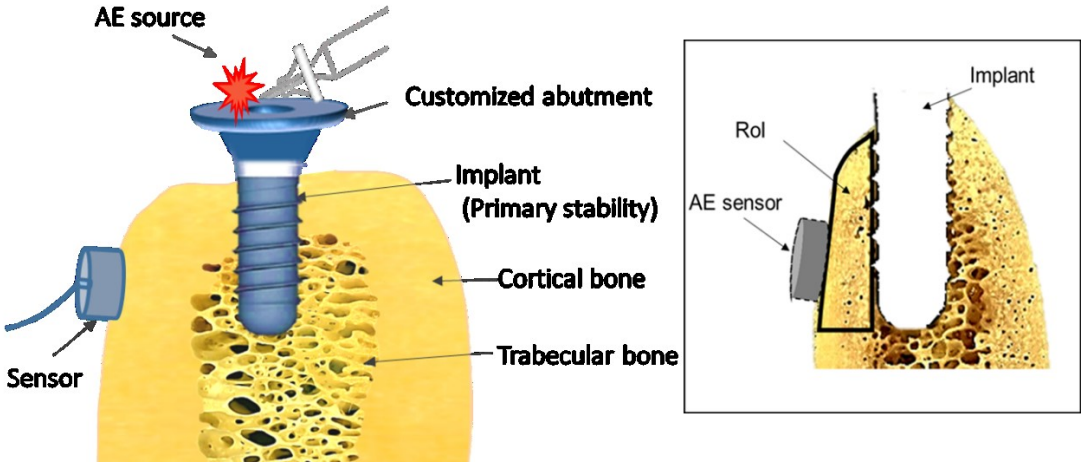

Figure 5.8: Source-sensor position for the transmission through bone, and region of interest (RoI)

As is evident from the bar chart, Figure 5.9, there is no systematic difference in microstructural parameters in the three bone sections which would account for the difference in AE energy with the possible exception of the trabecular horizontal mean free distance shown in more detail in Figure (5.10). The model for rate of energy loss developed in the previous section was also applied in the RoI for each of the sections and the pattern matches best with the pattern of cortical width in each of the sections, although this could be coincidence. Overall, it seems that the variation due to installation is likely to make it difficult to see the effect of bone microstructure over such small distances. This is positive from point of view of monitoring the bone-implant interface since it indicates that bone microstructure variations are likely to have little effect provided that any sensor is mounted close to the implant of interest.

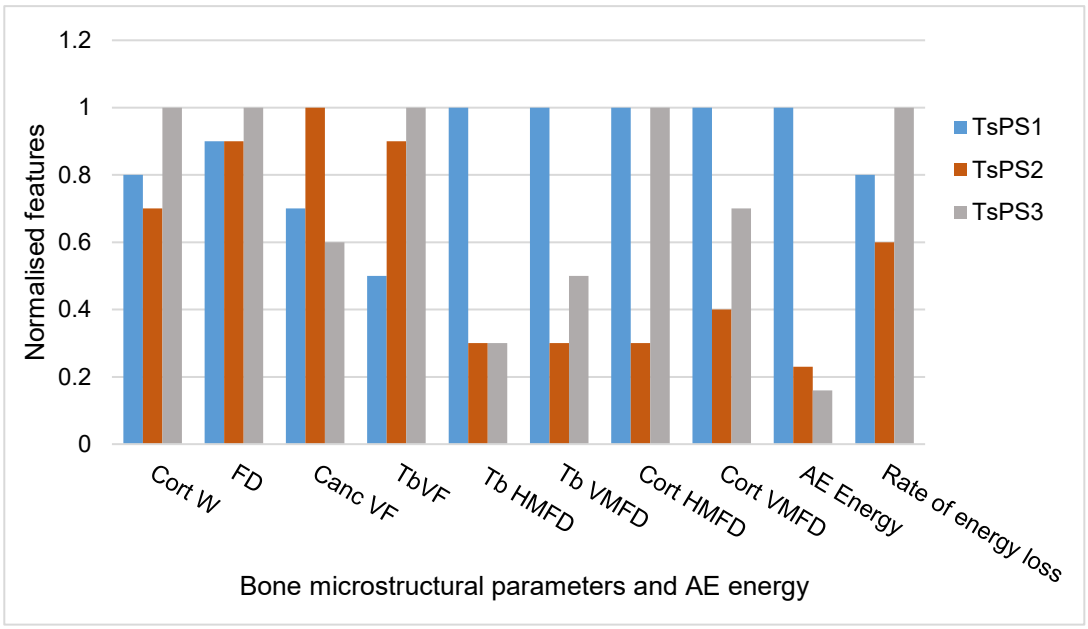

Figure 5.9: Relative AE energy and rate of energy loss vs. normalised bone microstructural parameters for transverse sections of primary stability configuration (TsPS1, TsPS2, TsPS3): Cortical width (Cort W), Fractal dimension (FD), Cancellous volume fraction (Canc VF), Trabecular volume fraction (Tb VF), Trabecular horizontal and vertical mean free distances (Tb HMFD, Tb VMFD), Cortical horizontal and vertical mean free distances (Cort HMVF, Cort VMFD).

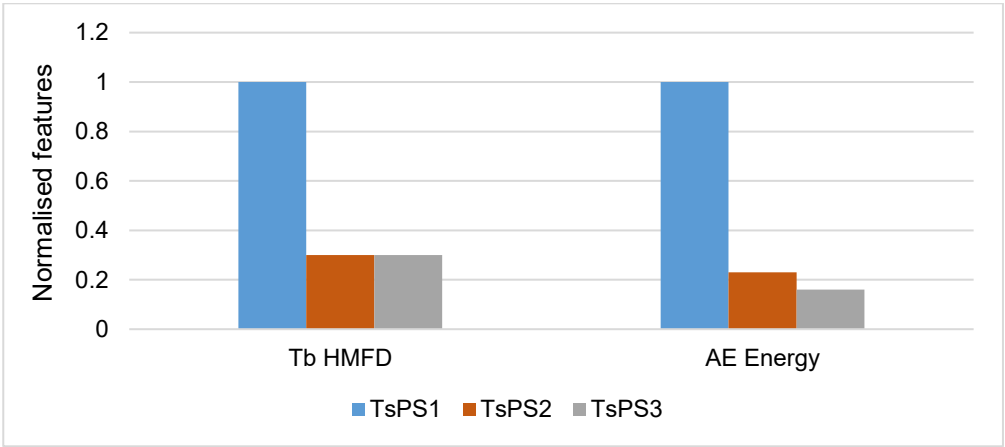

Figure 5.10: Correlation of AE energy and trabecular horizontal mean free distance (Tb HMFD)

5.2 Influence of simulated osseointegration and secondary stability on AE transmission

The focus in this experiment, described in Chapter 3 Section 3.2.2.2, was to examine the capacity of AE to monitor the development of secondary stability, using a simulated osseointegration model. The experiments involved measuring the AE energy transmitted from AE source to a sensor (S_1) positioned adjacent to the implant. A total of 12 new implants were inserted randomly into 2 fresh bones (B2, B3) with 3 different degrees of stability: primary stability, partial osseointegration and full osseointegration. In addition, 3 more primary stability models from other two bones (one in B1, two in B4) used in previous tests were also included in the analysis.

5.2.1 Effect of degree of secondary stability

Figure 5.11 shows the averages (bar height) and variation (error bars) of the AE energy measurements for each implant per each type of the stability configurations. In total, 15 installations were tested, each using 20 pencil lead breaks. As can be seen, there is a clear difference in the AE transmission through the three different stability configurations, with highest transmission being through the fully integrated models. As would be expected, the transmission reduced as the simulated bone-implant contact (the amount of cement-implant contact) decreased, from complete through partial to none in the fully integration, partially integration and primary stability models, respectively.

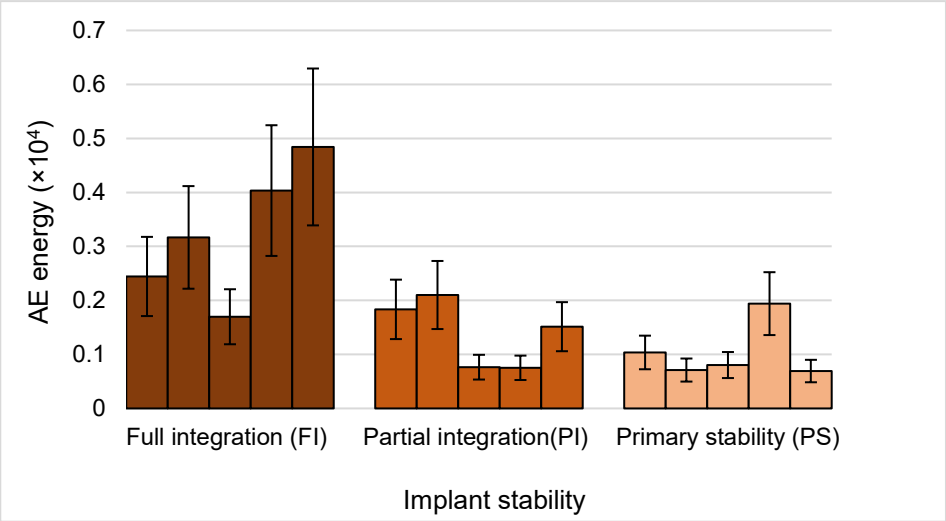

Figure 5.11: AE energy for each example of each of the stability configurations

To test the statistical significance of the observations in Figure 5.11, analysis of variance (ANOVA) was performed between the stability configurations (FI, PI, and PS) and the uncontrolled variability within each configuration (due to pencil lead breaks, bone local and global microstructure, and sensor coupling). The P-value (Table 5.1) was 0.003, indicating a significant difference in the transmission among the three different degrees of stability, although it might be noted that there is a larger drop in the mean between full and partial than between partial and primary stability. Finally, the variance in full integration is an order of magnitude larger than the other two. As can be seen, this increased variance is attributable both to the individual lead breaks and to the individual example.

ANOVA: Single Factor

Summary

Groups	*Count*	*Sum*	*Average*	*Variance*
Full integration	5	1.62×10^{-4}	3.24×10^{-5}	1.55×10^{-10}
Partial integration	5	6.97×10^{-5}	1.39×10^{-5}	3.79×10^{-11}
Primary stability	5	5.18×10^{-5}	1.04×10^{-5}	2.74×10^{-11}

ANOVA

Source of variation	*SS*	*df*	*MS*	*F*	*P-value*	*F crit*
Between groups	1.39×10^{-9}	2	6.97×10^{-10}	9.48	0.003	3.89
Within groups	8.83×10^{-10}	12	7.36×10^{-11}			
Total	2.28×10^{-9}	14				

Table 5.1: ANOVA for the effect of different stability configurations on the transmission

To quantify the observations in Table 5.1, the width of the simulated osseointegration layer around the implant (simulated bone-implant contact) was measured by calculating the average for the cement widths measured every 2 cm all around the implant. The average width per each degree of integration is plotted against the average AE energy in Figure 5.12, showing a very good correlation (R^2 =0.98) with the energy increasing by a factor of about 3 for each mm of osseointegrated layer. However, if the actual measured thickness for each installation is used (rather than the average for all in the class), Figure 5.13, the slope is still the same, but the correlation is much poorer (R^2 =0.64). It should, however, be noted that there is considerable scope for experimental error in assessing the osseointegrated thickness and in producing the models. First of all, the preparation of the full integration samples requires them to be cast into cement, which cannot always be done with the precision of drilling and screwing. Equally, for the partial integration model, the cement may not always be squeezed into the bone voids effectively. Finally, and for both models, only one section was used to assess thickness when, in fact, the entire circumference of the osseointegrated layer is transmitting the AE.

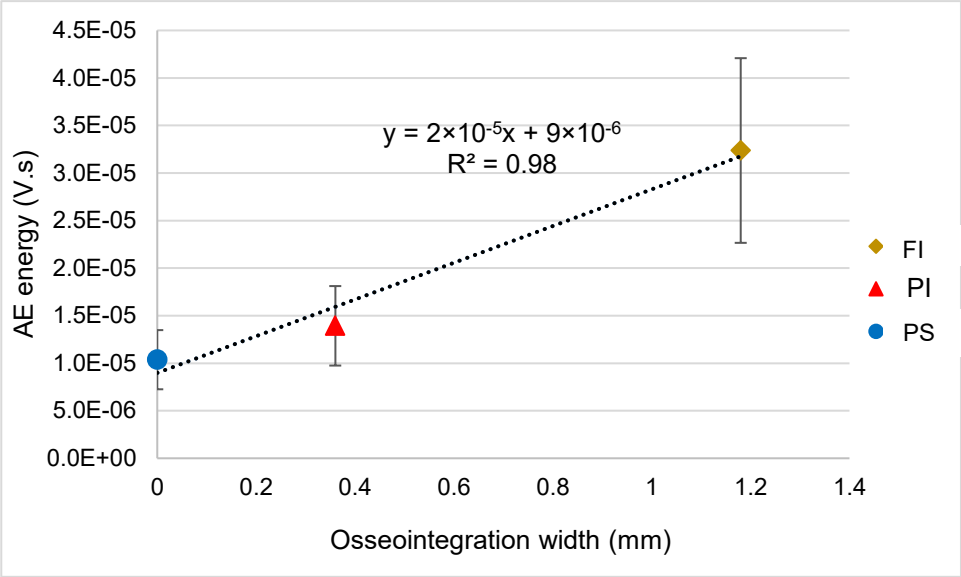

Figure 5.12: Average AE energy *vs*. average width of simulated osseointegration for each of the stability configurations; Ps: Primary stability, PI: Partial integration and FI: Full integration. Error bars represent the uncontrolled variation

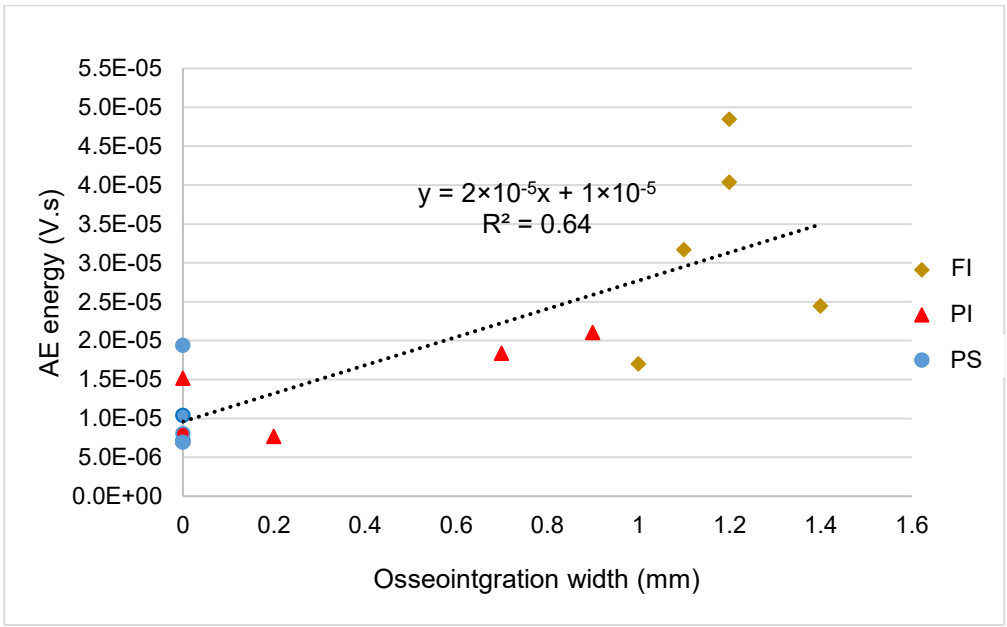

Figure 5.13: AE energy *vs*. width of simulated osseointegration for each implant per each stability configuration; Ps: Primary stability, PI: Partial integration, FI: Full integration

5.2.2 Effect of animal specificity for the different stability configurations

A subset of data from the previous test were used in this analysis in order to examine the effect of subject-related variations on the transmission through

the different stability configurations. Figure 5.14 shows the average AE energy for each implant for each stability configuration for each bone. As can be seen, there appears to be a difference in the AE transmission through the three different stability configurations between the two bones, most notably for the full integration models where transmission in the bone is a larger proportion of the path from source to sensor.

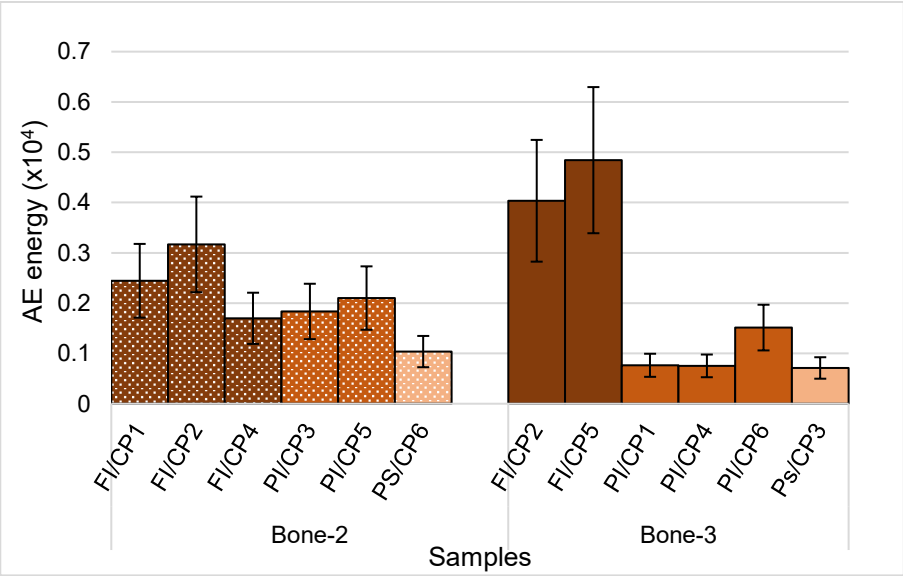

Figure 5.14: Transmitted energy for different stability models per each of the bone samples (C: buccal side, P: position of implant on bone sample, FI and PI; full and partial integration, PS: primary stability)

In order to assess the significance of the difference in the transmission between bone samples, an ANOVA test was applied to the AE data grouped as collected from bone (B2) or bone (B3) regardless of the stability condition, and tested at the 5% confidence level, so that the variation due to bones (between groups: B2, B3) can be compared with the variation due to stability configurations (within groups: FI, PI, PS). Table 5.2, shows that the P- value is 0.9, well above 0.05, which means that there no significant difference in the transmission between the two bones, B2 and B3, indicating that the stability configuration is a more important source of variation than the bone itself.

ANOVA: Single Factor

Summary

Groups	*Count*	*Sum*	*Average*	*Variance*
Bone-2	6	1.23×10^{-4}	2.05×10^{-5}	5.21×10^{-11}
Bone-3	6	1.26×10^{-4}	2.1×10^{-5}	3.43×10^{-10}

ANOVA

Source of Variation	*SS*	*df*	*MS*	*F*	*P-value*	*F crit*
Between Groups	9.47×10^{-13}	1	9.47×10^{-13}	0.005	0.946	4.96
Within Groups	1.97×10^{-9}	10	1.97×10^{-10}			
Total	1.98×10^{-9}	11				

Table 5.2: ANOVA for the effect of individual bone on the AE transmission (Buccal data)

The possible reasons for this outcome could be:

- there is no significant difference in the structure between the two bones,
- the variations in the embodiment of the configurations or the positions of the implant on the bone are bigger than that due to the bones.

The question then arises as to whether the bone has any significant effect on the transmission when considering each configuration separately.

Figure 5.15 (a-c) shows the energy values, plotted to highlight the effect of bone on the transmission for each individual stability configuration.

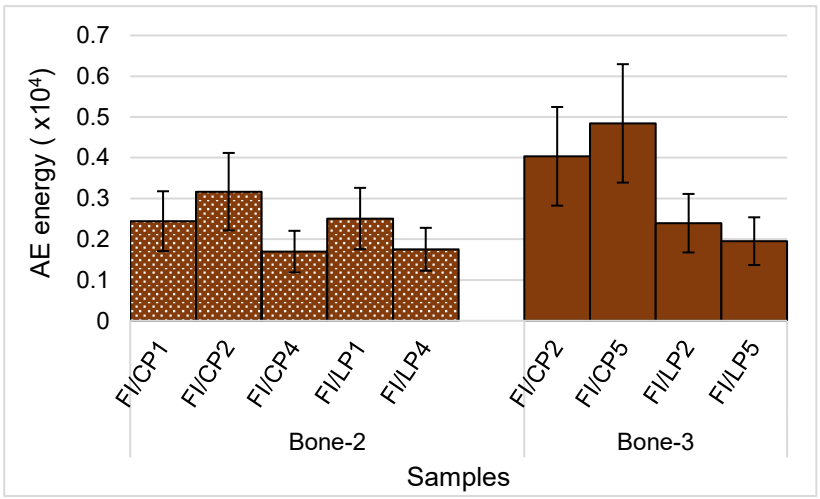
AE energy (x10⁴)
0.7
0.6
0.5
0.4
0.3
0.2
0.1
0
FI/CP1
FI/CP2
FI/CP4
FI/LP1
FI/LP4
FI/CP2
FI/CP5
FI/LP2
FI/LP5
Bone-2
Bone-3
Samples

(a)

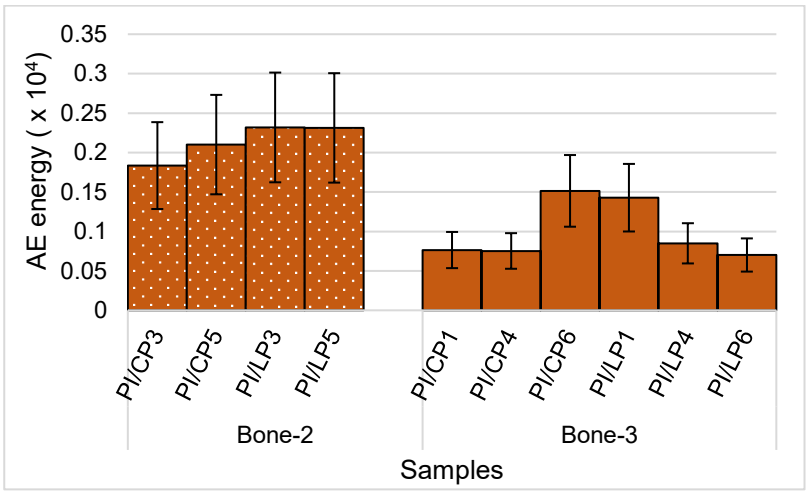
AE energy (x 10⁴)
0.35
0.3
0.25
0.2
0.15
0.1
0.05
0
PI/CP3
PI/CP5
PI/LP3
PI/LP5
PI/CP1
PI/CP4
PI/CP6
PI/LP1
PI/LP4
PI/LP6
Bone-2
Bone-3
Samples

(b)

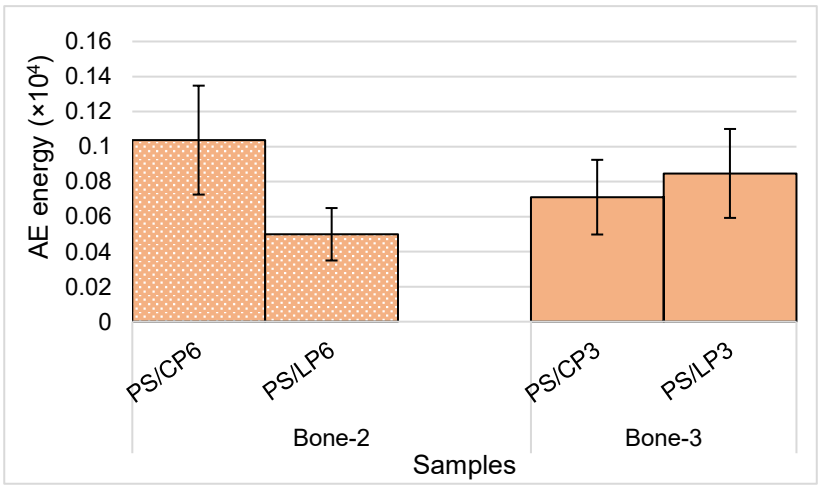
AE energy (×10⁴)
0.16
0.14
0.12
0.1
0.08
0.06
0.04
0.02
0
PS/CP6
PS/LP6
PS/CP3
PS/LP3
Bone-2
Bone-3
Samples

(c)

Figure 5.15 (a, b, c): Effect of individual bone across: (a) fully integrated implants, (b) partially integrated implants, (c) primary stability configuration. Data from both buccal (C) and lingual (L) sides for each of the bone samples have been used here to improve the statistical power.

Table 5.3 shows the summary of ANOVA for the effect of bone across each individual stability configuration. It can be seen that the particular bone has a significant effect only on the transmission across partially integrated implants.

	Full integration	Partial integration	Primary stability
P- value	0.184	0.0006	0.972

Table 5.3: Summary of ANOVA for the effect of bone per each stability configuration

5.3 Potential of AE energy for diagnosing peri-implant bone loss

The aim in this set of tests, described in Chapter 3 Section 3.2.2.3, was to assess whether AE transmission could be used to monitor peri-implant bone loss. Two types of models were used, simulating circumferential and vertical bone loss, respectively. These are discussed in turn below, followed by a summary of the overall effect of peri-implant bone loss.

5.3.1 Effect of simulated circumferential bone loss on AE transmission

In this test, 20 models were installed randomly in 5 bovine bone samples (B5-9), 4 models per bone. Four different degrees of bone loss were used, illustrated schematically in Figure 5.16 (adapted from Figure 3.16 for clarity).

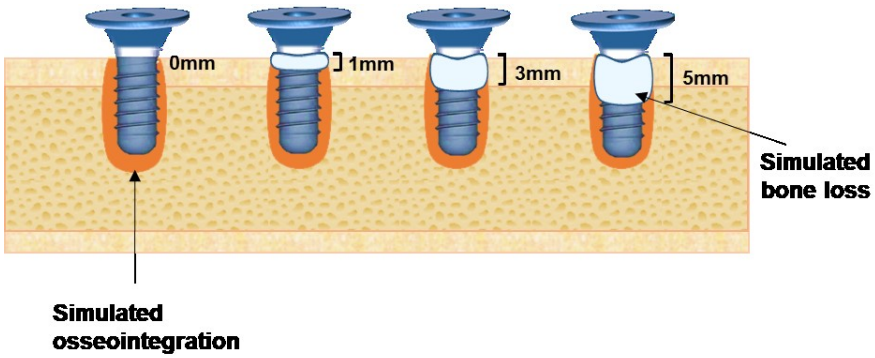

Figure 5.16: Schematic view of models for the circumferential bone loss to various depths

Figure 5.17 shows the average transmitted AE energy for each implant position for each bone sample. It is immediately apparent that the degree of bone loss affects transmission, but also that the reference condition (full integration model) varies between the individual bone samples used.

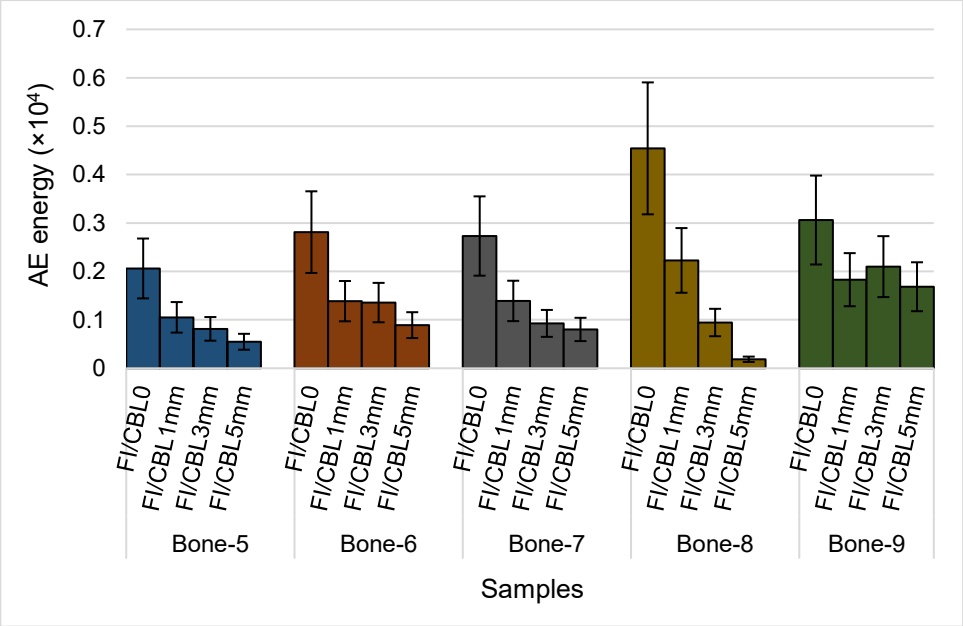

Figure 5.17: Transmitted energy for different interface conditions per each bone (FI: Full integration, CBL: circumferential bone loss)

In order to evaluate the relative effects of the bone sample and the bone loss on the transmission, a two-factor ANOVA test was applied to the AE data grouped at two levels, according to the amount of bone loss or having been collected from different bones, and then tested at 5% confidence level. Table 5.4 shows that P-values are 0.0002 and 0.13 for the effect of bone loss and individual bone, respectively, indicating that the circumferential bone loss was the main source of variation. However, a *post-hoc* comparison (Tukey's HSD test) making pair-wise comparisons between the means of different conditions of the interface showed significant differences in the AE energy between the

intact fully integrated implants and each of the levels of circumferential bone loss tested. However, the AE did not significantly differentiate between the varying severities of compromised interfaces, although the data for each bone sample clearly show progressive differences.

ANOVA: Two-Factor without Replication

Summary

Groups	*Count*	*Sum*	*Average*	*Variance*
Bone Loss-0mm	5	1.52×10^{-4}	3.04×10^{-5}	8.4×10^{-11}
Bone Loss-1mm	5	7.88×10^{-5}	1.58×10^{-5}	2.08×10^{-11}
Bone Loss-3mm	5	6.14×10^{-5}	1.23×10^{-5}	2.8×10^{-11}
Bone Loss-5mm	5	4.11×10^{-5}	8.22×10^{-6}	3.07×10^{-11}
Bone-5	4	4.47×10^{-5}	1.12×10^{-5}	4.38×10^{-11}
Bone-6	4	6.44×10^{-5}	1.61×10^{-5}	6.92×10^{-11}
Bone-7	4	5.85×10^{-5}	1.46×10^{-5}	7.8×10^{-11}
Bone-8	4	7.9×10^{-5}	1.97×10^{-5}	3.64×10^{-10}
Bone-9	4	8.67×10^{-5}	2.17×10^{-5}	3.84×10^{-11}

ANOVA

Source of variation	*SS*	*df*	*MS*	*F*	*P-value*	*F crit*
Rows (Bone loss)	1.4×10^{-9}	3	4.67×10^{-10}	14.9	0.0002	3.49
Column (Bone)	2.77×10^{-10}	4	6.92×10^{-11}	2.2	0.13	3.26
Error	3.77×10^{-10}	12	3.15×10^{-11}			
Total	2.06×10^{-9}	19				

Table 5.4: ANOVA for the effect of circumferential bone loss and individual bone on AE transmission

The averages and the standard deviations of the transmitted energy for intact and compromised interfaces are plotted in Figure 5.18. As can be observed, there is a clear distinction in the transmission between the intact interface and those with circumferential bone loss to depths of 1, 3 and 5 mm. The largest drop was between the intact interface and the circumferential defect of 1 mm depth. The energy also decreased as the defect depth increased from 1 to 5 mm, but to a lesser extent.

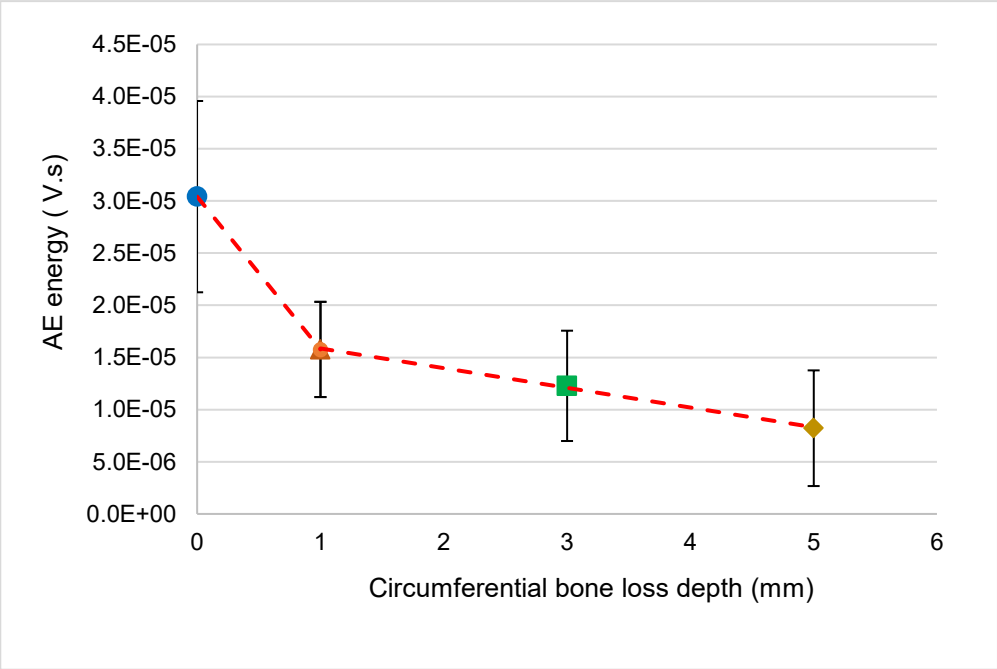

Figure 5.18: Average transmitted energy for the intact and compromised interfaces with circumferential bone loss

5.3.2 Effect of simulated vertical peri-implant bone loss on AE transmission.

In this test, 25 experimental models were installed randomly in 5 bovine bones (B10-14), 5 models per bone. The aim was to investigate the feasibility of acoustic signals to recognise the changes in the circumferential extent of a fixed-depth vertical bony defect adjacent to the osseointegrated implant, Figure 5.19 (adapted from Figure 3.17 for clarity). AE energy analysis was carried out on signals transmitted from the AE source applied to osseointegrated implants with varying circumferential widths of vertical bony defect, all extending 1mm apically. The AE energy of the defective interfaces was analysed and compared with the transmission through intact fully integrated implants.

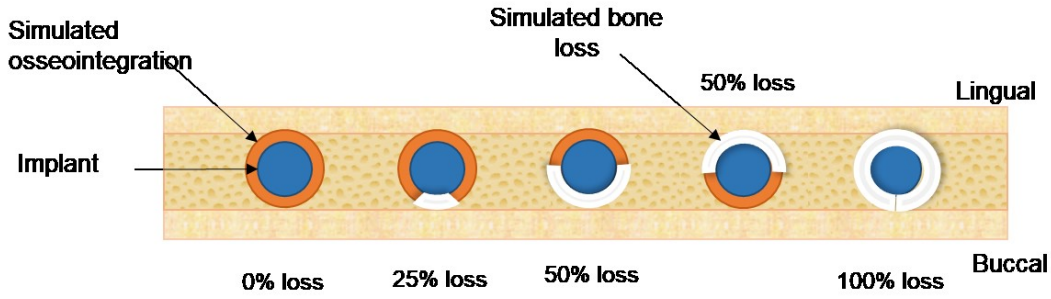

Figure 5.19: Schematic view for the circumferential extensions of simulated vertical bone loss

Figure 5.20 plots the averages and the standard deviations of 20 pencil lead breaks for the intact interface and compromised interfaces with varying widths of vertical bone loss. As can be seen, the transmitted energy reduces as the width of the vertical defect increases. As with the circumferential defect, the intact interface transmits significantly higher energy than those with any vertical bone loss. The energy showed a considerable drop (approximately by two thirds) when the osseointegrated implants lost 25% of the supporting bone at 1 mm depth. It also showed a further drop between 25% and 100% bone loss. However, the spread on all of the data is quite large and is greater for the intact interface than for the others.

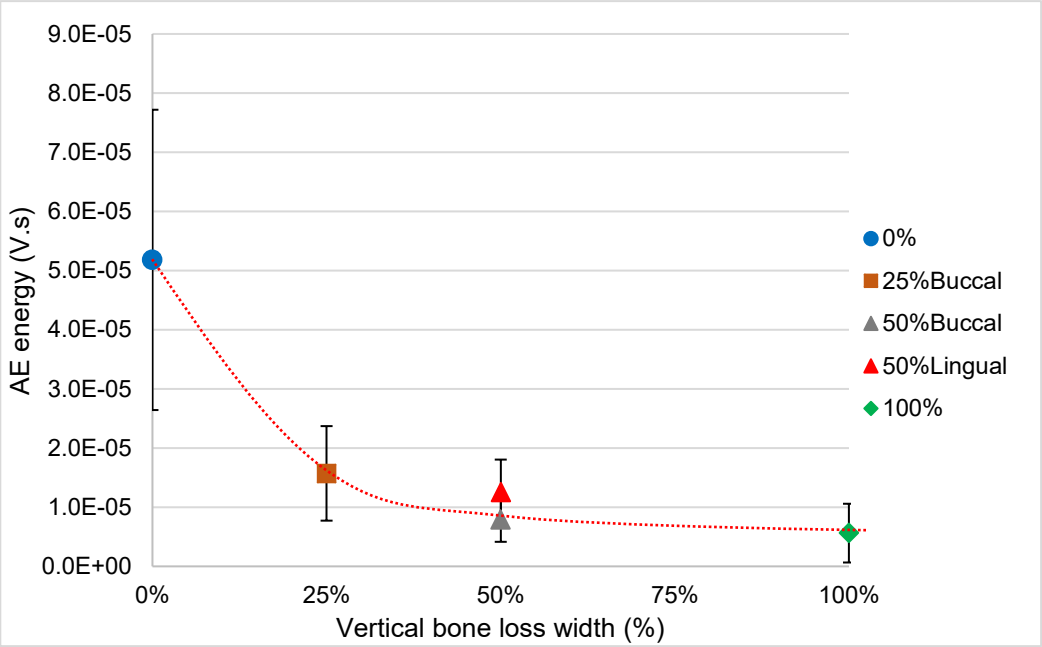

Figure 5.20: Averages and standard deviations for the intact integration and compromised interfaces with buccal or lingual vertical bone defect. Red trend line is hand drawing

Figure 5.21 shows the averages (bar height) and the uncontrolled variations (error bars) of the 20 AE readings for each implant for each type of the compromised configurations as well as the fully integrated implants.

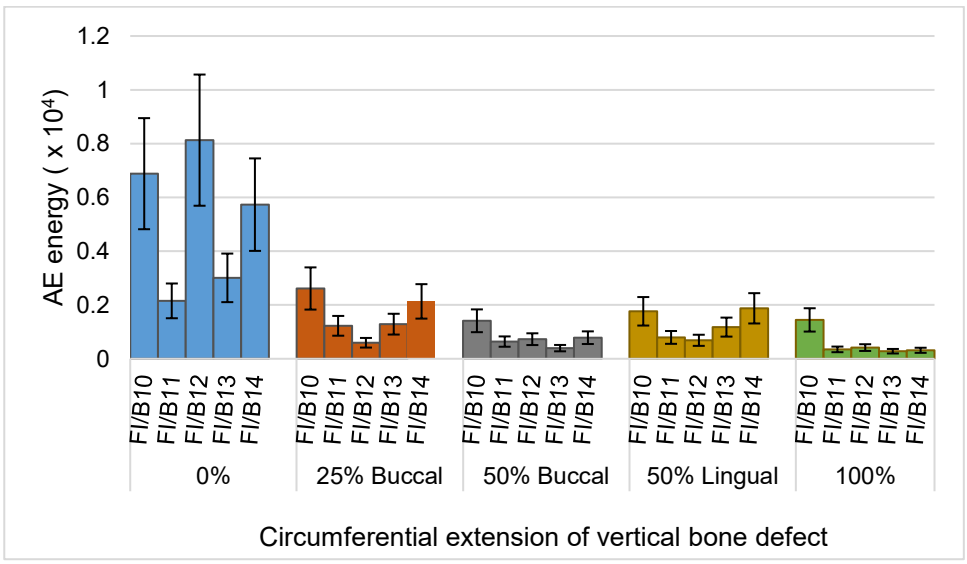

Figure 5.21: Average transmitted energy for each implant per each interface condition (FI: Full integration, B: Bone)

Analysis of variance (ANOVA) was carried out for the effect of vertical bone loss on AE transmission (Table 5.5). The 20 pencil lead breaks were grouped according to the extent of the defect around the implant, and tested at 5% confidence level. The P-value was 5.2 x 10^{-5}, indicating a significant effect of the vertical bone loss on the AE energy.

ANOVA: Single Factor

Summary

Groups	*Count*	*Sum*	*Average*	*Variance*
0% Loss	5	2.59×10^{-4}	5.18×10^{-5}	6.44×10^{-10}
25% Buccal loss	5	7.86×10^{-5}	1.57×10^{-5}	6.39×10^{-11}
50% Buccal loss	5	3.96×10^{-5}	7.93×10^{-6}	1.42×10^{-11}
50% Lingual loss	5	6.3×10^{-5}	1.26×10^{-5}	2.97×10^{-11}
100% Loss	5	2.81×10^{-5}	5.62×10^{-6}	2.47×10^{-11}

ANOVA

Source of variation	*SS*	*df*	*MS*	*F*	*P-value*	*Fcrit*
Between Groups	7.15×10^{-9}	4	1.79×10^{-9}	11.5	5.195×10^{-5}	2.87
Within Groups	3.11×10^{-9}	20	1.55×10^{-10}			
Total	1.03×10^{-8}	24				

Table 5.5: ANOVA for the effect of vertical bone loss on AE transmission

Tukey's test showed significant differences between the energy averages of intact integrated implants and every single condition of the vertical bone loss. However, the difference in the transmission between the subsequent compromised interfaces groups (25%, 50% and 100%) was not significant.

Figure 5.22 shows the data re-plotted to show the averages of AE energy for each implant position for each bone.

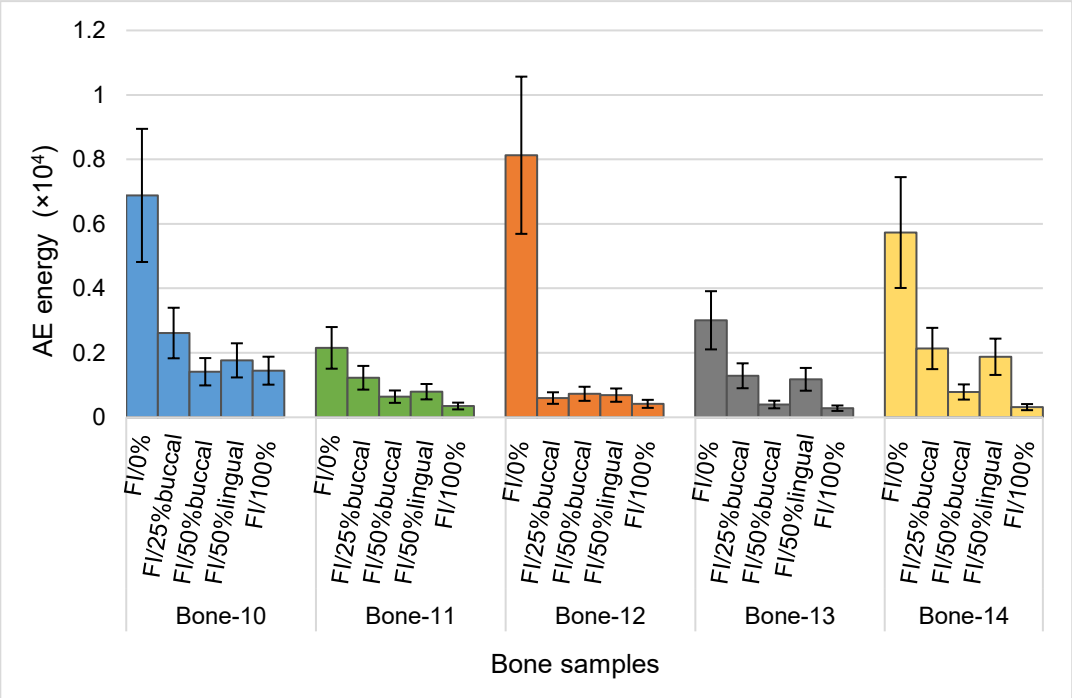

Figure 5.22: Averages of AE energy for each implant position per each bone

As for the circumferential defects, a two-factor ANOVA test was applied to assess the effect of the vertical bone loss and effect of the individual bone on the transmission (Table 5.6). The AE data were grouped at two levels, amount of bone loss and bone sample and then tested at the 5% confidence level. P-value was 4.06 x 10^{-5} for the effect of loss and 0.1 for the effect of individual bone on the transmission, indicating again that the bone loss was the main source of variation in the transmission between the groups and was not affected significantly by the individual bone.

ANOVA: Two-Factors without Replication

Summary

Groups	*Count*	*Sum*	*Average*	*Variance*
0% loss	5	2.59×10^{-4}	5.18×10^{-5}	6.44×10^{-10}
25% Buccal	5	7.86×10^{-5}	1.57×10^{-5}	6.39×10^{-11}
50% Buccal	5	3.96×10^{-5}	7.93×10^{-6}	1.42×10^{-11}
50% Lingual	5	6.3×10^{-5}	1.26×10^{-5}	2.97×10^{-11}
100%	5	2.81×10^{-5}	5.62×10^{-6}	2.47×10^{-11}

Bone-10	5	1.41×10^{-4}	2.82×10^{-5}	5.38×10^{-10}
Bone-11	5	5.16×10^{-5}	1.03×10^{-5}	4.93×10^{-11}
Bone-12	5	1.06×10^{-4}	2.11×10^{-5}	1.13×10^{-9}
Bone-13	5	6.15×10^{-5}	1.23×10^{-5}	1.19×10^{-10}
Bone-14	5	1.08×10^{-4}	2.17×10^{-5}	4.53×10^{-10}

ANOVA

Source of variation	*SS*	*df*	*MS*	*F*	*P-value*	*Fcrit*
Rows (Bone loss)	7.15×10^{-9}	4	1.79×10^{-9}	14.1	4.06×10^{-5}	3.01
Column (Bone)	1.08×10^{-9}	4	2.71×10^{-10}	2.14	0.122	3.01
Error	2.02×10^{-9}	16	1.26×10^{-10}	14.1		
Total	1.03×10^{-8}	24				

Table 5.6: ANOVA for the effect of vertical bone loss and individual bone on AE transmission

5.3.3 Combined effect of circumferential and vertical bone loss on the transmission

Figure 5.23 shows the collected data for degradation of interface and includes averages and the standard deviations of all the intact fully integrated implants and the compromised interfaces with circumferential or vertical bone loss. In all, the graph includes 10 fully integrated implants and 30 implants with compromised interfaces. There are two dimensions of bone loss; depth and circumferential extent. All of the vertically oriented defects are on 1 mm depth and are of varying circumferential extent, so they are shown in figure 5.23 as a proportion of 1 mm loss. The trend lines are calculated as exponential decay curves simply to give an indication of the degree of the defect rather than any expectation that the curve is genuinely exponential. As can be seen, plotted in this way, the effect of vertical defects is considerably stronger than circumferential ones, which suggests, that the data might be presented in a more clinically relevant way. To do this, all 15 fully integrated implants were included (i.e. those from Experiments: 5.1, 5.2, and 5.3) as will be seen in Figure 5.24.

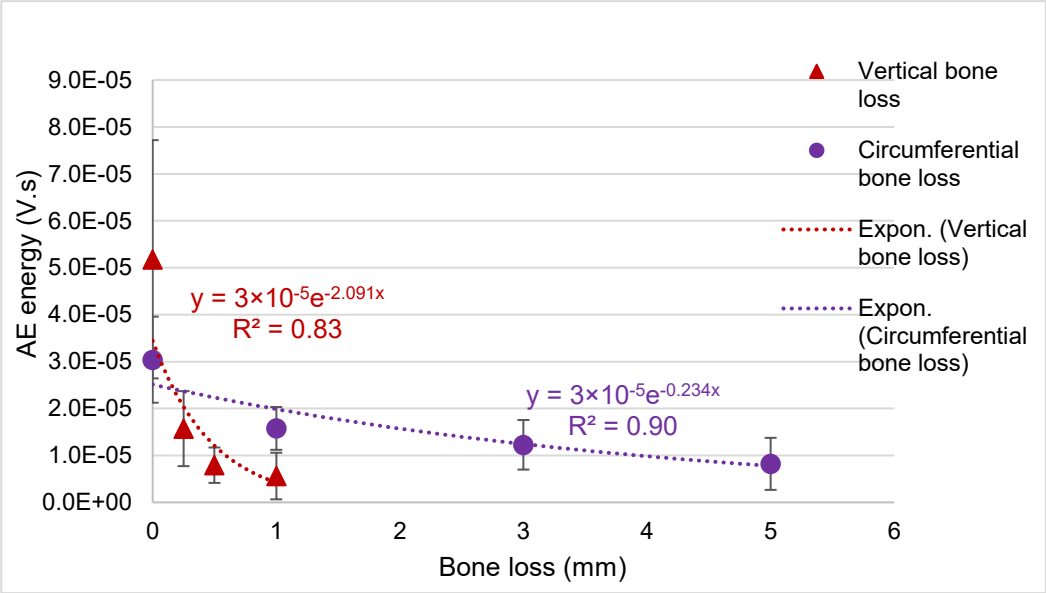

Figure 5.23: Averages and standard deviations of intact interfaces and compromised interfaces with circumferential or vertical bone loss

Accordingly, the proportion of the interface that has been compromised was calculated by taking the whole cylindrical area of the implant and determining the cylindrical area of the defect. If the cylindrical area is $2\pi rl$ (where r is the external radius of the implant and l is its axial length). Then the cylindrical area of the circumferential defects is $2\pi rh$ where h is the depth of the defect (1, 2 or 5 mm). For the vertical defects, where h is always 1 mm, the cylindrical area of the defect is $2\pi rc$, where c is the fraction of the circumferential affected (0.25, 0.5 or 1). As can be seen in Figure 5.24, the effect of the extent of the defect is relatively small, the most significant change being between intact interfaces and those which have been compromised in some way. Further points to note in Figure 5.24:

- Each point represents an implant installation and there is considerable variation between implants which may be due to the local bone structure and/or the reproducibility of the build of the interface models
- Each point involved its own sensor placement which can give rise to a variation of ± 20% in the recorded energy between points.
- Each point is an average over 20 pencil lead breaks, which can give rise to a variation of ± 10% in the recorded energy for each point.

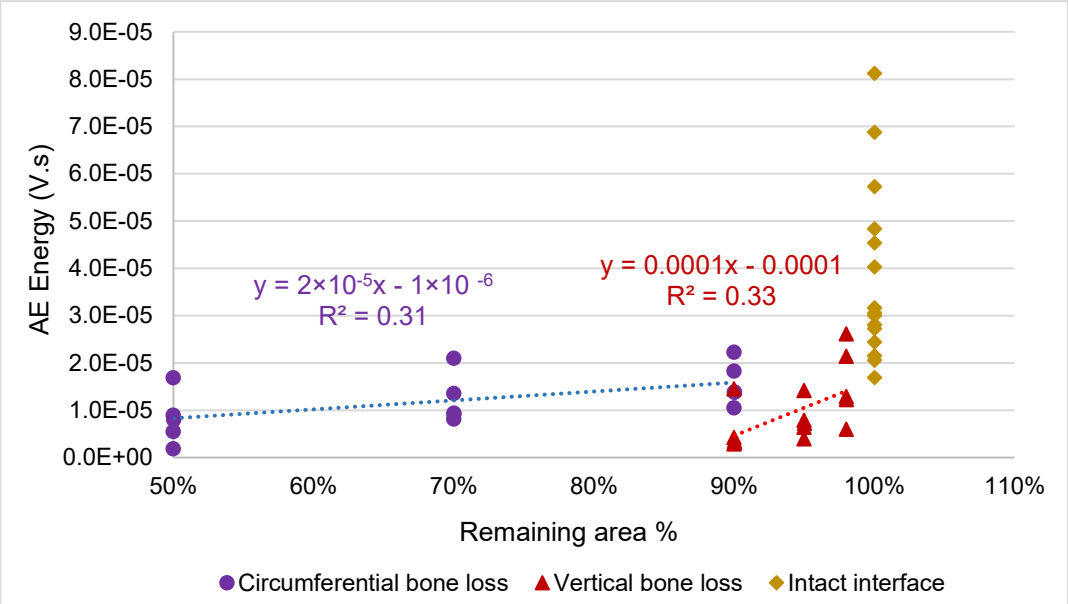

Figure 5.24: The correlation between the AE energy and the remaining unaffected area of osseointegrated implants

5.4 Summary of the Key findings

The key findings from all systematic experiments are as follows:

- The energy of AE wave travelling along a bone drops of in an approximately linear fashion with the propagated distance per cross-sectional area of the solid components of the bone. Although the main effect on the attenuation of energy is propagation distance, the transmission was also significantly affected by the underlying microstructure of the bone. For a given distance along the bone, the loss of energy is around 20% per cm propagated. Signal transmission through the bone, from the interface to the surface, was not significantly affected by microstructure or macrostructure of the bone, because the distances involved are quite small and the effect of variations (random and systematic) in the installation seemed to be largely responsible for loss in energy.

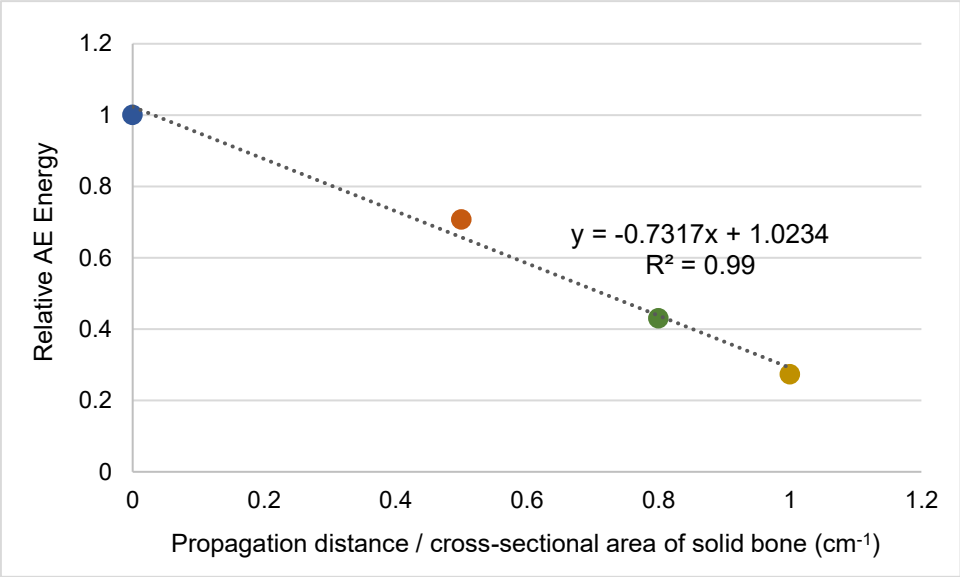

Figure 5.25: AE transmission along bone and per unit cross-sectional area of solid components of bone (cortex and trabeculae)

- AE can detect the development of osseointegration around dental implants. From primary stability to full integration, the proportion of the input energy transmitted to the sensor increases by a factor of 3 and the trend line for the data has a correlation coefficient of 0.98.

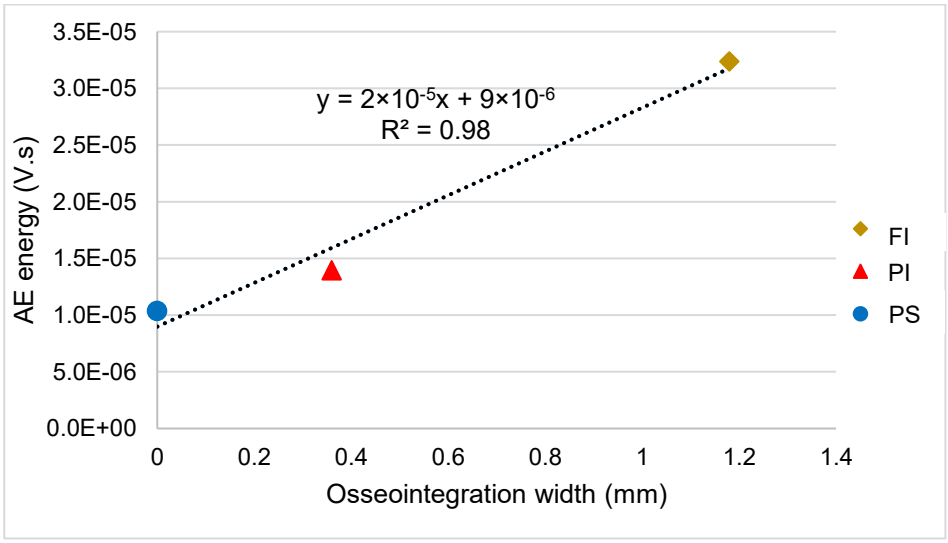

Figure 5.26: Average AE energy *vs.* average width of simulated osseointegration for each of the stability configurations; Ps: Primary stability, PI: Partial integration and FI: Full integration

- AE can recognise the circumferential and vertical peri-implant bone loss around osseointegrated implants. There is a substantial reduction in the transmission when fully integrated implants present circumferential or vertical marginal bone loss.

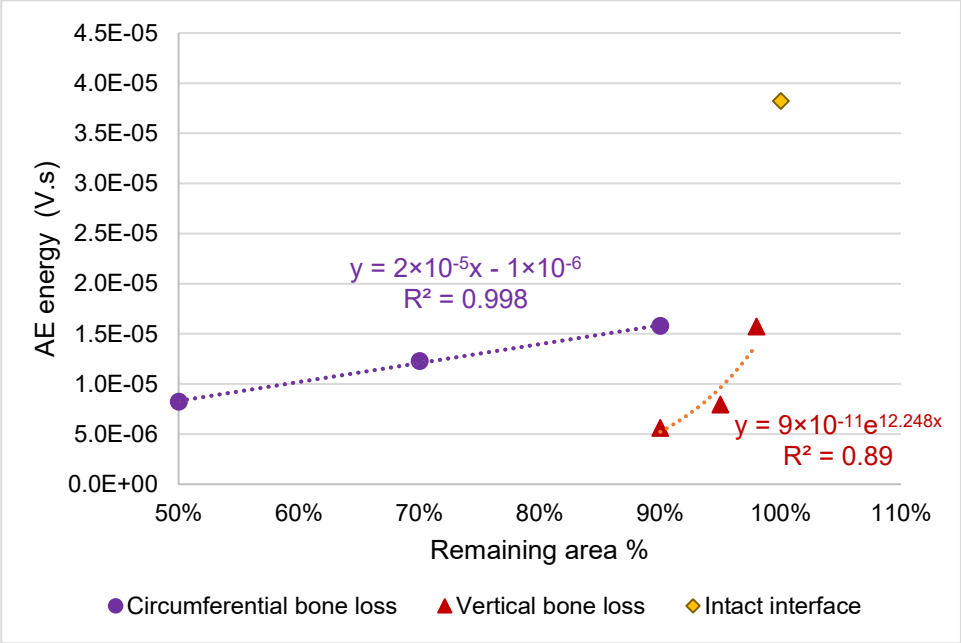

Figure 5.27: AE energy *vs.* proportion of the remaining supporting bone

There are a number of complicating factors that affect the clarity with which the systematic variations can identified:

1. Consistency of the AE probe (the pencil lead break). The energy recorded for an installation can vary due to a pencil lead break (on abutment) by about 10%.
2. Consistency of sensor coupling. The variation in the recorded energy due to sensor coupling is about 20%.
3. The variability of the individual bones both within samples and between samples.
4. The reproducibility of the installation of the implants and the build of the osseointegrated models.

5. Uncertainty in the measurements of bone microstructure and degree of osseointegration.

The implications of these limitations on the practical use of the technique will be discussed in the next chapter.

Chapter 6
Discussion

Monitoring bone-implant integration over time is valuable to assure long-term function. Various methods have been developed to assess implant stability and osseointegration longitudinally, each with limitations on its effectiveness and reliability. Acoustic emission, as presented in this thesis, is a non-invasive test that offers the potential to monitor implant stability efficiently, and at least as effectively as existing methods.

In this PhD study, the main aim was to investigate, using models of implants in various stability configurations, the potential of the AE technique to monitor bone-implant integration during healing and follow-up examination. The present results have demonstrated, in the model system, that the amount of AE energy transmitted from a source applied to the implant abutment could be used to recognise the development of osseointegration of dental implants. In addition, the AE energy effectively detected early changes in the marginal bone around the osseointegrated implants. These findings extend those of Ossi, (2013), confirming that AE energy transmission can be a successful tool for monitoring implant stability.

In this chapter, the discussion is structured into the following sections:

- suitability of the models used to represent the clinical application,
- reproducibility and accuracy of the histological and acoustic emission measurements,
- comparison of the proposed technique with existing methods,
- clinical implications of the study.

These are presented in turn below.

6.1 Suitability of the models to represent the clinical situation

No *in vivo* testing was carried out in this work and the animal model was confined to the bone itself. Whereas primary stability can be simulated in this animal model, secondary stability and degraded secondary stability both had to be simulated using physical models. These two aspects are discussed in the following sections.

6.1.1 Animal model

A cadaveric animal model was deemed preferable to avoid issues such as ethical implications, handling, availability and cost. Bovine rib bones have been used widely in dental implant research (Pinheiro et al., 2015, Vayron et al., 2014a) as a model for edentulous human jawbones because of their similar macroscopic relationship between cortical and cancellous bone, Figure 6.1. Each of the 14 ribs used in the systematic experiments were sourced from different bovine animals and showed varying anatomical configurations. Thus, the subject-related variations between these specimens can be used to assess the potential effect of patient variability in the clinical application. To avoid confusion with systematic variation, the positions of implants were randomized along each rib, so that any effect of type of bone surrounding each implant would reflect the intra-patient variability in bone density along the jaw (O' Mahony et al., 2000).

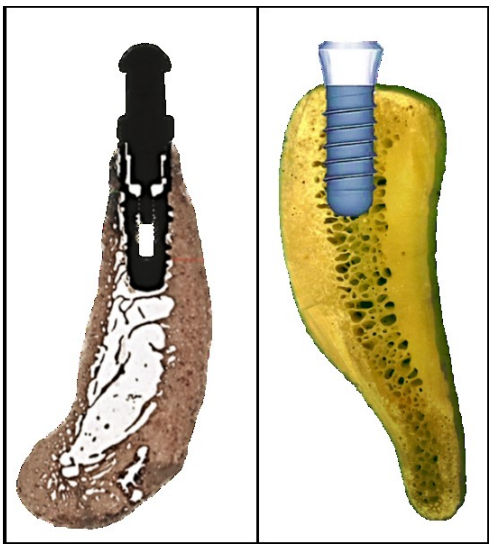

Figure 6.1: Cross-sectional view for human mandible (Nkenke et al., 2003) and bovine rib from this study

6.1.2 Interface simulations

The bone model was used for primary stability models, but was also developed for some stages of the work to simulate changes in the implant stability over time. Implants were inserted in the bones to mimic three stability configurations; primary stability, secondary stability (osseointegration) and compromised integration. These configurations were developed in the model in a way that imitates the sequence of changes that happen around an implant in a real installation, such as that shown in Figure 6.2. The series of radiographs in Figure 6.2 (A) and (B) show development of the primary stability of an implant into the secondary stability due to bone formation and maturation (osseointegration), whereas (C) shows signs of stability degradation due to marginal bone loss.

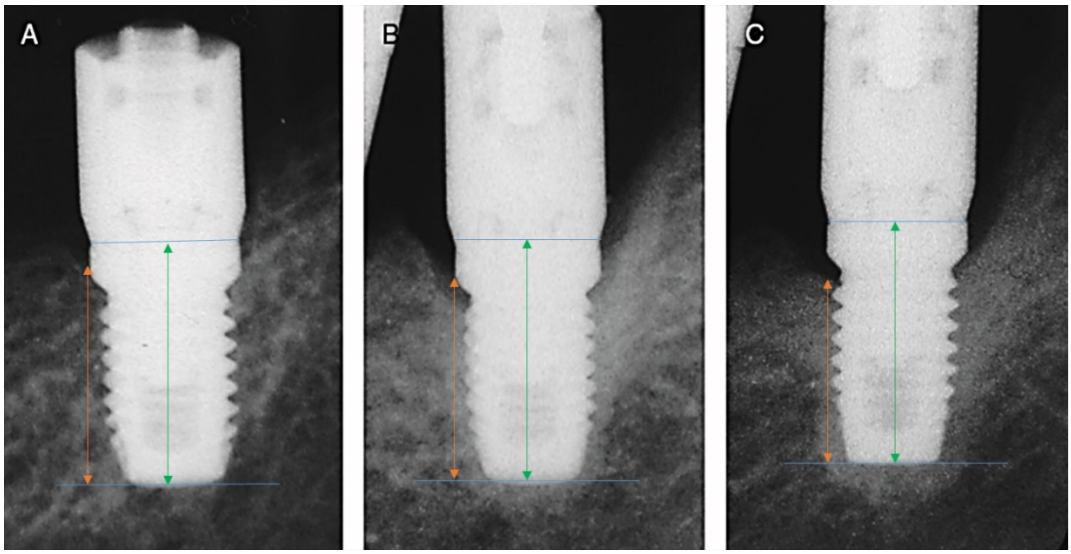

Figure 6.2: Bone response/ changes around an oral implant (Albrektsson et al., 2014). (A) Implant at the time of placement (primary stability). (B) The implant after 2 years with clear osseointegration layer (secondary stability). (C) The implant after 8 years with signs of marginal bone loss. The percentage of bone to implant (length) is estimated as (A) 96%, (B) 85%, (C) 74%.

At the time of placement, the mechanical integration of the implants into the surrounding bone (mostly cortical bone) simulated the primary stability situation. For secondary stability, obviously it was not possible for the implant to be osseointegrated, so glass ionomer cement (GIC) was used to integrate

the implants into the bone and to act as bone-implant interface. In earlier work, GIC was shown to have similar acoustic properties to bone (Ossi et al., 2013).

Two degrees of integrations were simulated; partial and full integration. On sectioning, as shown in Figure 6.3, partial integration (a) showed discrete cement masses of varying width attached to the implant surface, whereas the fully integrated model (b) displayed a distinct layer of cement at the interface between the implant and bone. These can be compared with real osseointegration in animal models where (c) shows low bone-implant contact and (d) shows high bone-implant contact. In this respect, the models for partial and full integration seem to be reasonably representative of the real situation.

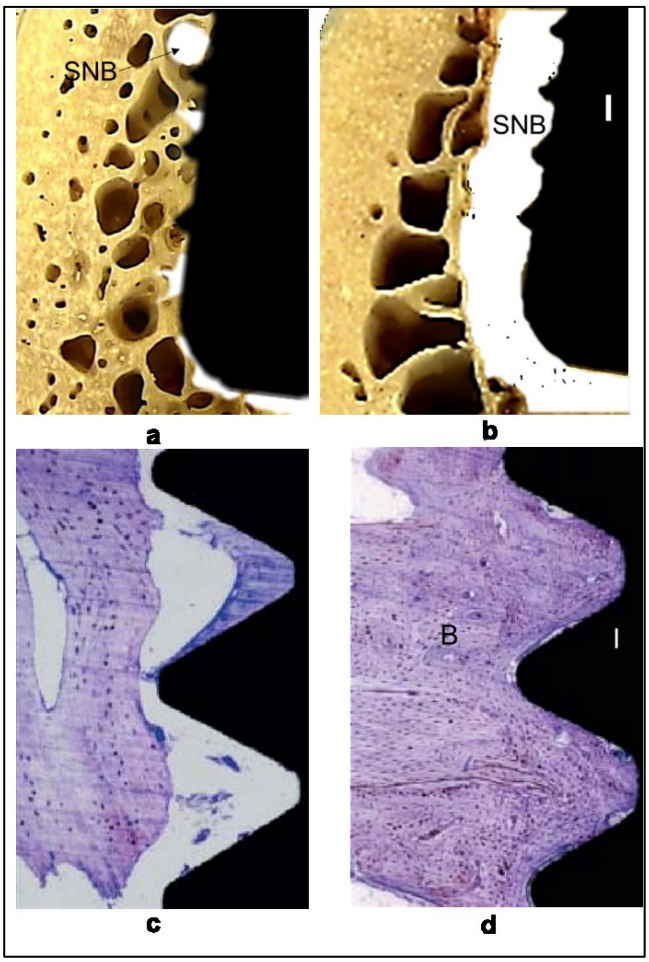

Figure 6.3: Comparison between the simulated osseointegration models used in this work (a: partial osseointegration and b: fully osseointegration) with real osseointegration in animal models (Albrektsson and Wennerberg, 2004) (c: low bone-implant contact, d: complete osseointegration and high bone-implant contact). B: Bone, I: Implant, SNB: Simulated New Bone.

For the compromised integration models, predetermined amounts of bone loss were created in the cervical region of the interface for fully integrated implants using adhesive paper pads to stop some of the transmission paths to the sensor. The pattern of loss of contact thus created around the implant, Figure 6.4 (a), seems to be a reasonable representation of *in vivo* peri-implant bone loss, Figure 6.4 (b).

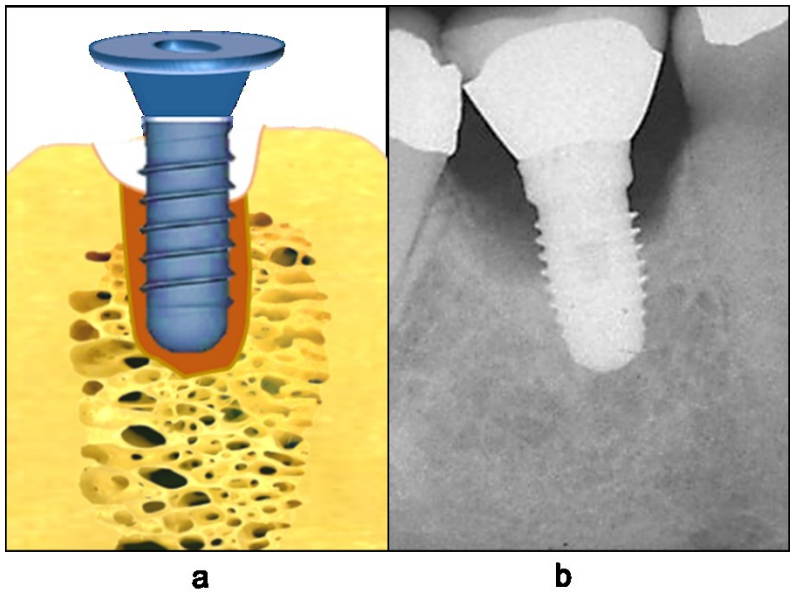

Figure 6.4: Comparison between (a) simulated compromised osseointegrated models used in this work and (b) real peri-implant bone loss in *in vivo* (Romanos and Weitz, 2012).

The accuracy of implant installation and obtaining nominally identical configurations, especially for primary stability, could have been affected by the skills of the investigator who is not a qualified surgeon and was essentially following the manufacturer's recommended surgical protocol. This could have influenced the reproducibility of AE measurements, but is taken into account in the measurements by having multiple versions of the same configuration. For the osseointegration models, although casting the implants into the restorative glass ionomer cement resulted in reproducible specimens for the fully integrated implants and the compromised versions, this might not be representative of the real architecture of osseointegration and pattern of peri-

implant bone loss *in vivo*. However, the advantage of reproducible specimens allowed a focus on the actual interface geometry free from the patient-specific variation that would no doubt ensue from real specimens. In addition, it was not technically possible to simulate exactly the same amount of cement-implant contact in each of the partially integrated models due to extrusion of the luting cement into the voids close to the implant. Nevertheless, this range of contact potentially simulated the real situation during the healing stage.

Another important limitation associated with using the bovine model (or any *in vitro* model) is that it was not possible to simulate the real oral environment between the implant and a surface-mounted sensor, including the cavity between the teeth and the cheek or lips, presence or absence of saliva, and soft tissue, any or all of which may have an influence on acoustic transmission. This matter is discussed in more detail in section 6.4.

6.2 Reproducibility and accuracy of the histological and acoustic emission measurements

This section is concerned with how well the measurements were made. There were two distinct types of measurement, the microstructure and macrostructure of bone-interface-implant configurations, and the measurement of transmitted AE.

6.2.1 Histological measurements

To better understand the transmission through the bone and the interface, it was necessary to quantify the microstructure and macrostructure, for which histological examination was necessary. Since AE is a type of structure-borne sound transmitted as elastic waves, the key thing was to quantify the continuous solid path from source to sensor for which an aggressive preparation was used to remove all non-solid components from the sections. Relevant measurements were made on a number of histological sections of bone and bone-implant interface and this process could be subjected to error due to some challenges in the preparation and analysis processes.

A limited number of the implants were allocated for the study, so they were removed before cutting the sections. This may have resulted in detachment of

some parts of the bone or cement, which might have been subsequently lost during sawing. To minimise this problem, the implants were removed as gently as possible, and the empty holes were filled with a wax to support the remaining structures during sectioning. To further preserve the structural integrity, sectioning was limited to only one histological section per implant. Despite these measures, loss of some materials still could obviously be seen in the photographic image for some sections, as shown in Figure 6.5. As far as was possible, areas of obvious post-test cement loss were compensated for the quantitative assessment of the interfacial contact. This was most difficult to do in the partial integration models, and so the degree of partial integration remains the least reliable of the quantitative interface contact measures.

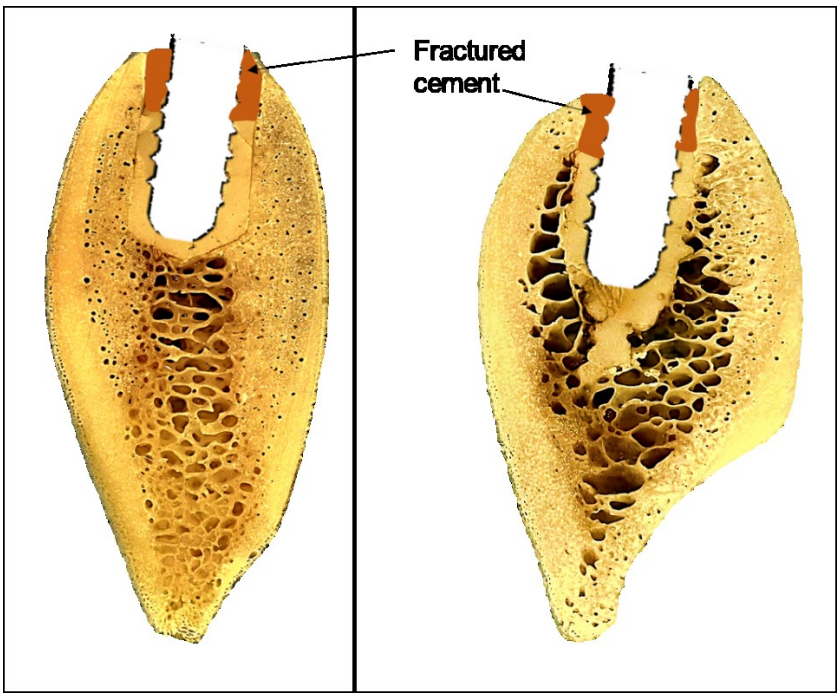

Figure 6.5: Example of histological preparation errors: fractured glass ionomer cement around the implant

Another source of error is that analysing histological sections provides only two-dimensional information which is only a sample of the entire 3D structure of either of the bone or the interface between bone and implant. This means

that any single histological measure has a non-quantifiable random error which can affect the certainty of any correlations with acoustic transmission. This may explain the weakness in the correlation between the width of the simulated osseointegration and the transmission which was measured from one view. As can be seen in Figure 6.6, there is a direct positive relationship between the transmission and the degree of osseointegration for the raw data, but this correlation is relatively weak as indicated by R^2 =0.64. As mentioned above, one of the experimental errors that could explain this is the reliance on one histological section to estimate the thickness of osseointegration layer rather than using the entire circumference of the layer, which is in fact transmitting the AE, but cannot be obtained from a 2D histological section produced in this work. This error is much more likely to affect partial integration models, because of the partial coverage of the surface of the implant.

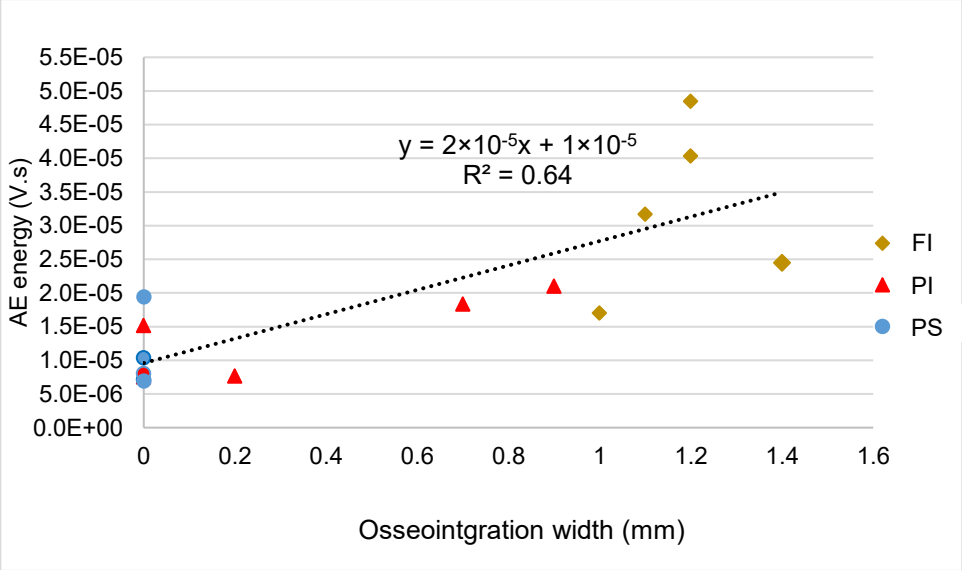

Figure 6.6: Correlation between AE and average width of the simulated osseointegration layer around the implant

Furthermore, as the analysis of the sections was done manually on photographic images acquired from a stereomicroscope, there were some difficulties in distinguishing the surface from the deeper parts of the porous structure of the cancellous bone. In order to better evaluate the sections and

retrieve the relevant data, the photographs were reviewed simultaneously on a computer screen.

Despite the above mentioned limitations in the histological quantification, the data were good enough to clearly show the effect of bone microstructure and density on the transmitted energy for relatively long distances along the bone, with an attenuation of approximately 20% per centimetre travelled. However, this was not of use for the transmission through the bone to a sensor adjacent to the implant on the surface, where the effect of the bone microstructure was far outweighed by the interface effect. This is positive in terms of the application (where the focus is on the transmission through the interface) but is scientifically a little unsatisfactory as the interface is also (in the real application) partly made of bone. Any future work needs to focus on this aspect using more realistic models of the bone-implant interface.

6.2.2 Acoustic emission measurements

This work has evaluated the capacity of AE to measure the changes in implant stability due to development or loss of osseointegration. The basis of the measurements was to introduce a controlled amount of ultrasonic energy, generated from a pencil lead break, into implants of varying stabilities in the bone. The amount of the transmitted energy is recorded using a sensor mounted on the surface of the specimens to express the amount of integration (stability) for those implants. Assuming the same amount of input energy (the pencil lead break is known to generate a reproducible amount of energy), losses can occur at the interface, within the bone, and between the bone and the sensor.

The main sources of uncontrolled variations in the systemic measurements were the pencil lead breaks and the coupling of the sensors to the bone surface. The recorded AE energy for a given installation can vary due the pencil lead break by approximately 10%, and due to the coupling of the sensor by about 20%. These variations are acceptable in terms of establishing the effect of the interface, but would not have adequate sensitivity (or specificity) for clinical use. Having said that, a clinical application would not involve pencil

lead breaks, nor would the surface mounting be directly onto the bone. This matter is discussed further in Section 6.4.

6.3 Comparison of the proposed technique with existing methods

A range of methods have been suggested to evaluate implant stability, some of which are in commercial use, some routinely. The most common of these are: radiography, Periotest™, resonance frequency analysis (RFA) and conventional ultrasound (CUS). This section summarises the way in which each technique works and then compares the clinical and practical value of each with the proposed method.

6.3.1 Basic principle of the methods

Figure 6.7 illustrates the basic physical principle of each technique for evaluation of the bone-implant interface.

A ***periapical radiograph***, Figure 6.7 (a), provides a two-dimensional projection for bone-implant system morphology and the output depends on the relative distribution of bone density. This is an imaging technique, providing a picture of bone density as a 2D projection of the implant and its surrounding bone.

The ***Periotest™*** (percussion test), Figure 6.7 (b), applies a transient force from an impactor to vibrate the implant and then measures the deceleration time by an accelerometer sensor. This method measures the mechanical fixity of the implant by a direct mechanical tap, and “feeling” the resistance.

Resonance frequency analysis (RFA), Figure 6.7 (c), involves excitation of implant with a vibrational stimulus (low frequency magnetic waves) and measures the displacement of the attached beam (the first flexure resonance frequency). This method also assesses mechanical fixity, this time less directly and is akin to plucking a guitar string, where higher frequencies indicate a tighter fixity.

Conventional ultrasound (CUS), Figure 6.7 (d), involves injection of ultrasonic pulse into the implant from a transponder which then measures the reflected pulse from the bone-implant interface. This method assesses the acoustic impedance of the interface, where good impedance matching results

in little ultrasound being reflected, whereas poor matching (poorly integrated interface) results in a large amount of reflection.

The *acoustic emission technique (AE)*, Figure 6.7 (e), introduces high frequency sound from an artificial source into the implant and records the transmission to a sensor on the patient's cheek. This method also assesses the acoustic impedance of the interface, good transmission being indicative of good matching (well-integrated) and poor matching (low transmission) being indicative of a poorly integrated interface.

Figure 6.7: Physical principle of each technique for examination of bone-implant interface

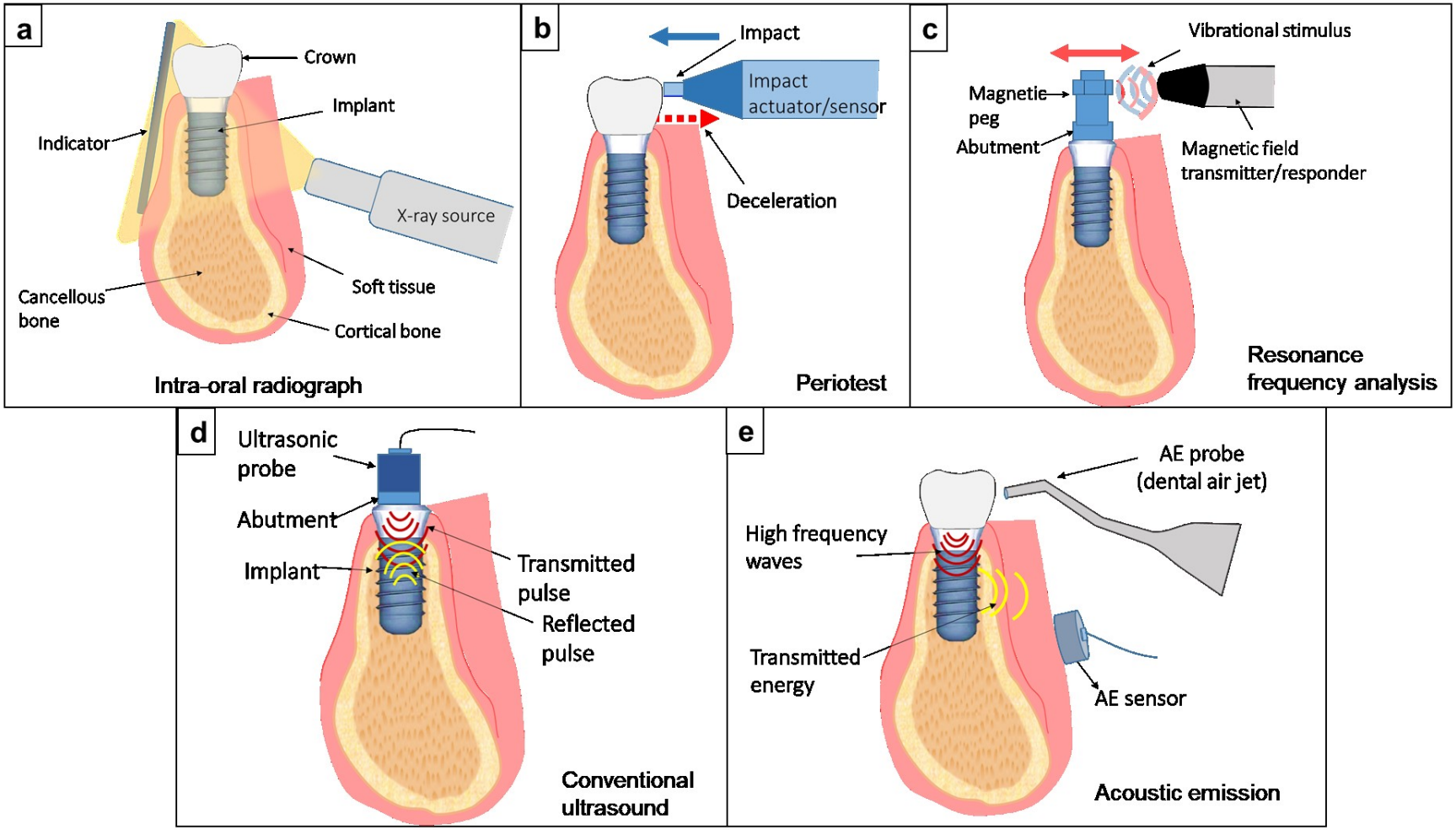

6.3.2 Advantages, limitations and reliability of methods for monitoring dental implants

Table 6.1 shows a comparison of the methods described in the previous section. Besides the different measurement outputs, from image to anchorage quality factor, the methods differ in the extent to which they have been commercially developed and/or are available in a typical clinic. Besides radiography, which is currently exploited to the maximum extent that it can be in normal clinical implantology practice, the only other commercially developed methods are those which measure the anchorage of the implant. For these, it is necessary to apply a force or displacement to the implant and/or attach a device to the abutment. The reliability and resolution of the methods are also limited, and they can be affected by operator skill.

The two remaining methods, CUS and AE both involve the propagation of high frequency waves, applied at the abutment. For CUS the amount of reflected wave energy is measured, whereas, for AE, the amount of transmitted energy is measured. The CUS method requires a transponder to be attached to the abutment, which carries an attendant risk of pain or damage. For AE, a simple source, such as an air jet pulse, would be preferred.

The cost of equipment for the commercially available techniques is nearly the same, ranging between $2000-5000. However, a periapical X-ray set is very versatile and may already be available in a dental practice for purposes other than monitoring implant stability. Periotest and Osstell are single-purpose instruments but, they are light, portable probes offering radiation free examination compared with radiography.

For both CUS and AE, technology suitable for this clinical application needs to be developed. Although it is not yet known what the commercial cost of either a CUS or an AE set would be, the equipment components (sensors, data acquisition and signal processing hardware and display hardware) would not be as expensive as the currently available units (radiography, Periotest and resonance frequency analysis).

Table 6.1: Comparison of techniques for examination of bone-implant interface

Technique	Relevant measurements	Advantages	Limitations	Reliability for monitoring dental implants
Periapical Radiographs	Image: 2-dimensional projection of bone-implant system morphology and bone density distribution.	Routinely available in the clinic. Well understood.	Radiation hazards. 2-dimensional, geometric distortion and anatomical superimposition. Requires interpretation by clinician,	Pre-operative bone quality assessment, evaluation of osseointegration and abutment fit, can only diagnose large mesial and distal defects.
Periotest™	Damping capacity of bone-implant structure (Implant mobility).	Commercially available. Portable non-contact device, patient and user friendly, less invasive than RFA and CUS. Gives a number indicative of quality.	Low sensitivity to partial peri-implant bone defects compared with RFA, lack of repeatability (susceptible to operator variability such as angulation and striking point of handpiece).	Measures fixity of implant into bone, provides objective measurement of implant stability, can diagnose circumferential bone loss >2mm.
Resonance frequency analysis (RFA): Osstell Mentor™; Osstell ISQ™	Implant vibration frequency under forced stimulus.	Commercially available. Portable, easy to use device, widely used.	Beam screwed to implant may endanger interface. No prognostic threshold value defined for implant failure.	Measures fixity of implant into bone, provides objective measurement of implant stability, can diagnose circumferential bone loss >1mm, and large partial vertical bone defect (3-walls at 5mm depth).

Technique	Relevant measurements	Advantages	Limitations	Reliability for monitoring dental implants
Conventional ultrasound (CUS)	Acoustic impedance of bone-implant interface as measure of intimate contact. Uses reflected energy.	Mild invasiveness, shows better sensitivity than vibrational methods.	Transponder screwed to implant may results in pain or damage, reproducibility affected by orientation of probe relative to implant axis, requires ultrasonic gel, bulky oral probe (transducer/ responder), currently not commercially available and cost is not yet known.	Measures implant osseointegration indirectly, but clinical sensitivity and specificity needs to be confirmed.
Acoustic emission (AE)	Acoustic impedance of bone-implant interface as measure of intimate contact. Uses transmitted energy.	Non-invasive, safer test, proposed oral probe (air jet) offers simple convenient test, patient and user friendly, high sensitivity to bone-implant anchorage and marginal bone loss.	Issues with the reproducibility of input stimulus and sensor coupling, pencil lead break test is not convenient for clinical application, currently not commercially available, extra-oral equipment needs to be developed for light and portable instrument, commercial cost is not yet known.	Measures implant osseointegration indirectly, detects mini-peri-implant marginal bone defects (circumferential loss extending for 1mm, vertical defect involving one wall extended 1mm), evaluate bone quality and density, clinical sensitivity and specificity needs to be confirmed.

6.4 Clinical implications of the study

It is well known that the demand is increasing for a non-invasive, clinically applicable method capable of providing a quantitative assessment of bone quality and measuring the degree of osseointegration as well as the level of peri-implant bone attachment. This demand has not been satisfied by the currently used methods in the clinic (Atsumi et al., 2007, Choi et al., 2014, Satwalekar et al., 2015, Garcia-Garcia et al., 2016, Zanetti et al., 2018).

The AE technique has been shown to offer a non-invasive, easily deployable test for routine clinical monitoring of implant osseointegration. Under the conditions of this study, the findings suggest that the AE technique may provide objective information about the condition of bone-implant interface at installation (anaesthetic permitting) immediately prior to loading and, subsequently, at follow-up examinations. AE has been able to detect the development of osseointegration of the implant which indicates that the technique can be applied to predict implant stability which may help to determine at which time point during healing the implant is ready for loading.

The technique has also shown its potential for detecting small changes in marginal bone height around dental implants. AE transmission for the osseointgrated implants showed a significant drop in the presence of a circumferential bone loss extending 1 mm apically, corresponding to the loss of the coronal cortical bone. Furthermore, AE can be used to detect a narrow, vertical bone defect including the first coronal 1 mm. It was not surprising that the major factor for the significant stability reduction was the loss of the coronal cortical bone, which has been proven to be critical for implant stability.

On the other hand, the AE energy was not able to differentiate significantly between the varying severities of compromised interfaces. In case of circumferential bone loss this can be explained by the fact that once the integrated implant has lost 1 mm of cortical support, most of the transmission is to the cancellous bone, and further loss of interface makes proportionately less difference.

As the bovine bones used in this study were long enough to accommodate the 10 mm long implant, there was no chance that the implants would have any bi-cortical stabilisation which would retain the AE transmission after removal of coronal cortical bone. Any future work needs to acknowledge this aspect and determine whether coronal cortical bone is the only contributor to the AE measurements.

The work has also shown that the changes in the AE energy can be observed when an osseointegrated implant loses as little as 2% of its supporting marginal bone area which is clinically equivalent to a defect of one wall extending 1 mm apically. This means that AE could detect peri-implant bone loss at a stage where other techniques are still not sensitive enough. The relatively low-resolution level makes it difficult for radiography to identify changes in the peri-implant bone structure and morphology until substantial amount of demineralization has occurred. For example, even in the high-resolution radiograph shown in Figure 6.2, the bone loss beyond that at implant placement (A), cannot be clearly seen on the radiograph until about 20% of the supporting marginal bone has been lost (C). For vibrational techniques, a clinically stable implant may maintain osseointegration laterally on some walls while experiencing small marginal bone defects on the other walls which may still limit the mobility of the implant and therefore be difficult to detect using vibration.

These findings could have a potential application in the early diagnosis of the conditions that affect peri-implant marginal bone health, such as peri-implantitis or any other form of loss of integration for implants used elsewhere in the body.

The AE technique can also provide additional information about the condition of the bone. The work that has been done on along-bone propagation identified in Chapter 5 suggests that AE may have a role in assessing and monitoring bone density in the jaw for patients who have had implants. This information could be calibrated against the bone density assessment that is made prior to implant placement by other techniques such as radiography to give a base-

line data for the patient which then can be compared with the subsequent measurements taken in the follow-up visits. Such an assessment would not necessarily replace established methods of bone density assessment but may help follow-up.

Figure 6.8 shows the potential anatomical landmarks for placing the AE sensor on the patient's jaw which include the skin over the temporomandibular joint (TMJ), zygomatic bone and mental foramen. These positions were tested by Ossi, (2013) to determine the optimal sensor position that can offer a stabilised mounting and allow sufficiently strong transmission. These landmarks were chosen because they have relatively little soft tissue covering providing good contact between the bone and sensor. Ossi's observations have shown clearly that mounting the sensor over mental foremen area provides the most stable placement and also provides the best transmission, with less consistent results for the other two positions. This difference could be attributed to factors such as; variations in the density of bone between the upper and lower jaw, the amount of soft tissue between bone and sensor or the proximity between the source and sensor. This highlights the need for further investigation to determine the best sensor mounting points on the patient's face considering the regional and anatomical variations of these positions.

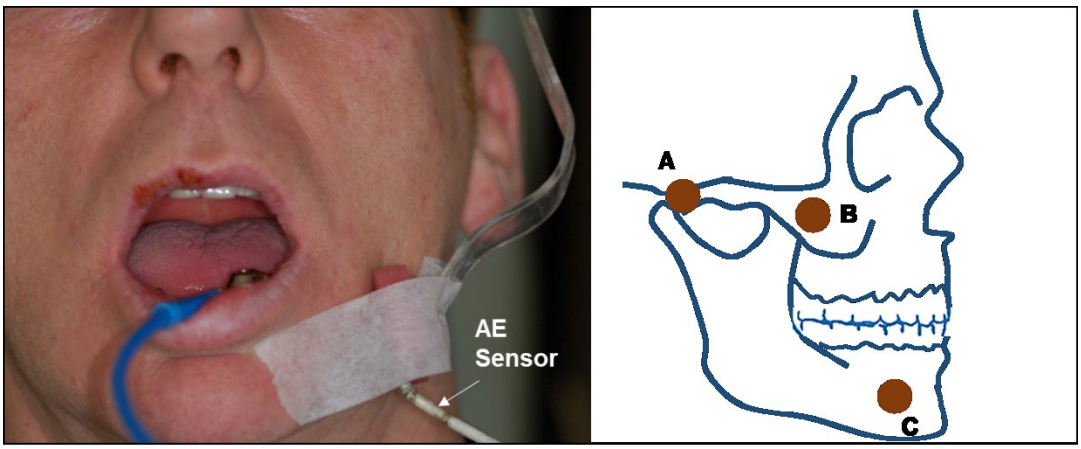

Figure 6.8: (a) Mounting of the AE sensor on patient's face (Ossi, 2013), (b) Potential anatomical positions for AE sensor mounting on patient's face on the areas of; A: TMJ, B: Zygoma, C: Mental foramen

As mentioned at the outset, it was not feasible to simulate the real oral environment so that its effect, as a confounding factor, on AE transmission remains unknown. A number of patient-specific variables such as the amount of soft tissue between bone and sensor, saliva level and tongue movements, although not assessed here, are expected to cause a reduction in the transmission. These variables have been explored using an air jet AE source, applied to an implant abutment in a number of different patient's mouths, recorded at a sensor mounted on the patient's faces (Ossi, 2013). Such patient-specific variables need to be taken into account in order that AE transmission can be used effectively to interrogate the interface.

In summary, the AE technique can be conveniently performed at any time interval during treatment or follow-up examinations to monitor variation in implant stability as well as the early changes in peri-implant marginal bone. However, in order that such a method can be used in the clinic, the following issues need to be addressed:

1. Introducing an impulsive source such as a pencil lead break is not appropriate for intra-oral use, so a more suitable source for clinical examination needs to be developed. This may be solved by using the

air jet from the dental chair as an oral AE probe and the feasibility of such a source has already been demonstrated in a previous study (Ossi, 2013). Ossi's results showed that the AE transmitted from an air jet source varied with the simulated degree of implant integration (loose or tight contact) and between large and small implants in a way similar to that of a pencil lead break test.

2. The air jet is not an impulsive source and is less easy to standardise than a pencil lead break. Accordingly, the distribution of frequency of transmitted AE can be used to discriminate between stability conditions.
3. The reproducibility of the source might be affected by the excitation conditions such as location of the striking (or jet landing) point and position of the source.
4. The difficulty in sensor placement and stabilisation on the patient's face due to variation in the soft tissue anatomy and patient attitude.
5. Patient specificity could also affect the reproducibility of the AE measurements. However, understanding the patient-specific effect (quality and quantity of bone) would help characterising the acoustic transmission parameters of the bone-implant interface as well as, potentially, the quality of bone in the patient's jaw.

Chapter 7
Conclusions and recommendations for future research

This chapter summarises the thesis findings and presents recommendations for future research.

The main objective of this work was to identify more reliable and precise parameter for measuring osseointegration and detecting compromised dental implants than those are currently available. Through a series of systematic investigations, presented in the preceding chapters, the acoustic emission technique has successfully offered a promising non-invasive method for assessing osseointegration and stability of dental implants.

7.1 Conclusions and key findings of the thesis

The conclusions for each of the systematic investigations are given below:

7.1.1 Effect of bone microstructure on acoustic transmission

The effect of bone micro and macrostructure on the AE transmission through and along bone has been measured in a primary stability model of a dental implant in bovine bone and established a base-line for assessing patient-specific acoustic characteristics. Strong attenuation was observed for AE signals travelling along bone and the degree of attenuation was influenced by the underlying microstructure and density of bone. The transmitted energy attenuated by approximately 20% per centimetre travelled and the correlation is considerable strengthened when the cross-section of solid bone along the transmission path is taken into account. This indicates the potential clinical usefulness of the technique for evaluating bone quality and provide a potential reference for changes / alterations in jaw bone density due to ageing or

systemic disease if a measurement is recorded at the time of implant installation and on first loading and then later in the follow-up visits.

Despite the sensitivity to bone structure, AE transmission through the bone from an implant to a sensor on the adjacent bone surface was more heavily conditioned by the quality of the bone-implant interface, which is the site of interest for stability monitoring. This indicates that AE is capable of providing quantitative information directly related to the bone-implant interface condition.

7.1.2 Influence of osseointegration and secondary stability on acoustic transmission

The reliability of acoustic emission for monitoring implant stability has been evaluated as a function of osseointegration in a simulation model. A positive correlation was found between the amount of simulated bone-implant contact and proportion of acoustic emission energy transmitted from a standard AE source to a sensor placed on the adjacent surface of the bone.

The transmitted energy has been found to differentiate between primary stability and partial and full integration, with a factor of over 3 in transmission between primary stability and full integration. These findings demonstrate that monitoring changes in acoustic emission transmission during the implant healing phase can provide valuable information on the progress of osseointegration. Such a measurement could allow the practitioner to predict indirectly implant stability during the early stages after implant placement which would be helpful in determining the appropriate loading approach and avoid early implant failure and/or accelerate healing and osseointegration. Subject-related variations had an influence on the acoustic transmission but did not dominate the effect of osseointegration.

7.1.3 Potential of acoustic energy for diagnosing peri-implant bone loss

The sensitivity of the acoustic emission technique has been investigated for simulated osseointegrated implants with various peri-implant bone defects. The results have shown that the transmitted energy can effectively detect small changes in the marginal bone around the osseointegrated implants. Circumferential or narrow vertical bone defects were clearly detectible for the

most coronal 1 mm of the marginal bone. Significant changes in the AE energy could be observed when the osseointegrated implants had lost as little as 2% of their supporting marginal bone area. These findings suggest that loss of contact between bone and implant surfaces can be identified at an earlier stage using acoustic emission, compared with existing techniques. This could have implications for the early diagnosis of peri-implantitis, the main cause of failure of dental implants, or other forms of loss of integration when used elsewhere in the body.

Overall, acoustic emission has shown efficacy in providing objective information about successful osseointegrated implants and compromised implants in an *in vitro* model. This could have clinical significance in a number of ways, including: 1) evaluating implant stability at different stages of healing until establishing a successful osseointegration, 2) helping in the decision process on when an implant should be loaded; 3) aiding in early failure diagnosis and critical treatment planning; 4) monitoring implant stability / function at follow-up examinations, and 5) monitoring the general bone health of patients with implants.

These findings are promising and worthy for clinical validation which could pave the way toward the development of a medical device for monitoring the bone-implant interface not only for dental implants, but also for other medical implant applications.

7.2 Limitations of the study

The work has some acknowledged imitations which condition the conclusions and inform the future work suggested. The main ones listed below.

1. The work was carried out in *in vitro* with implants being inserted in cadaveric animal bone (bovine ribs) and using artificial models for osseointegration.
2. An engineering drill was used instead of a dental handpiece for preparation of the implant bed.

3. For the studies presented in this thesis, one implant system with fixed diameter and length was used.
4. The pencil lead break and the sensors limit the frequency range to 0.1-1MHz. this source is not appropriate for intra-oral use, so a more suitable source for clinical examination needs to be developed, which may involve a different range of frequencies.
5. The variability associated with sensor placement and stabilisation on the bone surface has led to some scatter in results which, if not overcome, would limit sensitivity in the clinical setting.
6. Histological analysis provided only two-dimensional information about the simulated bone-implant contact.
7. This work was confined to transmission to the surface of the bone and did not consider the effect of soft tissue (mucosa, cheek) and any air spaces between the bone and sensors.

7.3 Recommendations for future research

The work presented here is not without its limitations, the most significant of which are that the work was carried out *in vitro* and that the osseointegration models were artificial. The following recommendations for future work are suggested to overcome these limitations.

1. This work has provided a basic understanding of the relationship between bone microstructure and acoustic transmission through a primary stability simulation. To gain further insight into patient-specific aspects of acoustic transmission, further studies considering different bone qualities in more realistic models (animal models) would be beneficial in establishing the correlation between acoustic emission and bone-implant contact.
2. So far, the work has been confined to transmission to the surface of the bone, which is not directly accessible *in vivo*. An extension of the study piloted by Ossi would be beneficial in quantifying the effects of adjacency of the implant to the most stable sensor mounting site, and

patient-specific aspects, such as bone quality and soft tissue (lip and cheek) anatomy.

3. Future longitudinal clinical studies are required to characterise the acoustic transmission for dental implants at various points during healing for monitoring osseointegration.
4. Longitudinal clinical studies are needed to validate the potential of the AE as an early detection tool for marginal peri-implant bone loss.
5. So far, the study has been confined to one type of implant. It would be of interest also to investigate the effect of different implant types, diameters and lengths.

Appendix

Full inventory of bone and bone-implant interface sections

Bone-1: (in reference to Figure 3.8a, Section 3.1.3 / Figure 5.2, Section 5.1)

A) Transverse sections at sensors positions including the reference position with primary stability model

B) Longitudinal sections of areas between sensor positions

Bone-2: Transverse sections of primary stability and partial and full osseointegration

(In reference to Figure 3.8b, Section 3.1.3 / Section 5.1 / Section 5.2)

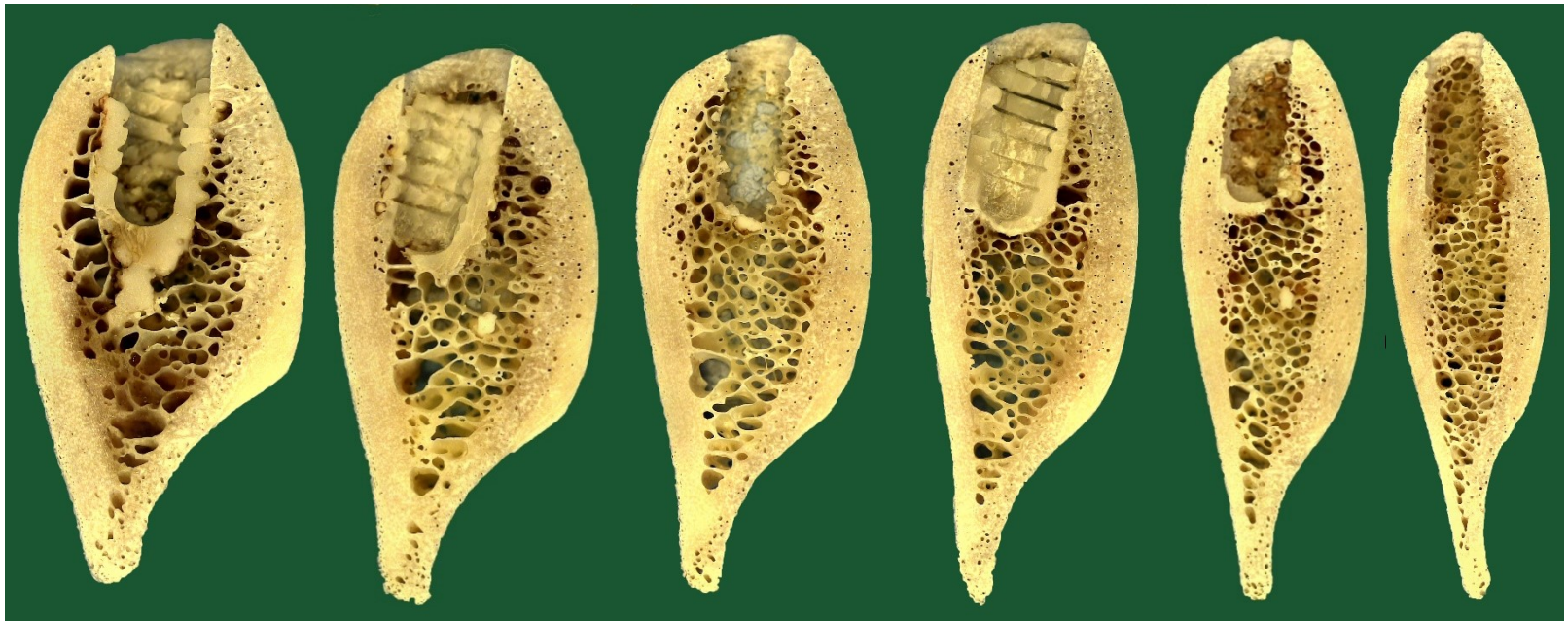

Bone-3: Transverse sections of primary stability and partial and full osseointegration

(In reference to Figure 3.8c, Section 3.1.3 / Section 5.1 / Section 5.2)

References

Acil, Y., SIevers, J., Gulses, A., Ayna, M., Wiltfang, J. & Terheyden, H. 2017. Correlation between resonance frequency, insertion torque and bone-implant contact in self-cutting threaded implants. Odontology, 105, 347-353.

Adell, R., Lekholm, U., Rockler, B. & Brånemark, P. I. 1981. A 15-year study of osseointegrated implants in the treatment of the edentulous jaw. International Journal of Oral Surgery, 10, 387-416.

Aggelis, D., Strantza, M., Louis, O., Boulpaep, F., Polyzos, D. & Van Hemelrijck, D. 2015. Fracture of human femur tissue monitored by acoustic emission sensors. Sensors, 15, 5803-5819.

Aguilar-Salvatierra, A., Calvo-Guirado, J. L., González-Jaranay, M., Moreu, G., Delgado-Ruiz, R. A. & Gómez-Moreno, G. 2016. Peri-implant evaluation of immediately loaded implants placed in aesthetic zone in patients with diabetes mellitus type 2: A two-year study. Clinical Oral Implants Research, 27,156-161.

Al-Sabbagh, M., & Bhavsar, I. 2015. Key local and surgical factors related to implant failure. Dental Clinics of North America, 59, 1-23.

Albrektsson, T., Brånemark, P. I., Hansson, H. A., Lindström, J., Albrektsson, J. & Brånemark, J. 1981. Osseointegrated titanium implants: Requirements for ensuring a long- lasting, direct bone-to-implant anchorage in man. Acta Orthopaedica, 52, 155-170.

Albrektsson, T., Buser, D. & Sennerby, L. 2012. On crestal/marginal bone loss around dental implants. The International Journal of Prosthodontics, 25, 320-322.

Albrektsson, T., Dahlin, C., Jemt, T., Sennerby, L., Turri, A. & Wennerberg, A. 2014. Is marginal bone loss around oral implants the result of a provoked foreign body reaction? Clinical Implant Dentistry and Related Research, 16, 155-165.

Albrektsson, T., & Isidor, F., 1994. Consensus Report of Session IV. In: Lang, N.P. and Karring, T., Eds., Proceedings of the First European Workshop on Periodontology, Quintessence Publishing, London, 365-369.

Albrektsson, T. & Jacobsson, M. 1987. Bone-metal interface in osseointegration. The Journal of Prosthetic Dentistry, 57, 597-607.

Albrektsson, T. & Wennerberg, A. 2004. Oral implant surfaces: Part 1-review focusing on topographic and chemical properties of different surfaces and *in vivo* responses to them. International Journal of Prosthodontics, 17, 536-543.

Albrektsson, T. & Zarb, G. A. 1993. Current interpretations of the osseointegrated response: clinical significance. The International Journal of Prosthodontics, 6, 95-105.

Albrektsson, T., Zarb, G., Worthington, P. & Eriksson, A. R. 1986. The long-term efficacy of currently used dental implants: A review and proposed criteria of success. The International Journal of Oral & Maxillofacial Implants, 1, 11.

Alghamdi, H., Anand, P. S. & Anil, S. 2011. Undersized implant site preparation to enhance primary implant stability in poor bone density: A prospective clinical study. Journal of Oral and Maxillofacial Surgery, 69, 506-512.

Alghamdi, S. 2018. Methods to improve osseointegration of dental implants in low quality (Type-IV) bone: An overview. Journal of Functional Biomaterials, 9, 7.

Alla, R. K., Ginjupalli, K., Upadhya, N., Shammas, M., Ravi, R. K. & Sekhar, R. 2011. Surface roughness of implants: A review (Report). Trends in Biomaterials and Artificial Organs, 25, 112.

Andersson, P., Pagliani, L., Verrocchi, D., Volpe, S., Sahlin, H. & Sennerby, L. 2019. Factors influencing resonance frequency analysis (RFA) measurements and 5-year survival of neoss dental implants. International Journal of Dentistry, 2019, 1-9.

Annibali, S., Bignozzi, I., La Monaca, G. & Cristalli, M. P. 2012. Usefulness of the aesthetic result as a success criterion for implant therapy: A review. Clinical Implant Dentistry and Related Research, 14, 3-40.

Ao, J., Li, T., Liu, Y., Ding, Y., Wu, G., Hu, K. & Kong, L. 2010. Optimal design of thread height and width on an immediately loaded cylinder implant: A finite element analysis. Computers in Biology and Medicine, 40, 681-686.

Aparicio, C., Lang, N., & Rangert, B. 2006. Validity and clinical significance of biomechanical testing of implant-bone interface. Clinical oral implants research, 17, 2–7.

As El, A. 1999. Why do dental implants fail? Part I. Implant Dentistry, 8, 173-185.

ASTM International. 2015. E976-15 Standard guide for determining the reproducibility of acoustic emission sensor response. West Conshohocken, PA; ASTM International.

Ata-Ali, J., Flichy-Fernández, A. J., Alegre-Domingo, T., Ata-Ali, F. & Peñarrocha-Diago, M. 2016. Impact of heavy smoking on the clinical, microbiological and immunological parameters of patients with dental implants: A prospective cross-sectional study. Journal of Investigative and Clinical Dentistry, 7, 401-409.

Atsumi, M., Park, S. H. & Wang, H. L. 2007. Methods used to assess implant stability: Current status. The International Journal of Oral & Maxillofacial Implants, 22, 743-754.

Baldi, D., Lombardi, T., Colombo, J., Cervino, G., Perinetti, G., Lenarda, R. & Stacchi, C. 2018. Correlation between insertion torque and implant stability quotient in tapered implants with knife-edge thread design. Bio Med Research International, 2018.

Baqain, Z. H., Moqbel, W. Y. & Sawair, F. A. 2012. Early dental implant failure: risk factors. British Journal of Oral & Maxillofacial Surgery, 50, 239-243.

Barfeie, A., Wilson, J. & Rees, J. 2015. Implant surface characteristics and their effect on osseointegration. British Dental Journal, 218, e9.

Barikani, H., Rashtak, S., Akbari, S., Fard, M. K. & Rokn, A. 2014. The effect of shape, length and diameter of implants on primary stability based on resonance frequency analysis. Dental Research Journal, 11, 87-91.

Berglundh, T., Armitage, G., Araujo, M. G., Avila-Ortiz, G., Blanco, J., Camargo, P. M., Chen, S., Cochran, D., Derks, J. & Figuero, E. 2018. Peri-implant diseases and conditions: Consensus report of workgroup 4 of the 2017 world workshop on the classification of periodontal and peri-Implant diseases and conditions. Journal of Periodontology, 89, 313-318.

Bhandari, M. A. 2019. Effect of surface design and morphology on primary stability of dental implant: A systematic review. EC Dental Science, 18, 401-409.

Bilhan, H., Cilingir, A., Bural, C., Bilmenoglu, C., Sakar, O. & Geckili, O. 2015. The evaluation of the reliability of Periotest for implant stability measurements: An *in vitro* study. Journal of Oral Implantology, 41, 90-95.

Bilhan, H., Geckili, O., Mumcu, E., Bozdag, E., Sünbüloğlu, E. & Kutay, O. 2010. Influence of surgical technique, implant shape and diameter on the primary stability in cancellous bone. Journal of Oral Rehabilitation, 37, 900-907.

Bohra, A., Chandrasekaran, M. & Teyi, N. 2019. Bone drilling investigation and possible research: A state of the art review, 2128.

Brånemark, P. I., Breine, U., Adell, R., Hansson, B. O., Lindström, J. & Ohlsson, Å. 1969. Intra-osseous anchorage of dental prostheses: I. Experimental Studies. Scandinavian Journal of Plastic and Reconstructive Surgery, 3, 81-100.

Brånemark P. I., Hansson B. O., Adell R., Breine U., Lindström J., Hallán O. & Öhman A. 1977. Osseointegrated implants in the treatment of the edentulous jaw. Stockholm: Almqvist and Wiksell, 1977, 132.

Brocard, D., Barthet, P., Baysse, E., Duffort, J. F., Eller, P., Justumus, P., Marin, P., Oscaby, F., Simonet, T. & Benqué, E. 2000. A multicenter report on 1,022 consecutively placed ITI implants: A 7-year longitudinal study. International Journal of Oral & Maxillofacial Implants, 15, 691-700.

Brunette, D. M., Tengvall, M., Textor, M. & Thomsen, P. 2002. Titanium in medicine: Material science, surface science, engineering, biological responses and medical applications. Springer-Verlag, Berlin Heidelberg, pp 87.

Bugea, C., Luongo, R., Di Iorio, D., Cocchetto, R. & Celletti, R. 2008. Bone contact around osseointegrated implants: Histologic analysis of a dual-acid-etched surface implant in a diabetic patient. International Journal of Periodontics and Restorative Dentistry, 28, 145-151.

Busenlechner, D., Fürhauser, R., Haas, R., Watzek, G., Mailath, G. & Pommer, B. 2014. Long-term implant success at the Academy for Oral Implantology: 8-year follow-up and risk factor analysis. Journal of Periodontal & Implant Science, 44, 102-108.

Buser, D., Janner, S. F., Wittneben, J. G., Brägger, U., Ramseier, C. A. & Salvi, G. E. 2012. 10-Year Survival and success rates of 511 titanium implants with a sandblasted and acid-etched surface: A retrospective study in 303 partially edentulous patients. Clinical Implant Dentistry and Related Research, 14, 839-851.

Buser, D., Weber, H. P. & Lang, N. P. 1990. Tissue integration of non-submerged implants. 1-year results of a prospective study with 100 ITI hollow-cylinder and hollow-screw implants. Clinical Oral Implants Research, 1, 33-40.

Canullo, L., Peñarrocha-Oltra, D., Covani, U., Botticelli, D., Serino, G. & Penarrocha, M. 2016. Clinical and microbiological findings in patients with peri-implantitis: A cross-sectional study. Clinical Oral Implants Research, 27,376-382.

Carcuac, O., Abrahamsson, I., Albouy, J. P., Linder, E., Larsson, L. & Berglundh, T. 2013. Experimental periodontitis and peri-implantitis in dogs. Clinical Oral Implants Research, 24, 363-371.

Carr, A. B. 2012. Survival of short implants is improved with greater implant length, placement in the mandible compared with the maxilla, and in nonsmokers. The journal of Evidence-Based Dental Practice, 12, 18-20.

Carrasco-García, A., Castellanos-Cosano, L., Corcuera-Flores, J. R., Rodríguez-Pérez, A., Torres-Lagares, D. & Machuca-Portillo, G. 2019. Influence of marginal bone loss on peri-implantitis: Systematic review of literature. Journal of Clinical and Experimental Dentistry, 11, 1045-1071.

Cassetta, M., Di Giorgio, R. & Barbato, E. 2018. Are intraoral radiographs accurate in determining the peri-implant marginal bone level? International Journal of Oral & Maxillofacial Implants, 33, 847-852.

Çavuşoğlu, Y., Şahin, E. & Akça, K. 2012. Efficacy of resonance frequency analysis in the diagnosis of compromised bone-implant interface. Implant Dentistry, 21, 394–398.

César-Neto, J. B., Duarte, P. M., Sallum, E. A., Barbieri, D., Moreno, H. & Nociti, F. H. 2003. A comparative study on the effect of nicotine administration and cigarette smoke inhalation on bone healing around titanium implants. Journal of Periodontology, 74, 1454-1459.

Chambrone, L., Chambrone, L. A. & Lima, L. A. 2010. Effects of occlusal overload on peri-implant tissue health: A systematic review of animal-model studies. Journal of Periodontology, 81, 1367-1378.

Chang, P. K., Chen, Y. C., Huang, C. C., Lu, W. H., Chen, Y. C. & Tsai, H. H. 2012. Distribution of micromotion in implants and alveolar bone with different thread profiles in immediate loading: A finite element study. International Journal of Oral & Maxillofacial Implants, 27, 96-101.

Chen, H., Liu, N., Xu, X., Qu, X., Lu, E. & Baradaran, H. R. 2013. Smoking, radiotherapy, diabetes and osteoporosis as risk factors for dental implant failure: A meta-analysis. PLoS ONE, 8, e71955.

Cheng, T., Chen, Y. & Nie, X. 2013. Insertion torques influenced by bone density and surface roughness of HA-TiO2 coatings. Thin Solid Films, 549, 123-130.

Choi, H. H., Chung, C. H., Kim, S. G. & Son, M. K. 2014. Reliability of 2 implant stability measuring methods in assessment of various peri-implant bone loss: An *in vitro* study with the Periotest and Osstell Mentor. Implant Dentistry, 23, 51-56.

Chrcanovic, B. R., Albrektsson, T. & Wennerberg, A. 2014a. Diabetes and oral implant failure. Journal of Dental Restoration, 93, 859-867.

Chrcanovic, B. R., Albrektsson, T. & Wennerberg, A. 2014b. Reasons for failures of oral implants. Journal of Oral Rehabilitation, 41, 443-476.

Chrcanovic, B. R., Albrektsson, T. & Wennerberg, A. 2015. Smoking and dental implants: A systematic review and meta-analysis. Journal of Dentistry, 43, 487-498.

Claudio, S., Federico, B., Giuseppe, P., Andrea, F., Teresa, L., Aiman, K., Francesca, A. & Roberto Di, L. 2016. Risk factors for peri-implantitis: Effect of history of periodontal disease and smoking habits. A systematic review and meta-analysis. E-Journal of Oral Maxillofacial Research, 7, e3.

Clementini, M., Rossetti, P. H., Penarrocha, D., Micarelli, C., Bonachela, W. C. & Canullo, L. 2014. Systemic risk factors for peri-implant bone loss: A systematic review and meta-analysis. International Journal of Oral & Maxillofacial Surgery, 43, 323-334.

Coelho, P. G., Granato, R., Marin, C., Teixeira, H. S., Suzuki, M., Valverde, G. B., Janal, M. N., Lilin, T. & Bonfante, E. A. 2011. The effect of different implant macrogeometries and surface treatment in early biomechanical fixation: An experimental study in dogs. Journal of Mechanical Behaviour of Biomedical Materials, 4, 1974-1981.

Coli, P., Christiaens, V., Sennerby, L. & Bruyn, H. 2017. Reliability of periodontal diagnostic tools for monitoring peri-implant health and disease. Periodontology 2000, 73, 203-217.

Coli, P. & Sennerby, L. 2019. Is peri-implant probing causing over-diagnosis and over-treatment of dental implants? Journal of Clinical Medicine, 8, 1123-1136.

Crespi, R., Capparè, P., Gherlone, E. & Romanos, G. E. 2007. Immediate occlusal loading of implants placed in fresh sockets after tooth extraction. International Journal of Oral & Maxillofacial Implants, 22, 955-962.

Crespi, R., Capparé, P., Gherlone, E. & Romanos, G. E. 2008. Immediate versus delayed loading of dental implants placed in fresh extraction sockets in the maxillary aesthetic zone: A clinical comparative study. International Journal of Oral & Maxillofacial Implants, 23,753-758.

Da Costa Valente, M. L., De Castro, D. T., Shimano, A. C., Lepri, C. P. & Dos Reis, A. C. 2016. Analysing the influence of a new dental implant design on primary stability. Clinical Implant Dentistry and Related Research, 18, 168-173.

Da Silva, E. S., Feres, M., Figueiredo, L. C., Shibli, J. A., Ramiro, F. S. & Faveri, M. 2014. Microbiological diversity of peri-implantitis biofilm by Sanger sequencing. Clinical Oral Implants Research, 25, 1192-1199.

Dagher, M., Mokbel, N., Jabbour, G. & Naaman, N. 2014. Resonance frequency analysis, insertion torque, and bone to implant contact of 4 implant surfaces: Comparison and correlation study in sheep. Implant Dentistry, 23, 672-678.

Daubert, D. M., Weinstein, B. F., Bordin, S., Leroux, B. G. & Flemmig, T. F. 2015. Prevalence and predictive factors for peri-implant disease and implant failure: A cross-sectional analysis. Journal of Periodontology, 86, 337-347.

Davies, J. E. 1998. Mechanisms of endosseous integration. The International Journal of Prosthodontics, 11, 391-401.

De Oliveira, R. C., Leles, C. R., Lindh, C. & Ribeiro-Rotta, R. F. 2012. Bone tissue microarchitectural characteristics at dental implant sites. Part 1: identification of clinical-related parameters. Clinical Oral Implants Research, 23, 981-986.

Decker, A. M. & Wang, H. L. 2020. Diabetes and smoking as the potential risk factors for peri-implant diseases. Risk factors for peri-implant diseases. Springer.

Degidi, M., Nardi, D. & Piattelli, A. 2009. Immediate restoration of small-diameter implants in cases of partial posterior edentulism: A 4-year case series. Journal of Periodontology, 80, 1006-1012.

Denis, B., Alberto, B., Antonio, K., Aleksandar, I., Leksandar, S., Florent, B., Elitsa, G. D. & Elizabeta, G. 2018. Assessment of primary and secondary implant stability by resonance frequency analysis in anterior and posterior segments of maxillary edentulous ridges. Journal of IMAB, 24, 2058-2064.

Dias, D., Leles, C., Lindh, C. & Ribeiro-Rotta, R. 2014. The effect of marginal bone level changes on the stability of dental implants in a short-term evaluation. Clinical Oral Implants Research, 26, 1185-1190.

Diaz Castro, M. C., Falcao, A., Lopez-Jarana, P., Costa, C., Rios-Santos, J. V., Fernandez-Palacin, A. & Climent, M. 2019. Repeatability of the resonance frequency analysis values in implants with a new technology. Medicina Oral Patología Oraly Cirugia Bucal, 24, 636–642.

Donati, M., Ekestubbe, A., Lindhe, J. & Wennström, J. L. 2018. Marginal bone loss at implants with different surface characteristics: A 20-year follow-up of a randomized controlled clinical trial. Clinical Oral Implants Research, 29, 480-487.

Dos Santos, M. V., Elias, C. N. & Cavalcanti Lima, J. H. 2011. The effects of superficial roughness and design on the primary stability of dental implants. Clinical Implant Dentistry and Related Research, 13, 215-223.

Eickholz, P., Grotkamp, F. L., Staehle, H. J., Steveling, H. & Mühling, J. 2001. Reproducibility of peri-implant probing using a force-controlled probe. Clinical Oral Implants Research, 12, 153-158.

El Shaib, M. N. 2013. Predicting acoustic emission attenuation in solids using ray-tracing within a 3D solid model. Heriot-Watt University UK.

Elias, C. N., Rocha, F. A., Nascimento, A. L. & Coelho, P. G. 2012. Influence of implant shape, surface morphology, surgical technique and bone quality on the primary stability of dental implants. Journal of the Mechanical Behaviour of Biomedical Materials, 16, 169-180.

Elsyad, M. A., Elsaih, E. A. & Khairallah, A. S. 2014. Marginal bone resorption around immediate and delayed loaded implants supporting a locator-retained mandibular overdenture. A 1-year randomised controlled trial. Journal of Oral Rehabilitation, 41, 608-618.

Eriksson, R. A. & Albrektsson, T. 1984. The effect of heat on bone regeneration: An experimental study in the rabbit using the bone growth chamber. Journal of Oral and Maxillofacial Surgery, 42, 705-711.

Esposito, M. 1999. On biological failures of osseointegrated oral implants. ProQuest Dissertations Publishing.

Esposito, M., Hirsch, J. M., Lekholm, U. & Thomsen, P. 1997. Failure patterns of four osseointegrated oral implant systems. Journal of Materials Science: Materials in Medicine, 8, 843-847.

Esposito, M., Hirsch, J. M., Lekholm, U. & Thomsen, P. 1998. Biological factors contributing to failures of osseointegrated oral implants, (I). Success criteria and epidemiology. Copenhagen, DK.

Esposito, M., Hirsch, J. M., Lekholm, U. & Thomsen, P. 1999. Differential diagnosis and treatment strategies for biologic complications and failing oral implants: A review of the literature. The International Journal of Oral & Maxillofacial Implants, 14, 473-490.

Esposito, M., Pellegrino, G., Pistilli, R. & Felice, P. 2011. Rehabilitation of posterior atrophic edentulous jaws: prostheses supported by 5 mm short implants or by longer implants in augmented bone? One-year results from a pilot randomised clinical trial. European Journal of Oral Implantology 4, 21-30.

Falco, A., Berardini, M. & Trisi, P. 2018. Correlation between implant geometry, implant surface, insertion torque, and primary stability: *In vitro* biomechanical analysis. The International Journal of Oral & Maxillofacial Implants, 33, 824-830.

Fazzalari, N.L., Parkinson, I.H.1996. Fractal properties of cancellous bone in osteoporosis. Science Direct Journals, 3,140-149.

Feller, L., Chandran, R., Khammissa, R., Meyerov, R., Jadwat, Y., Bouckaert, M., Schechter, I. & Lemmer, J. 2014. Osseointegration: biological events in relation to characteristics of the implant surface. South African Dental Journal, 69, 112-117.

Fernandes, C. B., Aquino, D. R., Franco, G. C., Cortelli, S. C., Costa, F. O. & Cortelli, J. R. 2010. Do elderly edentulous patients with a history of periodontitis harbour periodontal pathogens? Clinical Oral Implants Research, 21, 618-623.

Ferreira, S. D., Martins, C. C., Amaral, S. A., Vieira, T. R., Albuquerque, B. N., Cota, L. O., Esteves Lima, R. P. & Costa, F. O. 2018. Periodontitis as a risk factor for peri-implantitis: Systematic review and meta-analysis of observational studies. Journal of Dentistry, 79, 1-10.

Fiorellini, J. P., Luan, K. W., Chang, Y. C., Kim, D. M. & Sarmiento, H. L. 2019. Peri-implant mucosal tissues and inflammation: Clinical implications. The International Journal of Oral & Maxillofacial Implants, 34, 25-33.

Fischer, K., Backstrom, M. & Sennerby, L. 2009. Immediate and early loading of oxidized tapered implants in the partially edentulous maxilla: A 1-year prospective clinical, radiographic, and resonance frequency analysis study. Clinical Implant Dentistry and Related Research, 11, 69-80.

Fitzpatrick, A. J., Rodgers, G. W., Hooper, G. J. & Woodfield, T. B. 2017. Development and validation of an acoustic emission device to measure wear in total hip replacements *in-vitro* and *in-vivo*. Biomedical Signal Processing and Control, 33, 281-288.

Flanagan, D. 2010. Osteotomy irrigation: Is it necessary? Implant dentistry, 19, 241–249.

Fu, J. H., Hsu, Y. T. & Wang, H. L. 2012. Identifying occlusal overload and how to deal with it to avoid marginal bone loss around implants. European Journal of Oral Implantology, 5, 91-103.

Fu, M. W., Fu, E., Lin, F. G., Chang, W. J., Hsieh, Y. D. & Shen, E. C. 2017. Correlation between resonance frequency analysis and bone quality

assessments at dental implant recipient sites. International Journal of Oral Maxillofacial Implants, 32, 180-187.

Gaetti-Jardim, C. E., Santiago-Junior, F. J., Goiato, C. M., Pellizer, P. E., Magro-Filho, G. O. & Jardim, G. E. 2011. Dental implants in patients with osteoporosis: A clinical reality? Journal of Craniofacial Surgery, 22, 1111-1113.

Garcia-Garcia, M., Mir-Mari, J., Benic, G. I., Figueiredo, R. & Valmaseda-Castellon, E. 2016. Accuracy of periapical radiography in assessing bone level in implants affected by peri-implantitis: A cross-sectional study. Journal of Clinical Periodontology 43, 85-91.

Gehrke, S. A., Da Silva, U. T. & Del Fabbro, M. 2015. Does implant design affect implant primary stability? A resonance frequency analysis–based randomized split-mouth clinical trial. Journal of Oral Implantology, 41, e281-286.

Gómez-Moreno, G., Aguilar-Salvatierra, A., Rubio Roldán, J., Guardia, J., Gargallo, J. & Calvo-Guirado, J. L. 2015. Peri-implant evaluation in type 2 diabetes mellitus patients: A 3-year study. Clinical Oral Implants Research, 26, 1031-1035.

Gómez-Polo, M., Ortega, R., Gómez-Polo, C., Martín, C., Celemín, A. & Del Río, J. 2016. Does length, diameter, or bone quality affect primary and secondary stability in self-tapping dental implants? Journal of Oral and Maxillofacial Surgery, 74, 1344-1353.

Gonzalez-Martin, O., Oteo, C., Ortega, R., Alandez, J., Sanz, M. & Veltri, M. 2016. Evaluation of peri-implant buccal bone by computed tomography: An experimental study. Clinical Oral Implants Research, 27, 950-955.

Goodson, J., Haffajee, A. & Socransky, S. 1984. The relationship between attachment level loss and alveolar bone loss. Journal of Clinical Periodontology, 11, 348-359.

Gottlow, J., Sennerby, L., Rosengren, A. & Flynn, M. 2010. An experimental evaluation of a new craniofacial implant using the rabbit tibia model: part I. Histologic findings. Otol Neurotology, 31, 832-839.

Grisa, A. & Veitz-Keenan, A. 2018. Is osteoporosis a risk factor for implant survival or failure? Question: Is there a difference in survival rate between implants placed in patients with osteoporosis compared to patients without osteoporosis? Evidence-Based Dentistry, 19, 51-52.

Grosse, C. U. & Ohtsu, M. 2008. Acoustic emission testing, Springer Science & Business Media.

Gueiral, N. & Nogueira, E. 2012. Acoustic emission studies in hip arthroplasty. Peak Stress Impact *in Vitro* Cemented Prosthesis. Recent Advances in Arthroplasty, 131-145.

Hall, J., Miranda-Burgos, P. & Sennerby, L. 2005. Stimulation of directed bone growth at oxidized titanium implants by macroscopic grooves: An *in vivo* study. Clinical Implant Dentistry and Related Research, 7, 76-82.

Harris, D. O. & Bell, R. L. 1977. The measurement and significance of energy in acoustic-emission testing. Experimental Mechanics Journal, 17, 347-353.

Hellier, C. 2003. Handbook of non-destructive evaluation. New York: McGraw-Hill, pp. 11.

Helmy, M. H., Alqutaibi, A. Y., El-Ella, A. A. & Shawky, A. F. 2018. Effect of implant loading protocols on failure and marginal bone loss with unsplinted two-implant-supported mandibular overdentures: Systematic review and meta-analysis. International Journal of Oral & Maxillofacial Surgery, 47, 642-650.

Herrmann, I., Lekholm, U., Holm, S. & Kultje, C. 2005. Evaluation of patient and implant characteristics as potential prognostic factors for oral implant failures. International Journal of Oral and Maxillofacial Implants, 20, 731-736.

Hsu, J. T., Shen, Y. W., Kuo, C. W., Wang, R. T., Fuh, L. J. & Huang, H. L. 2017. Impacts of 3D bone-to- implant contact and implant diameter on primary stability of dental implant. Journal of the Formosan Medical Association, 116, 582-590.

Huang, H. L., Chang, C. H., Hsu, J. T., Fallgatter, A. M. & Ko, C. C. 2007. Comparison of implant body designs and threaded designs of dental implants: A 3-dimensional finite element analysis. International Journal of Oral & Maxillofacial Implants, 22, 551-562.

Huang, H. L., Tu, M. G., Fuh, L. J., Chen, Y. C., Wu, C. L., Chen, S. I. & Hsu, J. T. 2010. Effects of elasticity and structure of trabecular bone on the primary stability of dental implants. Journal of Medical and Biological Engineering, 30, 85-89.

Hui, C., Nizhou, L., Xinchen, X., Xinhua, Q. & Eryi, L. 2013. Smoking, radiotherapy, diabetes and osteoporosis as risk factors for dental implant failure: A meta-analysis. PLoS ONE, 8, e71955.

Ibañez, C., Catena, A., Galindo-Moreno, P., Noguerol, B., Magán-Fernández, A. & Mesa, F. 2016. Relationship between long-term marginal bone loss and bone quality, implant width, and surface. The International Journal of Oral & Maxillofacial Implants, 31, 398-405.

Isidor, F. 2006. Influence of forces on peri-implant bone. Clinical Oral Implants Research, 17, 8-18.

Jaffin, R. A. & Berman, C. L. 1991. The excessive loss of Brånemark fixtures in type IV bone: A 5-year analysis. Journal of Periodontology, 62, 2-4.

Jaramillo, V. R., Santos, V. R., Lázaro, V. P., Romero, V. M., Rios-Santos, V. J., Bullón, V. P., Fernández-Palacín, V. A. & Herrero-Climent, V. M. 2014. Comparative analysis of 2 resonance frequency measurement devices: Osstell Mentor and Osstell ISQ. Implant Dentistry, 23, 351-356.

Javed, F., Ahmed, H. B., Crespi, R. & Romanos, G. E. 2013. Role of primary stability for successful osseointegration of dental implants: Factors of influence and evaluation. Interventional Medicine & Applied Science, 5, 162-167.

Javed, F. & Romanos, G. 2010. The role of primary stability for successful immediate loading of dental implants. A literature review. Journal of Dentistry, 38, 612-620.

Jemt, T., Olsson, M. & Franke Stenport, V. 2015. Incidence of first implant failure: A retroprospective study of 27 years of implant operations at one specialist clinic. Clinical Implant Dentistry and Related Research, 17, 501-510.

Jimbo, R. & Albrektsson, T. 2015. Long-term clinical success of minimally and moderately rough oral implants: A review of 71 studies with 5 years or more of follow-up. Implant Dentistry, 24, 62-69.

John, G., Becker, J. & Schwarz, F. 2015. Modified implant surface with slower and less initial biofilm formation. Clinical Implant Dentistry and Related Research, 17, 461-468.

Jordana, F., Susbielles, L. & Colat-Parros, J. 2018. Peri-implantitis and implant body roughness: A systematic review of literature. Implant Dentistry, 27, 672-681.

Kang, S. R., Bok, S. C., Choi, S. C., Lee, S. S., Heo, M. S., Huh, K. H., Kim, T. I. & Yi, W. J. 2016. The relationship between dental implant stability and trabecular bone structure using cone-beam computed tomography. Journal of Periodontal Implant Science, 46, 116-127.

Kapur, R. A. 2016. Acoustic emission in orthopaedics: A state of the art review. Journal of Biomechanics, 49, 4065-4072.

Kim, R. J., Kim, Y. J., Choi, N. S. & Lee, I. B. 2015. Polymerization shrinkage, modulus, and shrinkage stress related to tooth-restoration interfacial de-bonding in bulk-fill composites. Journal of Dentistry, 43, 430-439.

Knabe, C., Klar, F., Fitzner, R., Radlanski, R. J. & Gross, U. 2002. *In vitro* investigation of titanium and hydroxyapatite dental implant surfaces using a rat bone marrow stromal cell culture system. Biomaterials, 23, 3235-3245.

Kong, L., Liu, B. L., Hu, K. J., Li, D. H., Song, Y. L., Ma, P. & Yang, J. 2006. Optimized thread pitch design and stress analysis of the cylinder screwed dental implant. West China Journal of Stomatology, 24, 509-515.

Kühl, S., Zürcher, S., Zitzmann, N. U., Filippl, A., Payer, M. & Dagassan-Berndt, D. 2016. Detection of peri-implant bone defects with different radiographic techniques – a human cadaver study. Clinical Oral Implants Research, 27, 529-534.

Lachmann, S., Laval, J. Y., Axmann, D. & Weber, H. 2011. Influence of implant geometry on primary insertion stability and simulated peri-implant bone loss: an *in vitro* study using resonance frequency analysis and damping capacity assessment. The International Journal of Oral & Maxillofacial Implants, 26, 347-355.

Lachmann, S., Laval, J. Y., Jager, B., Axmann, D., Gomez-Roman, G., Groten, M. & Weber, H. 2006. Resonance frequency analysis and damping capacity assessment. Part 2: Peri-implant bone loss follow-up. An *in vitro* study with the Periotest and Osstell instruments. Clinical Oral Implants Research, 17, 80-84.

Lages, F. S., Douglas-De Oliveira, D. W. & Costa, F. O. 2018. Relationship between implant stability measurements obtained by insertion torque and resonance frequency analysis: A systematic review. Clinical Implant Dentistry and Related Research, 20, 26-33.

Lambert, P. M., Morris, H. & Ochi, S. 1997. Positive effect of surgical experience with implants on second-stage implant survival. Journal of Oral and Maxillofacial Surgery: Official Journal of the American Association of Oral and Maxillofacial Surgeons, 55, 12-18.

Lan, T. H., Du, J. K., Pan, C. Y., Lee, H. E. & Chung, W. H. 2011. Biomechanical analysis of alveolar bone stress around implants with different thread designs and pitches in the mandibular molar area. Clinical Oral Investigations, 16, 363-369.

Le Guéhennec, L., Soueidan, A., Layrolle, P. & Amouriq, Y. 2007. Surface treatments of titanium dental implants for rapid osseointegration. Dental Materials, 23, 844-854.

Lee, J. W., An, J., Park, S. H., Chong, J. H., Kim, G. S., Han, J., Jung, S., Kook, M. S., Oh, H. K., Ryu, S. Y. & Park, H. J. 2016. Retrospective clinical study of an implant with a sandblasted, large-grit, acid-etched surface and

internal connection: Analysis of short-term success rate and marginal bone loss. Maxillofacial Plastic and Reconstructive Surgery, 38, 1-7.

Lekholm, U., Van Steenberghe, D., Herrmann, I., Bolender, C., Folmer, T., Gunne, J., Henry, P., Higuchi, K., Laney, W. R. & Lindén, U. 1994. Osseointegrated implants in the treatment of partially edentulous jaws: A prospective 5-year multicenter study. International Journal of Oral & Maxillofacial Implants, 9.

Lekholm, U., Zarb, G. 1985. Patient selection and preparation. In Brånkmark P I, Zarb G A, Albrektsson T, editors. Tissue-integrated prostheses. Osseointegration in clinical dentistry. Chicago: Quintessence: 199-209.

Leite, F. R., Nascimento, G. G., Baake, S., Pedersen, L. D., Scheutz, F. & López, R. 2019. Impact of smoking cessation on periodontitis: A systematic review and meta-analysis of prospective longitudinal observational and interventional studies. Nicotine and Tobacco Research, 21, 1600-1608.

Lemos, C. A., De Souza Batista, V. E., Almeida, D. A., Santiago Júnior, J. F., Verri, F. R. & Pellizzer, E. P. 2016. Evaluation of cement-retained versus screw-retained implant-supported restorations for marginal bone loss. The Journal of Prosthetic Dentistry, 115, 419-427.

Li, H., Li, J., Yun, X., Liu, X. & Fok, A. S. 2011. Non-destructive examination of interfacial de-bonding using acoustic emission. Dental Materials, 27, 964-971.

Linkevicius, T., Puisys, A., Vindasiute, E., Linkeviciene, L. & Apse, P. 2013. Does residual cement around implant-supported restorations cause peri-implant disease? A retrospective case analysis. Clinical Oral Implants Research, 24, 1179-1184.

Machuca, G., Rosales, I., Lacalle, J. R., Machuca, C. & Bullón, P. 2000. Effect of cigarette smoking on periodontal status of healthy young adults. Journal of Periodontology, 71, 73-78.

Mandelbrot, B. B. 1967. How long is the coast of Britain? Statistical self-similarity and fractional dimension. Science, 156, 636–638

Mantovani, A., Mattias Sartori, I., Azevedo-Alanis, L., Tiossi, R. & Fontão, F. 2018. Influence of cortical bone anchorage on the primary stability of dental implants. Oral and Maxillofacial Surgery, 22, 297-301.

Manzano, G., Montero, J., Martín-Vallejo, J., Del Fabbro, M., Bravo, M. & Testori, T. 2016. Risk Factors in Early Implant Failure: A Meta-Analysis. Implant Dentistry, 25,272-280.

Marković, A., Mišić, T., Mančić, D., Jovanović, I., Šćepanović, M. & Jezdić, Z. 2014. Real-time thermographic analysis of low-density bone during implant placement: A randomized parallel-group clinical study comparing lateral condensation with bone drilling surgical technique. Clinical Oral Implants Research, 25, 910-918.

Marquezan, M., Osório, A., Sant' Anna, E., Souza, M. M. & Maia, L. 2012. Does bone mineral density influence the primary stability of dental implants? A systematic review. Clinical Oral Implants Research, 23, 767-774.

Marrone, A., Lasserre, J., Bercy, P. & Brecx, M. C. 2013. Prevalence and risk factors for peri-implant disease in Belgian adults. Clinical Oral Implants Research, 24, 934-940.

Mathieu, V., Anagnostou, F., Soffer, E. & Haïat, G. 2011. Ultrasonic evaluation of dental implant biomechanical stability: An *in vitro* Study. Ultrasound in Medicine and Biology, 37, 262-270.

Matthews, J. R. 1983. Acoustic emission, CRC Press.

Mavrogenis, A. F., Dimitriou, R., Parvizi, J. & Babis, G. C. 2009. Biology of implant osseointegration. Journal of Musculoskeletal & Neuronal interactions, 9, 61-71.

Meredith, N. 1998. Assessment of implant stability as a prognostic determinant. The International Journal of Prosthodontics, 11, 491-501.

Meredith, N., Alleyne, D. & Cawley, P. 1996. Quantitative determination of the stability of the implant-tissue interface using resonance frequency analysis. Clinical Oral Implants Research, 7, 261-267.

Meredith, N., Friberg, B., Sennerby, L. & Aparicio, C. 1998. Relationship between contact time measurements and PTV values when using the Periotest to measure implant stability. International Journal of Prosthodontics, 11, 269-275.

Merheb, J., Graham, J., Coucke, W., Roberts, M., Quirynen, M., Jacobs, R. & Devlin, H. 2015. Prediction of implant loss and marginal bone loss by analysis of dental panoramic radiographs. International Journal of Oral & Maxillofacial Implants, 30, 372-377.

Merheb, J., Van Assche, N., Coucke, W., Jacobs, R., Naert, I. & Quirynen, M. 2010. Relationship between cortical bone thickness and computerized tomography-derived bone density values and implant stability. Clinical Oral Implants Research, 21, 612-617.

Merli, M., Moscatelli, M., Mariotti, G., Piemontese, M. & Nieri, M. 2012. Immediate versus early non-occlusal loading of dental implants placed flapless in partially edentulous patients: A 3-year randomized clinical trial. Journal of Clinical Periodontology, 39, 196-202.

Meyle, J., Casado, P., Fourmousis, I., Kumar, P., Quirynen, M. & Salvi, G. E. 2019. General genetic and acquired risk factors, and prevalence of peri-implant diseases – Consensus report of working group 1. International Dental Journal, 69, 3-6.

Misch, C., 1989. Bone classification, training keys to implant success. Dentistry today, 8, 39-44.

Misch, C., 2005. An implant is not a tooth: A comparison of periodontal indexes. Dental Implant Prosthetics, 1, 18-31.

Misch, C. 2015. Dental implant prosthetics, St. Louis, Missouri: Elsevier Mosby.

Misch, C., Perel, L. M., Wang, A. H., Sammartino, K. G., Galindo-Moreno, K. P., Trisi, K. P., Steigmann, K. M., Rebaudi, K. A., Palti, K. A., Pikos, K. M., Schwartz-Arad, K. D., Choukroun, K. J., Gutierrez-Perez, K. J., Marenzi, K. G. & Valavanis, K. D. 2008. Implant success, survival, and failure: The International Congress of Oral Implantologists (ICOI) Pisa Consensus Conference. Implant Dentistry, 17, 5-15.

Misch, C., Steigenga, J., Cianciola, L. & Kazor, C. 2006. Short Dental Implants in Posterior Partial Edentulism: A multicenter Retrospective 6-Year Case Series Study. Journal of Periodontology, 1340-1347.

Mishra, S., Kumar, M. & Chowdhary, R. 2017. Anodized dental implant surface (Systematic Review). Indian Journal of Dental Research, 28, 76-99.

Moedano, D. E., Irigoyen, M. E., Borges-YAEZ, A., Flores-Sanchez, I. & Rotter, R. C. 2011. Osteoporosis, the risk of vertebral fracture, and periodontal disease in an elderly group in Mexico City (Report). Gerodontology, 28, 19-29.

Möhlhenrich, S. C., Modabber, A., Steiner, T., Mitchell, D. A. & Hölzle, F. 2015. Heat generation and drill wear during preparation of sites for dental implants: Systematic review. British Journal of Oral & Maxillofacial Surgery, 53, 679-689.

Monje, A., Ortega-Oller, I., Galindo-Moreno, P., Catena, A., Monje, F., O'Valle, F., Suarez, F. & Wang, H. L. 2014. Sensitivity of resonance frequency analysis for detecting early implant failure: A case-control study. The International Journal of Oral & Maxillofacial Implants, 29, 456-461.

Moraschini, V., Barboza, E. S. & Peixoto, G. A. 2016. The impact of diabetes on dental implant failure: A systematic review and meta-analysis. International Journal of Oral & Maxillofacial Surgery, 45, 1237-1245.

Naujokat, H., Kunzendorf, B. & Wiltfang, J. 2016. Dental implants and diabetes mellitus: A systematic review. International Journal of Implant Dentistry, 2, 1-10.

Nicholson, J. W. 1998. Glass-ionomers in medicine and dentistry. Proceedings of the Institution of Mechanical Engineers. Part H, Journal of Engineering in Medicine, 212, 121–126.

Nivesrangsan P. 2005. Multi source, multi sensor approaches to diesel engine monitoring using acoustic emission, PhD Thesis, Heriot Watt University, Edinburgh.

Nkenke, E., Hahn, M., Weinzierl, K., Radespiel-Troger, M., Neukam, F. W., Engelke, K. 2003. Implant stability and histomorphometry: A correlation study in human cadavers using stepped cylinder implants. Clinical Oral Implants Research, 14, 601-609.

Noda, K., Arakawa, H., Kimura-Ono, A., Yamazaki, S., Hara, E. S., Sonoyama, W., Maekawa, K., Okura, K., Shintani, A., Matsuka, Y. & Kuboki, T. 2015. A longitudinal retrospective study of the analysis of the risk factors of implant failure by the application of generalized estimating equations. Journal of Prosthodontic Research, 59, 178-184.

Novaes, A. B., Souza, S. L., De Oliveira, P. T. & Souza, A. M. 2002. Histomorphometric analysis of the bone-implant contact obtained with 4 different implant surface treatments placed side by side in the dog mandible. The International Journal of Oral & Maxillofacial Implants, 17, 377-383.

O' Mahony, A. M., Williams, J. L., Katz, J. O. & Spencer, P. 2000. Anisotropic elastic properties of cancellous bone from a human edentulous mandible. Clinical Oral Implants Research, 11, 415-421.

O'Neill, C. & Ruff, B. 2004. Estimating human long bone cross-sectional geometric properties: A comparison of non-invasive methods. Journal of Human Evolution, 4, 221-235.

Obagbemiro, K., Ajayi, Y., Akeredolu, P., Adeoye, J. & Arotiba, G. 2018. The effect of implant characteristics on the implant stability of immediately loaded single implant cases: A prospective study. Journal of Dental Implants, 8, 48-53.

Ogle, O. E. 2015. Implant surface material, design, and osseointegration. Dental Clinics of North America, 59, 505-520.

Okonkwo, U. A. & Di Pietro, L. A. 2017. Diabetes and wound angiogenesis. International Journal of Molecular Sciences, 18, 1419.

Olate, S., Lyrio, M. C., De Moraes, M., Mazzonetto, R. & Moreira, R. W. 2010. Influence of diameter and length of implant on early dental implant failure. Journal of Oral and Maxillofacial Surgery, 68, 414-419.

Olivé, J. & Aparicio, C. 1990. The Periotest method as a measure of osseointegrated oral implant stability. International Journal of Oral & Maxillofacial Implants, 5, 390-400.

Olson, J. W., Shernoff, A. F., Tarlow, J. L., Colwell, J. A., Scheetz, J. P. & Bingham, S. F. 2000. Dental endosseous implant assessments in a type 2 diabetic population: A prospective study. International Journal of Oral & Maxillofacial Implants, 15, 811-818.

Ossi, Z. 2013. Monitoring the stability of dental implant using acoustic emission method. ProQuest Dissertations Publishing.

Ossi, Z., Abdou, W., Reuben, R., Ibbetson, R. 2011. *In vitro* assessment of bone-implant interface using an acoustic emission transmission test. Proceedings of the institution of Mechanical Engineers. Part H, Journal of Engineering in Medicine, 226, 63-69.

Ossi, Z., Abdou, W., Reuben, R., Ibbetson, R. 2013. Transmission of acoustic emission in bones, implants and dental materials. Proceedings of the Institution of Mechanical Engineers, Part H: Journal of Engineering in Medicine, 227, 1237-1245.

Östman, P. O., Hellman, M., Wendelhag, I. & Sennerby, L. 2006. Resonance frequency analysis measurements of implants at placement surgery. International Journal of Prosthodontics, 19, 77-83.

Oswal, M., Amasi, U., Oswal, M. & Bhagat, A. 2016. Influence of three different implant thread designs on stress distribution: A three-dimensional finite element analysis. (Report). The Journal of Indian Prosthodontic, 16, 359-365.

Pan, C. Y., Liu, P. H., Tseng, Y. C., Chou, S. T., Wu, C. Y. & Chang, H. P. 2019. Effects of cortical bone thickness and trabecular bone density on primary stability of orthodontic mini-implants. Journal of Dental Sciences, 14, 383-388.

Papaspyridakos, P., Chen, C. J., Singh, M., Weber, H. P. & Gallucci, G. 2012. Success criteria in implant dentistry: A systematic review. Journal of Dental Research, 91, 242-248.

Parvini, P., Saminsky, M., Stanner, J., Klum, M., Nickles, K. & Eickholz, P. 2019. Discomfort/pain due to periodontal and peri-implant probing with/without platform switching. Clinical Oral Implants Research, 30, 997-1004.

Paul, S., Petsch, M. & Held, U. 2017. Modelling of crestal bone after submerged vs transmucosal implant placement: A systematic review with meta-analysis. The International Journal of Oral & Maxillofacial Implants, 32, 1039–1050.

Pechon, P. H., Pullin, R., Eaton, M. J., Jones, S. A. & Evans, S. 2018. Acoustic emission technology can warn of impending iatrogenic femur fracture during femoral canal preparation for uncemented hip replacement. A cadaveric animal bone study. Journal of Medical Engineering & Technology, 42, 72-87.

Pesce, P., Canullo, L., Grusovin, M. G., De Bruyn, H., Cosyn, J. & Pera, P. 2015. Systematic review of some prosthetic risk factors for peri-implantitis. The Journal of Prosthetic Dentistry, 114, 346-350.

Petrov, S. D., Xing, Y., Khandelwal, N. & Drew, H. J. 2014. A novel technique for osteotome internal sinus lifts with simultaneous placement of tapered implants to improve primary stability. Journal of Oral Implantology, 40, 607-613.

Pikner, S. S. & Gröndahl, K. 2009. Radiographic analyses of “Advanced” marginal bone loss around Brånemark dental implants. Clinical Implant Dentistry and Related Research, 11, 120-133.

Pimentel, S. P., Shiota, R., Cirano, F. R., Casarin, R. C., Pecorari, V. G., Casati, M. Z., Haas, A. N. & Ribeiro, F. V. 2018. Occurrence of peri-implant diseases and risk indicators at the patient and implant levels: A multilevel cross-sectional study. Journal of Periodontology, 89, 1091-1100.

Pinheiro, L. R., Gaia, B. F., Oliveira De Sales, M. A., Umetsubo, O. S., Santos Junior, O. & Paraíso Cavalcanti, M. G. 2015. Effect of field of view in the detection of chemically created peri-implant bone defects in bovine ribs using cone beam computed tomography: an *in vitro* study. Oral Surgery, Oral Medicine, Oral Pathology and Oral Radiology, 120, 69-77.

Quaranta, A., Lim, Z., Tang, J., Perrotti, V. & Leichter, J. 2017. The Impact of residual subgingival cement on biological complications around dental implants: A systematic review. Implant Dentistry, 26, 465-474.

Quirynen, M., Abarca, M., Van Assche, N., Nevins, M. & Van Steenberghe, D. 2007. Impact of supportive periodontal therapy and implant surface roughness on implant outcome in patients with a history of periodontitis. Journal of Clinical Periodontology, 34, 805-815.

Rakic, M., Galindo-Moreno, P., Monje, A., Radovanovic, S., Wang, H. L., Cochran, D., Sculean, A. & Canullo, L. 2018. How frequent does peri-implantitis occur? A systematic review and meta-analysis. Clinical Oral Investigations, 22, 1805-1816.

Rashid, M. S. & Pullin, R. 2014. The sound of orthopaedic surgery—the application of acoustic emission technology in orthopaedic surgery: A review. European Journal of Orthopaedic Surgery & Traumatology, 24, 1-6.

Renvert, S. & Quirynen, M. 2015. Risk indicators for peri-implantitis. A narrative review. Clinical Oral Implants Research, 26, 15-44.

Reuben, R. L. 2017. Acoustic emission and ultrasound for monitoring the bone-implant interface. In: Piattelli, A. (ed.) Bone Response to Dental Implant Materials. Woodhead Publishing.

Revell, P. A. 1983. Histomorphometry of bone. Journal of Clinical Pathology, 36, 1323.

Ribeiro-Rotta, R. F., Lindh, C., Pereira, A. C. & Rohlin, M. 2011. Ambiguity in bone tissue characteristics as presented in studies on dental implant planning and placement: A systematic review. Clinical Oral Implants research, 22, 789-792.

Romanos, G. E. 2009. Bone quality and the immediate loading of implants-critical aspects based on literature, research, and clinical experience. Implant Dentistry, 18, 203-209.

Romanos, G. E., Ciornei, G., Jucan, A., Malmstrom, H. & Gupta, B. 2014. *In vitro* assessment of primary stability of Straumann implant designs. Clinical Implant Dentistry and Related Research, 16, 89-95.

Romanos, G. E. & Weitz, D. 2012. Therapy of peri-implant diseases. Where is the evidence? Journal of Evidence Based Dental Practice, 12, 204-208.

Romhány, G., Czigány, T. & Karger-Kocsis, J. 2017. Failure assessment and evaluation of damage development and crack growth in polymer composites via localization of acoustic emission events: A review. Polymer Reviews, 57, 397-439.

Rosen, P., Clem, D., Cochran, D., Froum, S., Mcallister, B., Renvert, S. & Wang, H. L. 2013. Academy Report: Peri-implant mucositis and peri-implantitis: A current understanding of their diagnoses and clinical implications. Journal of Periodontology, 84, 436-443.

Rozé, J., Babu, S., Saffarzadeh, A., Gayet-Delacroix, M., Hoornaert, A. & Layrolle, P. 2009. Correlating implant stability to bone structure. Clinical Oral Implants Research, 20, 1140-1145.

Rupp, F., Liang, L., Geis-Gerstorfer, J., Scheideler, L. & Huttig, F. 2018. Surface characteristics of dental implants: A review. Dental Materials, 34, 40-57.

Ryu, H. S., Namgung, C., Lee, J. H. & Lim, Y. J. 2014. The influence of thread geometry on implant osseointegration under immediate loading: A literature review. The Journal of Advanced Prosthodontics, 6, 547-554.

Sachdeva, A., Dhawan, P. & Sindwani, S. 2016. Assessment of implant stability: Methods and recent advances. British Journal of Medicine and Medical Research, 12, 1-10.

Sahrmann, P., Gilli, F., Wiedemeier D. B., Attin T., Schmidlin P. R., & Karygianni L. 2020. The Microbiome of peri-implantitis: A systematic review and meta-Analysis. Microorganisms (Basel), 8, 661-686.

Salimov, F., Tatli, U., Kürkçü, M., Akoğlan, M., Öztunç, H. & Kurtoğlu, C. 2014. Evaluation of relationship between preoperative bone density values derived from cone beam computed tomography and implant stability parameters: A clinical study. Clinical Oral Implants Research, 25, 1016-1021.

Salvi, G. E., Aglietta, M., Eick, S., Sculean, A., Lang, N. P. & Ramseier, C. A. 2012. Reversibility of experimental peri-implant mucositis compared with experimental gingivitis in humans. Clinical Oral Implants Research, 23, 182-190.

Salvi, G. E. & Lang, N. P. 2004. Diagnostic parameters for monitoring peri-implant conditions. The International Journal of Oral & Maxillofacial Implants, 19, 116-127.

Sánchez-Siles, M., Ilha, J. B., Ruizc, J. A., Alonsod, F. C. & Alonso, F. C. 2019. Evaluation of primary stability and early healing of 2 implant macrodesigns placed in the posterior maxilla: A split-mouth prospective randomized controlled clinical study. Journal of Oral Science and Rehabilitation, 5, 8-15.

Santamaría-Arrieta, G., Brizuela-Velasco, A., Fernández-González, F. J., Chávarri-Prado, D., Chento-Valiente, Y., Solaberrieta, E., Diéguez-Pereira, M., Vega, J. A. & Yurrebaso-Asúa, J. 2016. Biomechanical evaluation of oversized drilling technique on primary implant stability measured by insertion torque and resonance frequency analysis. Journal of Clinical and Experimental Dentistry, 8, 307-311.

Sanz-Sánchez, I., Sanz-Martín, I., Figuero, E. & Sanz, M. 2015. Clinical efficacy of immediate implant loading protocols compared to conventional loading depending on the type of the restoration: A systematic review. Clinical Oral Implants Research, 26, 964-982.

Satwalekar, P., Nalla, S., Reddy, R. & Chowdary, S. 2015. Clinical evaluation of osseointegration using resonance frequency analysis. The journal of Indian Prosthodontic Society, 15, 192-199.

Sause, M. G. 2011. Investigation of pencil-lead breaks as acoustic emission sources. Journal of Acoustic Emission, 29, 184.

Schnitman, P. A. & Shulman, L. B. 1979. Recommendations of the consensus development conference on dental implants. The Journal of the American Dental Association, 98, 373-377.

Schulte, W. & Lukas, D. 1992. The Periotest method. International Dental Journal, 42, 433-440.

Schulze, R. K. & D'Hoedt, B. 2001. Mathematical analysis of projection errors in “paralleling technique” with respect to implant geometry. Clinical Oral Implants Research, 12, 364-371.

Schwartz-Arad, D., Herzberg, R. & Levin, L. 2005. Evaluation of long-term implant success. Journal of Periodontology, 76, 1623-1628.

Sennerby, L. & Meredith, N. 2008. Implant stability measurements using resonance frequency analysis: Biological and biomechanical aspects and clinical implications. Periodontology 2000, 47, 51-66.

Sennerby, L. & Roos, J. 1998. Surgical determinants of clinical success of osseointegrated oral implants: A review of the literature. International Journal of Prosthodontics, 11, 408-420.

Seong, W. J., Conrad, H. J. & Hinrichs, J. E. 2009. Potential damage to bone-implant interface when measuring initial implant stability. Journal of Periodontology, 80, 1868-1874.

Gao, S. S., Zhang, Y. R., Zhu, Z. L. & Yu, H. Y. 2012. Micro-motions and combined damages at the dental implant-bone interface. International Journal of Oral Science, 4, 182-188.

Shin, S. Y., Shin, S. I., Kye, S. B., Chang, S. W., Hong, J., Paeng, J. Y. & Yang, S. M. 2015. Bone cement grafting increases implant primary stability in circumferential cortical bone defects. Journal of Periodontal Implant Science, 45, 30-35.

Smeets, R., Henningsen, A., Jung, O., Heiland, M., Hammacher, C. & Stein, J. M. 2014. Definition, aetiology, prevention and treatment of peri-implantitis - A review. Head & Face Medicine, 10.

Smeets, R., Stadlinger, B., Schwarz, F., Beck-Broichsitter, B., Jung, O., Precht, C., Kloss, F., Gröbe, A., Heiland, M. & Ebker, T. 2016. Impact of dental implant

surface modifications on osseointegration. Bio-Medical Research International, 2016.

Smith, D. E. & Zarb, G. A. 1989. Criteria for success of osseointegrated endosseous implants. The Journal of Prosthetic Dentistry, 62, 567-572.

Srisuthep, C. 2019. Outcome of immediate versus delayed loading of full arch implant-supported fixed prosthesis: A systematic review and meta-Analysis. Dental Theses.

Staubli, N., Walter, C., Schmidt, J. C., Weiger, R. & Zitzmann, N. U. 2017. Excess cement and the risk of peri-implant disease: A systematic review. Clinical Oral Implants Research, 28, 1278-1290.

Steigenga, T. J., Al-Shammari, F. K., Nociti, H. F., Misch, E. C. & Wang, E. H. 2003. Dental implant design and its relationship to long-term implant success. Implant Dentistry, 12, 306-317.

Sugiura, T., Yamamoto, K., Horita, S., Murakami, K. & Kirita, T. 2019. Evaluation of primary stability of cylindrical and tapered implants in different bone types by measuring implant displacement: An *In vitro* Study. Contemporary Clinical Dentistry, 10, 471-476.

Sullivan, D. Y., Sherwood, R. L., Collins, T. A. & Krogh, P. H. 1996. The reverse-torque test: A clinical report. International Journal of Oral & Maxillofacial Implants, 11, 179-185.

Summers, R. B. 1994. A new concept in maxillary implant surgery: The osteotome technique. Compendium (Newtown, Pa.), 15, 152-158.

Tabassum, A., Meijer, G. J., Wolke, J. G. & Jansen, J. A. 2010. Influence of surgical technique and surface roughness on the primary stability of an implant in artificial bone with different cortical thickness: A laboratory study. Clinical Oral Implants Research, 21, 213-220.

Tettamanti, L., Andrisani, C., Bassi, M. A., Vinci, R., Silvestre-Rangil, J. & Tagliabue, A. 2017. Immediate loading implants: Review of the critical aspects. Oral & Implantology, 10, 129-139.

Tricio, J., Laohapand, P., Van Steenberghe, D., Quirynen, M. & Naert, I. 1994. Mechanical state assessment of the implant-bone continuum: A better understanding of the Periotest method. The International Journal of Oral & Maxillofacial Implants, 10, 43-49.

Trisi, P. & Rao, W. 1999. Bone classification: Clinical-histomorphometric comparison. Clinical Oral Implants Research, 10, 1-7.

Troiano, G., Lo Russo, L., Canullo, L., Ciavarella, D., Lo Muzio, L. & Laino, L. 2018. Early and late implant failure of submerged versus non-submerged implant healing: A systematic review, meta-analysis and trial sequential analysis (Report). Journal of Clinical Periodontology, 45, 613-624.

Turkyilmaz, I. & Mcglumphy, E. A. 2008. Influence of bone density on implant stability parameters and implant success: A retrospective clinical study. BMC Oral Health, 8, 32-40.

Underwood, E. E. 1979. Quantification of microstructures by stereological analysis. The Journal of Histochemistry and Cytochemistry, 27, 1536–1537.

Vandamme, K., Naert, I., Geris, L., Sloten, J. V., Puers, R. & Duyck, J. 2007. Influence of controlled immediate loading and implant design on peri-implant bone formation. Journal of Clinical Periodontology, 34, 172-181.

Vayron, R. & Haiat, G. 2015. Assessing dental implant stability using quantitative ultrasound methods: Experimental approach and numerical validation. The Journal of the Acoustical Society of America, 138, 1799.

Vayron, R., Hieu Nguyen, V., Lecuelle, B. & Haiat, G. 2018. Evaluation of dental implant stability in bone phantoms: comparison between a quantitative ultrasound technique and resonance frequency analysis. Clinical Implant Dentistry and Related Research. 20, 470-478.

Vayron, R., Mathieu, V., Michel, A. & Haiat, G. 2014a. Assessment of *in vitro* dental implant primary stability using an ultrasonic method. Ultrasound in Medicine & Biology, 40, 2885-2894.

Vayron, R., Nguyen, V. H., Bosc, R., Naili, S. & Haïat, G. 2016. Assessment of the biomechanical stability of a dental implant with quantitative ultrasound: A three-dimensional finite element study. The Journal of the Acoustical Society of America, 139, 773.

Vayron, R., Soffer, E., Anagnostou, F. & Haïat, G. 2014b. Ultrasonic evaluation of dental implant osseointegration. Journal of Biomechanics, 47, 3562-3568.

Veltri, M., Gonzalez-Martin, O. & Belser, U. C. 2014. Influence of simulated bone-implant contact and implant diameter on secondary stability: A resonance frequency *in vitro* study. Clinical Oral Implants Research, 25, 899-904.

Vervaeke, S., Collaert, B., Cosyn, J., Deschepper, E. & De Bruyn, H. 2015. A multifactorial analysis to identify predictors of implant failure and peri-implant bone loss. (Report). 17, 298-300.

Vicente Neto, P., Franco Micheloni, A. L., Scarduelli, C. R., Pizzol, K. E., Mollo Júnior, F. D. & Marcantônio Júnior, E. 2018. Predictability and success rate of short implants. Journal of Research in Dentistry, 5, 28.

Wadhwani, C. P. 2015. Complications related to cemented implant restoration. Dental Implant Complications: Aetiology, Prevention, and Treatment, 187-208.

Wennström, J. & Palmer, R. 1999. Proceedings of the 3rd European Workshop on Periodontology. Implant Dentistry.

Wilson Jr, T. G. 2009. The positive relationship between excess cement and peri-implant disease: A prospective clinical endoscopic study. Journal of Periodontology, 80, 1388-1392.

Winkler, S., Morris, H. F. & Ochi, S. 2000. Implant survival to 36 months as related to length and diameter. Annals of periodontology, 5, 22-31.

Winter, W., Möhrle, S., Holst, S. & Karl, M. 2010. Parameters of implant stability measurements based on resonance frequency and damping capacity: A comparative finite element analysis. The International Journal of Oral & Maxillofacial Implants, 25, 532-539.

Yang, B., Guo, J., Huang, Q., Heo, Y., Fok, A. & Wang, Y. 2016. Acoustic properties of interfacial de-bonding and their relationship with shrinkage stress in Class-I restorations. Dental Materials, 32, 742-748.

Yao, C., Ma, L. & Mattheos, N. 2017. Can resonance frequency analysis (RFA) detect narrow marginal bone defects around dental implants? An *ex-vivo* animal pilot study. Australian Dental Journal. 62, 433-439.

Zanetti, M. E., Pascoletti, G., Calì, M., Bignardi, C. & Franceschini, G. 2018. Clinical assessment of dental implant stability during follow-up: What is actually measured, and perspectives. Biosensors, 8, 68-76.

Zhang, S., Wang, S. & Song, Y. 2017. Immediate loading for implant restoration compared with early or conventional loading: A meta-analysis. Journal of Cranio-Maxillo-Facial Surgery, 45, 793-803.

Zitzmann, N. U. & Berglundh, T. 2008. Definition and prevalence of peri-implant diseases. Journal of Clinical Periodontology, 35, 286-291.

Zoghbi, S. A., De Lima, L. A., Saraiva, L. & Romito, G. A. 2011. Surgical experience influences 2-stage implant osseointegration. Journal of Oral and Maxillofacial Surgery, 69, 2771-2776.